

Journal of Structural Engineering

Optimization Based Improved Softened Membrane Model for Rectangular Reinforced Concrete Members under Combined Shear and Torsion --Manuscript Draft--

Manuscript Number:	STENG-6964R2
Full Title:	Optimization Based Improved Softened Membrane Model for Rectangular Reinforced Concrete Members under Combined Shear and Torsion
Manuscript Region of Origin:	INDIA
Article Type:	Technical Paper
Section/Category:	Analysis and Computation
Funding Information:	Science and Engineering Research Board (SB/S3/CEE/0060/2013) Dr Suriya Prakash
Abstract:	<p>Reinforced concrete (RC) elements are often subjected to combined actions including torsion under seismic events. Understanding the behavior of RC members under combined actions including torsion is essential for safe design. Behavioral predictions of RC columns under combined loading can be improved by including the bi-directional stress effects. The objective of this work is to propose improved combined actions softened membrane model (CA-SMM) for predicting the behavior of RC elements under combined torsion (T) and shear loading (V). In this approach, the rectangular cross-section is modeled as an assembly of four cracked shear panels. The applied external loads are distributed among these four shear panels. This assumption helps in reducing the complex stress state from combined loading to four different simple stress states on these panels. Additional equilibrium and compatibility conditions are imposed, and the system of non-linear equations are solved by using an optimization technique called gradient descent method. The developed improved model (CA-SMM) is validated with the experimental data available in the literature. After that, an interaction between the shear and torsion is developed to understand the behavior under various combinations of torsion and shear. A parametric study is carried out for understanding the effect of various sectional parameters such as longitudinal reinforcement ratio, transverse reinforcement ratio, and concrete strength. The predictions of the improved model had a close correlation with the test results.</p>
Corresponding Author:	Suriya Prakash, Ph.D., Indian Institute of Technology Hyderabad Sangareddy, Telangana INDIA
Corresponding Author E-Mail:	suriyap@iith.ac.in
Order of Authors:	Sriharsha Reddy Kothamuthyala, Mtech Nikesh Thammishetti, Mtech Suriya Prakash, Ph.D., Chandrika Prakash Vyasarayani
Suggested Reviewers:	<p>Ashraf Ayoub, PhD Professor, City University of London</p> <p>Professor Ayoub and his group have worked extensively on behavior of RC members under combined loading including torsion.</p> <p>Mohamad Elgawady, PhD Professor, Missouri University of Science and Technology</p> <p>Dr. Elgawady has extensively worked on behavior of RC members under torsional loading.</p> <p>Abdeldjelil Belarbi, PhD Professor, University of Houston</p>

	Has extensively worked on development of improved models for combined loading including torsion
	Ananth Ramaswamy, PhD Professor, Indian Institute of Science
	Has extensively worked on behavior of RC members and on development of improved models
Opposed Reviewers:	
Additional Information:	
Question	Response
Authors are required to attain permission to re-use content, figures, tables, charts, maps, and photographs for which the authors do not hold copyright. Figures created by the authors but previously published under copyright elsewhere may require permission. For more information see http://ascelibrary.org/doi/abs/10.1061/9780784479018.ch03 . All permissions must be uploaded as a permission file in PDF format. Are there any required permissions that have not yet been secured? If yes, please explain in the comment box.	No
ASCE does not review manuscripts that are being considered elsewhere to include other ASCE Journals and all conference proceedings. Is the article or parts of it being considered for any other publication? If your answer is yes, please explain in the comments box below.	No
Is this article or parts of it already published in print or online in any language? ASCE does not review content already published (see next questions for conference papers and posted theses/dissertations). If your answer is yes, please explain in the comments box below.	No
Has this paper or parts of it been published as a conference proceeding? A conference proceeding may be reviewed for publication only if it has been significantly revised and contains 50% new content. Any content overlap should be reworded and/or properly referenced. If your answer is yes, please explain in the comments box below and be prepared to provide the conference paper.	No
ASCE allows submissions of papers that are based on theses and dissertations so long as the paper has been modified to fit the journal page limits, format, and tailored for the audience. ASCE will	No

<p>consider such papers even if the thesis or dissertation has been posted online provided that the degree-granting institution requires that the thesis or dissertation be posted.</p> <p>Is this paper a derivative of a thesis or dissertation posted or about to be posted on the Internet? If yes, please provide the URL or DOI permalink in the comment box below.</p>	
<p>Each submission to ASCE must stand on its own and represent significant new information, which may include disproving the work of others. While it is acceptable to build upon one's own work or replicate other's work, it is not appropriate to fragment the research to maximize the number of manuscripts or to submit papers that represent very small incremental changes. ASCE may use tools such as CrossCheck, Duplicate Submission Checks, and Google Scholar to verify that submissions are novel. Does the manuscript constitute incremental work (i.e. restating raw data, models, or conclusions from a previously published study)?</p>	No
<p>Authors are expected to present their papers within the page limitations described in Publishing in ASCE Journals: A Guide for Authors. Technical papers and Case Studies must not exceed 30 double-spaced manuscript pages, including all figures and tables. Technical notes must not exceed 7 double-spaced manuscript pages. Papers that exceed the limits must be justified. Grossly over-length papers may be returned without review. Does this paper exceed the ASCE length limitations? If yes, please provide justification in the comments box below.</p>	No
<p>All authors listed on the manuscript must have contributed to the study and must approve the current version of the manuscript. Are there any authors on the paper that do not meet these criteria? If the answer is yes, please explain in the comments.</p>	No
<p>Was this paper previously declined or withdrawn from this or another ASCE journal? If so, please provide the previous manuscript number and explain what you have changed in this current version in the comments box below. You may upload a separate response to reviewers</p>	No

if your comments are extensive.	
<p>Companion manuscripts are discouraged as all papers published must be able to stand on their own. Justification must be provided to the editor if an author feels as though the work must be presented in two parts and published simultaneously. There is no guarantee that companions will be reviewed by the same reviewers, which complicates the review process, increases the risk for rejection and potentially lengthens the review time. If this is a companion paper, please indicate the part number and provide the title, authors and manuscript number (if available) for the companion papers along with your detailed justification for the editor in the comments box below. If there is no justification provided, or if there is insufficient justification, the papers will be returned without review.</p>	No
<p>If this manuscript is intended as part of a Special Issue or Collection, please provide the Special Collection title and name of the guest editor in the comments box below.</p>	No
<p>Recognizing that science and engineering are best served when data are made available during the review and discussion of manuscripts and journal articles, and to allow others to replicate and build on work published in ASCE journals, all reasonable requests by reviewers for materials, data, and associated protocols must be fulfilled. If you are restricted from sharing your data and materials, please explain below.</p>	No
<p>Papers published in ASCE Journals must make a contribution to the core body of knowledge and to the advancement of the field. Authors must consider how their new knowledge and/or innovations add value to the state of the art and/or state of the practice. Please outline the specific contributions of this research in the comments box.</p>	<p>Accurate predictions of the behaviour of RC members subjected to combined loading is essential for optimal design solutions. Only limited analytical models are available for predicting the response of rectangular RC members subjected to combined loading including torsion. This study presents an improved and robust combined actions softened membrane model (CA-SMM) for the analysis of rectangular RC members. In particular, the following advancements are made in the CA-SMM model developed in this study:</p> <ol style="list-style-type: none"> 1. Sophisticated softened membrane based model is adopted for analysing the behaviour of RC members subjected to combined shear and torsion loading. 2. The effect of bi-directional stress (Poisson's effect) is considered in the formulations of CA-SMM for improved post-peak predictions. 3. An improved tension stiffening effect model is used to account for the strain gradient effect. 4. A robust optimization based solution algorithm is proposed for significantly reducing the computational time involved in the analysis of RC members under combined actions including torsion.
<p>The flat fee for including color figures in print is \$800, regardless of the number of color figures. There is no fee for online only color figures. If you decide to not print figures in color, please ensure that the color figures will also make sense</p>	No

<p>when printed in black-and-white, and remove any reference to color in the text. Only one file is accepted for each figure. Do you intend to pay to include color figures in print? If yes, please indicate which figures in the comments box.</p>	
<p>If there is anything else you wish to communicate to the editor of the journal, please do so in this box.</p>	No

Optimization-Based Improved Softened Membrane Model for Rectangular Reinforced Concrete Members under Combined Shear and Torsion

Sriharsha Reddy Kothamuthyala⁽¹⁾, Nikesh Thammishetti⁽²⁾, Suriya Prakash S⁽³⁾,
Chandrika Prakash Vyasarayani⁽⁴⁾

⁽¹⁾ Graduate Student, Email: ce15mtech11023@iith.ac.in
Department of Civil Engineering, IIT Hyderabad, India

⁽²⁾ Ph.D. Candidate, Email: ce16resch11005@iith.ac.in
Department of Civil Engineering, IIT Hyderabad, India

⁽³⁾ Associate Professor and Corresponding Author, Email: suriyap@iith.ac.in
Department of Civil Engineering, IIT Hyderabad, India

⁽⁴⁾ Associate Professor, Email: vcprakash@iith.ac.in
Department of Mechanical and Aerospace Engineering, IIT Hyderabad, India

Abstract

Reinforced concrete (RC) elements are often subjected to combined actions including torsion under seismic events. Understanding the behavior of RC members under combined actions including torsion is essential for safe design. Behavioral predictions of RC columns under combined loading can be improved by including the bi-directional stress effects. The objective of this work is to propose improved combined actions softened membrane model (CA-SMM) for predicting the behavior of RC elements under combined torsion (T) and shear loading (V). In this approach, the rectangular cross-section is modeled as an assembly of four cracked shear panels. The applied external loads are distributed among these four shear panels. This assumption helps in reducing the complex stress state from combined loading to four different simple stress states on these panels. Additional equilibrium and compatibility conditions are imposed, and the system of non-linear equations are solved by using an optimization technique called gradient descent method. The developed improved model (CA-SMM) is validated with the experimental data available in the literature. After that, an interaction between the shear and torsion is developed to understand the behavior under various combinations of torsion and shear. A parametric study is carried out for understanding the effect of various sectional parameters such as longitudinal reinforcement ratio, transverse reinforcement ratio, and concrete strength. The predictions of the improved model had a close correlation with the test results.

Keywords: Combined loading; RC Member; Shear; Softened Membrane Model (SMM); Torsion

35 INTRODUCTION

36 Reinforced concrete (RC) bridge columns are subjected to combined loading including torsion under
37 seismic events. In general, numerous structural elements namely arch ribs, L-shaped bridge columns, and
38 spiral staircases are subjected to combinations of loading. General system of forces and moments acting in
39 RC member subjected to combined loading are shown in Fig. 1. Accurate predictions of the behavior of RC
40 members subjected to combined loading is essential for optimal design solutions. In typical design practices
41 of RC members, the effect of the torsional moment is ignored or indirectly considered in the design.
42 However, previous studies indicate that the presence of torsion during seismic events could significantly
43 affect the performance of the RC members (Tirasit and Kawashima 2007, Prakash et al. 2010, Prakash et
44 al. 2012). Previous researchers have extensively studied predicting the behavior of RC columns subjected
45 to torsional loading analytically through various approaches (Onsongo 1978, Chalioris 2007, Prakash and
46 Belarbi 2010, Belarbi et al. 2010, Deifalla 2015, Mondal et al. 2017). The cyclic torsional behavior of the
47 square and circular RC columns has also been investigated (Li 2012, Chalioris and Karayannis 2013, Li
48 and Belarbi 2013). In the past, only few studies (Klus 1968, Lampert and Thurlimann 1969, McMullen and
49 Warwaruk 1970, Onsongo 1978, Ewida and McMullen 1982, Greene and Belarbi 2009) have
50 experimentally investigated the effect of combined bending moment, shear and torsional loads on the
51 behavior of RC members.

52
53 Noncircular RC members warp under torsional loading (Collins and Mitchell 1997, Hsu 1993, Jeng 2014,
54 Zhang and Hsu 1998; Mullapudi and Ayoub 2013) and pose challenges in developing a rational model
55 under combined loading including torsion. Different analytical models such as softened truss model (STM)
56 from University of Houston (Hsu and Belarbi; Hsu and Zhu 2002; Greene and Belarbi 2009; Mondal and
57 Prakash 2015) and modified compression field theory (MCFT) from University of Toronto (Onsongo 1978;
58 Rahal 1993, Rahal and Collins 1995) were developed. These rational models were based on the principles
59 of mechanics and evolved over the years with increasing sophistication. The present study comes in the
60 purview of studies that include modeling the behavior of cracked concrete using STM developed at the
61 University of Houston. Mondal and Prakash (2015a, 2015b) showed that inclusion of tension stiffening

62 could significantly improve the torque twist prediction using STM. The effect of Poisson's ratio is observed
63 by the researchers and is found to be significant in the prediction of the behavior of RC members. Due to
64 the Poisson effect, the stresses get induced in the direction perpendicular to the direction in which loads are
65 applied. This stress state is known as bi-directional stress state and occurs due to Poisson effect. Zhu and
66 Hsu (2002) proposed a softened membrane model (SMM) including the effect of bi-directional stress states.
67 Jeng and Hsu (2009) proposed a softened membrane model for torsion (SMMT) for rectangular cross
68 sections by considering the effect of strain gradient. The consideration of bi-directional stresses using
69 Poisson's ratio helps in predicting the post-peak behavior accurately (Hsu and Zhu 2002). The fundamental
70 differences between CA-STM and CA-SMM are summarised in Table 1. SMMT was extended to other
71 geometries, and configuration like box girders (Greene and Belarbi 2009), hollow RC members (Jeng and
72 Hsu 2009), and rectangular sections strengthened with fiber reinforced polymer (FRP) composites
73 (Ganganagoudar et al. 2016) under pure torsion. Ganganagoudar et al. (2016) have also extended the SMM
74 based model for torsion (SMMT) for circular members and validated with the experimental test results.

75

76 Previous researchers have developed rational models for analysis of RC members under bending, shear,
77 axial load and their combinations (Rahal and Collins 1995; Mullapudi and Ayoub 2010, 2013). However,
78 combined loading with torsion can result in brittle failure of RC members and calls for deeper understanding
79 and development of improved models. Using MCFT, Rahal and Collins (1995) proposed a theoretical
80 model for predicting the behavior of RC rectangular columns subjected to combined torsion and shear
81 loading. They have modeled the rectangular section as an assembly of four cracked shear panels. The
82 applied loads are distributed among the shear panels in such a way that equilibrium and compatibility
83 conditions are satisfied. The stress states in each shear panels will be different due to different loads acting
84 on it. Greene and Belarbi (2009a, 2009b) developed a softened truss model (STM) based approach for
85 predicting the response of rectangular girder subjected to combined loading. Greene's model is developed
86 based on STM and can predict the behavior until peak load. Also, both the previous MCFT and STM
87 approaches were iterative and ignored the bi-directional stress effects. Recently, Silva et al. (2017) adopted
88 an optimization technique for solving the system of equations for analyzing the behavior of concrete

89 members. Adopting such optimization technique significantly reduces the computation time in the case of
90 multiple variables in the system. Developing a more sophisticated SMM theory for combined loading
91 analysis and solving the system by adopting an optimization technique is the focus of this study.

92

93 **RESEARCH SIGNIFICANCE AND OBJECTIVES**

94 Only limited analytical models are available for predicting the response of rectangular RC members
95 subjected to combined loading including torsion. This study presents an improved and robust combined
96 action softened membrane model (CA-SMM) for the analysis of rectangular RC members. To include the
97 effects of combined actions, the cross-section of the concrete member is modeled as an assembly of four
98 shear panels. The equations satisfying the equilibrium and compatibility conditions between the panels are
99 developed. Solving the nonlinear set of equations using trial and error is tedious especially in the case of
100 combined loading. In this study, an optimization technique namely gradient descent method is adopted to
101 solve the CA-SMM system of non-linear equations rather than conventional trial and error approach. In
102 particular, the following advancements are made in the CA-SMM model developed in this study:

- 103 1. Sophisticated softened membrane based model is adopted for analyzing the behavior of RC
104 members subjected to combined shear and torsion loading.
- 105 2. The effect of bi-directional stress (Poisson's effect) is considered in the formulations of CA-SMM
106 for improved post-peak predictions.
- 107 3. An improved tension stiffening effect model is used to account for the strain gradient effect.
- 108 4. A robust optimization based solution algorithm is proposed for significantly reducing the
109 computational time involved in the analysis of RC members under combined actions including
110 torsion.

111

112 **COMBINED ACTION-SOFTENED MEMBRANE MODEL (CA-SMM)**

113 **Assumptions of the model**

114 The improved CA-SMM model makes the following assumptions for satisfying the equilibrium and
115 compatibility conditions. The assumptions made are related to the modeling of geometry, strain profile, and
116 various material aspects as given below:

- 117 i. The rectangular cross-section is divided into four RC shear panels. The overall distribution of stresses
118 across the section are consolidated into four stress states, and each panel corresponds to a particular
119 stress state.
- 120 ii. The concrete member is assumed to act as a truss after cracking, i.e., concrete in diagonal struts is
121 assumed to resist the compression stresses, steel in longitudinal and transverse directions resist the
122 tensile stresses.
- 123 iii. The externally applied loads on the member are distributed to each of the panels as uniform normal
124 and shear stresses.
- 125 iv. The model neglects the dowel action of the reinforcement and assumes a perfect bond between
126 concrete and reinforcement.
- 127 v. Bredt's thin tube theory is considered for satisfying the torsion equilibrium at the sectional level. In
128 case of solid sections, the core of the member does not contribute to the torsional resistance and
129 therefore, neglected as per this theory.

130 The assumption of a concrete member acting as a truss is valid for a cracked RC member. The behavior of
131 the concrete member is known to be linear until cracking. The stress and strain at cracking can be calculated
132 from the expressions given by Collins and Mitchel (1991). The behavior is linear until cracking, and the
133 post-cracking behavior is predicted using the proposed CA-SMM theory.

134 **The idealization of RC cross-section:**

135 A rectangular RC section can be idealized as a thin-tube, assuming the shear stress due to torsion to be
136 constant over the thickness of the thin-tube. The centreline of the shear flow zone in a rectangular cross-
137 section has dimensions of by b_0 , and a constant thickness of $t_{d,i}$ along each side as shown in Fig. 2. The
138 modeled thickness of each panel is the depth of the shear flow zone t_d in that panel. The width of panels
139 1 and 3 is h_0 , and b_0 for panels 2 and 4. The cross-sectional area of a panel (A_o) is equal to a product of

140 its modeled width and thickness. The idealised b_o , h_o , A_o and p_o are calculated using Eq. 1, formulated by
141 Greene and Belarbi (2009). The panel dimensions used to analyse the cross-section and the cross-sectional
142 area of panel one is shown in Fig. 2.

$$143 \quad b_o = b - \left(\frac{t_{d,1} + t_{d,3}}{2} \right) \quad (1a)$$

$$144 \quad h_o = h - \left(\frac{t_{d,2} + t_{d,4}}{2} \right) \quad (1b)$$

$$145 \quad A_o = b_o h_o \quad (1c)$$

$$146 \quad p_o = 2(b_o + h_o) \quad (1d)$$

147 The longitudinal and transverse reinforcement in the section also has to be distributed among the shear
148 panels. If the sections have symmetrical reinforcement, then longitudinal steel and transverse steel are
149 distributed equally among all the shear panels. The transverse reinforcement is distributed equally among
150 all the shear panels as it is symmetric for all the specimens adopted in the current study. The longitudinal
151 steel area is assigned to that shear panel in which the longitudinal bar is located. In the cases of overlap of
152 steel area between two shear panels, it is distributed as a function of the width of the shear panels that are
153 overlapping. A detailed account of the distribution of longitudinal reinforcement can be obtained from
154 Greene and Belarbi (2009).

155

156 **Equilibrium equations**

157 The applied external loads are distributed as normal, and shear stresses on the membrane element. Fig. 3
158 depicts the stress state at the element level. The normal stresses are distributed among the concrete and steel
159 components of membrane element. The principle of transformation is used for determining the stresses in
160 principal directions 1 and 2, making an angle α_i with l -direction. It is worth mentioning that SMM is based
161 on fixed angle theory. More details on fixed angle theory can be found elsewhere (Hsu and Zhu 2002,
162 Ganganagoudar et al. 2016). The cracks are assumed to occur in the principal directions of RC composite
163 element. The crack angle in the concrete element will be different as it is subjected to shear stresses. The
164 equilibrium equations (Eqs. 2-4) of membrane element can be derived using the principle of transformation.

165 The planes of primary interest in the membrane element are the principal planes (1-2 planes) and the planes
 166 in which loads are applied (L-T planes), as shown in the Fig. 3.

167

$$168 \quad \sigma_{l,i} = \sigma_{2c,i} \cos^2 \alpha_i + \sigma_{1c,i} \sin^2 \alpha_i + 2\tau_{12c,i} \sin \alpha_i \cos \alpha_i + \rho_l f_l \quad (2)$$

$$169 \quad \sigma_{t,i} = \sigma_{2c,i} \sin^2 \alpha_i + \sigma_{1c,i} \cos^2 \alpha_i - 2\tau_{12c,i} \sin \alpha_i \cos \alpha_i - \rho_t f_t \quad (3)$$

$$170 \quad \tau_{lt,i} = \left((-\sigma_{2c,i} + \sigma_{1c,i}) \sin \alpha_i \cos \alpha_i + \tau_{12c,i} (\cos^2 \alpha_i - \sin^2 \alpha_i) \right) \cdot \text{sign}(q_i) \quad (4)$$

171

172 The shear flow due to torsional loading is constant along the cross-section. The applied shear loads are
 173 distributed in accordance with the direction of load application as shown below in the Fig. 4. The shear load
 174 is added to loads on one of the panels and is subtracted from the other panel due to combined shear and
 175 torsion loading (Fig. 4). Eq. 5 (Rahal and Collins 1995, Greene and Belarbi 2009) gives the net shear flow
 176 (q_i) in each panel.

$$177 \quad q_1 = \frac{T_x}{2A_0} + \frac{V_y}{2h_0} \quad (5a)$$

$$178 \quad q_2 = \frac{T_x}{2A_0} + \frac{V_z}{2b_0} \quad (5b)$$

$$179 \quad q_3 = \frac{T_x}{2A_0} - \frac{V_y}{2h_0} \quad (5c)$$

$$180 \quad q_4 = \frac{T_x}{2A_0} - \frac{V_z}{2b_0} \quad (5d)$$

181

182 **Bredt's thin tube theory:**

183 When torsion acts on an RC member, it induces shear stress within the member. Bredt's thin tube theory
 184 assumes that the applied torsion is resisted by the shear stresses developed across a tube of thickness known
 185 as shear flow depth. The elastic shear stress distribution varies linearly across the section with maximum
 186 stress at the surface and reaches zero at the center. However, Bredt's thin tube theory assumes the stress
 187 distribution to be constant across the depth of thin tube as shown in Fig. 5. The relation between the external
 188 torque and shear flow is given by Bredt's thin tube theory, as in Eq 6.

$$T_x = q \left[2 \left(\frac{b_0}{2} h_0 + \frac{h_0}{2} b_0 \right) \right] \quad (6a)$$

From the Fig. 6 (Hsu 1993), the integration around the cross section gives twice the area inscribed by shear flow region:

$$\left[2 \left(\frac{b_0}{2} h_0 + \frac{h_0}{2} b_0 \right) \right] = 2A_0$$

$$T_x = 2A_0 q \quad (6b)$$

Compatibility equations:

The equations of compatibility (Eqs. 7-10) are derived using the principle of transformation (Hsu and Zhu 2002). In-plane strain compatibility should be satisfied for all the membrane elements.

$$\varepsilon_{l,i} = \varepsilon_{2,i} \cos^2 \alpha_i + \varepsilon_{1,i} \sin^2 \alpha_i + \gamma_{12,i} \sin \alpha_i \cos \alpha_i \quad (7)$$

$$\varepsilon_{t,i} = \varepsilon_{2,i} \sin^2 \alpha_i + \varepsilon_{1,i} \cos^2 \alpha_i - \gamma_{12,i} \sin \alpha_i \cos \alpha_i \quad (8)$$

$$\gamma_{LT,i} = (2(-\varepsilon_{2,i} + \varepsilon_{1,i}) \sin \alpha_i \cos \alpha_i + \gamma_{12,i} (\cos^2 \alpha_i - \sin^2 \alpha_i)) \cdot \text{sign}(q_i) \quad (9)$$

$$\varepsilon_{t,i} = \varepsilon_{2,i} + \varepsilon_{1,i} - \varepsilon_{l,i} \quad (10)$$

The equations of compatibility are derived at the section level by imposing the strain compatibility requirement at the center of the cross-section. It is assumed that shear stress due to combined shear flows from an applied torsion and shear acts as a uniformly distributed shear stress, τ_{LT} , over the thickness of the shear flow zone. Eq. 11 gives the curvature of the concrete strut of each panel.

$$\Psi_i = \frac{-\overline{\varepsilon_{2s,l}}}{t_{d,i}} \quad (11)$$

The thickness of shear flow zone ($t_{d,i}$) is calculated using a simplified expression given by Ganganagouadar et al. (2016), as given below

$$t_{d,i} = \frac{-\overline{\varepsilon_{2s,l}}}{\Psi_i} \quad \left(\leq \frac{b_0}{2} \right) \quad (12a)$$

$$\Psi_i = \theta \sin(2\alpha_i) \quad (12b)$$

$$H_i = \frac{4\bar{\varepsilon}_{2,i}}{\gamma_{LT,i}\sin(2\alpha_i)} \quad (12c)$$

$$t_{d,i} = \frac{1}{2(H+4)} \left[P_c \left(1 + \frac{H}{2} \right) - \sqrt{\left(1 + \frac{H}{2} \right)^2 - 4H(H+4)A_c} \right] \quad (12d)$$

$$\text{where} \quad \theta = \left[(\gamma_{LT,1} + \gamma_{LT,3})h_0 + (\gamma_{LT,2} + \gamma_{LT,4})b_0 \right] \frac{1}{2A_0} \quad (13)$$

The calculated shear flow depth $t_{d,i}$ should be limited to the thickness of the wall in the case of hollow specimen and should be limited to half of the depth of the idealized cross-section $\left(\frac{b_0}{2}\right)$ in the case of solid cross-sections.

218

219 **Constitutive laws:**

220 The constitutive laws shown in Fig. [7, 8] are adopted in this study. The constitutive laws used in this study
 221 are developed based on flat panels which are a 2D element (Vecchio and Collins 1986, Hsu 1993) and
 222 includes the effects of softening and tension stiffening. Torsion is a 3-dimension problem. However, these
 223 constitutive laws are the current state of the art. The evaluation of constitutive laws for a 3-dimension panel
 224 is recently investigated by Labib et al. (2017). These constitutive laws for compression and tension based
 225 on a warped 3-dimension panel, Poisson effect on these 3-D panels and their application for torsion are not
 226 fully understood yet and is scope for further work.

227

228 **Concrete in compression:**

229 The presence of tensile cracks in principle compression plane causes softening of concrete struts. The
 230 softening coefficient (ζ) of concrete is a function of principle tensile strain (Vecchio and Collins 1986),
 231 compressive strength (Zhang and Hsu 1998) and deviation angle (β). The softening co-efficient used by
 232 Jeng and Hsu (2009), that accounts for all the above effects has been used in the present study. The concrete
 233 compression law has been given in Eq. 14.

$$\beta_i = \frac{1}{2} \left[\tan^{-1} \left(\frac{\gamma_{12c,i}}{\varepsilon_{2c,i} - \varepsilon_{1c,i}} \right) \right] \quad (14a)$$

234

$$\zeta_i = \frac{5.8}{\sqrt{f_c'}} \frac{0.9}{\sqrt{1+400\bar{\varepsilon}_{2c,i}}} \left(\frac{1-\beta_i}{24^0} \right) \quad (14b)$$

$$\sigma_{2c,i} = K_{2c,i} \zeta f_c' \quad (14c)$$

$$K_{2c,i} = \left[\frac{\bar{\varepsilon}_{2s,i}}{\zeta_i \varepsilon_0} - \frac{\varepsilon_{2s,i}^2}{3(\zeta_i \varepsilon_0)^2} \right] \quad \text{for } \frac{\bar{\varepsilon}_{2s,i}}{\zeta_i \varepsilon_0} \leq 1 \quad (14d)$$

$$K_{2c,i} = 1 - \frac{\zeta_i \varepsilon_0}{3\bar{\varepsilon}_{2s,i}} - \frac{1}{3\bar{\varepsilon}_{2s,i}} \left[\frac{(\bar{\varepsilon}_{2s,i} - \zeta_i \varepsilon_0)^3}{(4\varepsilon_0 - \zeta_i \varepsilon_0)^2} \right] \quad \text{for } \frac{\bar{\varepsilon}_{2s,i}}{\zeta_i \varepsilon_0} \geq 1 \quad (14e)$$

239 Concrete in tension:

240 The current study employs the tension stiffening relation used by Jeng and Hsu (2009) for modeling the
241 tension behavior of concrete. Fig. 9 shows the tension constitutive law of the concrete.

$$242 \quad f_{cr} = 0.652 \sqrt{f_{ck}} \quad (15a)$$

$$243 \quad E_c = 5620 \sqrt{f_{ck}} \quad (15b)$$

$$244 \quad \sigma_{1c,i} = E_c \bar{\varepsilon}_{1,i} \quad \text{for } \frac{\bar{\varepsilon}_{1s}}{\varepsilon_{cr}} \leq 1 \quad (15c)$$

$$245 \quad \sigma_{1c,i} = f_{cr} \left(\frac{\varepsilon_{cr}}{\bar{\varepsilon}_{1,i}} \right)^{0.4} \quad \text{for } \frac{\bar{\varepsilon}_{1s}}{\varepsilon_{cr}} \geq 1 \quad (15d)$$

246

247 Stress-strain relationship of steel:

248 The smeared stress-strain behavior of steel embedded in concrete as adopted by Jeng (2009) and
249 Ganganagoudar et al. (2016) in the previous SMMT formulations is used in the present study (Fig. 9). In
250 the below equations, $f_{s,i}$ represents both longitudinal and transverse steel.

$$251 \quad f_{s,i} = E_s \bar{\varepsilon}_{l,i} \quad \text{for } \bar{\varepsilon}_{l,i} \leq \bar{\varepsilon}_{ln,i} \quad (16a)$$

$$252 \quad f_{s,i} = \left[(0.91 - 2B_i) + (0.02 + 0.25B_i) \frac{\bar{\varepsilon}_{l,i}}{\varepsilon_{ly}} \right] \quad \text{for } \bar{\varepsilon}_{l,i} \leq \bar{\varepsilon}_{ln,i} \quad (16b)$$

$$253 \quad B_i = \left[\frac{(f_{cr}/f_{ly})^{1.5}}{\rho_i} \right] \quad (16c)$$

254
$$\overline{\varepsilon_{ln,i}} = \varepsilon_{ly} (0.93 - B_i) \quad (16d)$$

255

256 **The constitutive relation for concrete in shear**

257 The shear modulus is expressed as a function of normal stresses and strains in concrete element. The
 258 relation is given in Eq. 17.

259
$$\tau_{12c,i} = \frac{(-\sigma_{2c,i} + \sigma_{1c,i})}{2(\varepsilon_{1,i} - \varepsilon_{2,i})} \gamma_{12c,i} \quad (17)$$

260

261 **Poisson's effect in SMMT:**

262 Stresses in one direction can result in the development of stresses in its perpendicular direction due to
 263 Poisson's effect. This Poisson's ratio is considered in the formulation of CA-SMM. The strain in one
 264 direction is not only a function of stress in its direction but will also depend on the stress in its perpendicular
 265 direction. Zhu and Hsu (2002) investigated the Poisson's ratio of shear panels experimentally and proposed
 266 a parameter called Hsu/Zhu ratio, which quantifies the bi-directional stress effect. Hsu/Zhu ratio relates the
 267 strains and bi-directional stresses as given in equation 17.

268

269
$$\varepsilon_1 = \frac{\sigma_{1c}}{E_{1c}} - \nu_{12} \frac{\sigma_{2c}}{E_{2c}} \quad (17a)$$

270
$$\varepsilon_2 = \frac{\sigma_{2c}}{E_{2c}} - \nu_{21} \frac{\sigma_{1c}}{E_{1c}} \quad (17b)$$

271 where

272
$$\nu_{12} = (0.16 + 680\varepsilon_{sf}) \quad \text{for } \varepsilon_{sf} \leq \varepsilon_y \quad (18a)$$

273
$$\nu_{12} = 1.52 \quad \text{for } \varepsilon_{sf} \geq \varepsilon_y$$

274
$$\nu_{21} = 0 \quad (18b)$$

275

276 Here, v_{12} is the strain increment in direction 1 for an applied unit strain in direction 2. Now, defining
 277 uniaxial strains as $\bar{\varepsilon}_1 = \frac{\sigma_{1c}}{E_{1c}}$ and $\bar{\varepsilon}_2 = \frac{\sigma_{2c}}{E_{2c}}$ and re-writing the equation (17), the relation between uniaxial
 278 strains and biaxial strains can be arrived.

$$279 \quad \varepsilon_1 = \bar{\varepsilon}_1 - v_{12}\bar{\varepsilon}_2 \quad (19a)$$

$$280 \quad \varepsilon_2 = \bar{\varepsilon}_2 - v_{21}\bar{\varepsilon}_1 \quad (19b)$$

281 After re-arranging the equations (19), one can get

$$282 \quad \bar{\varepsilon}_1 = \frac{\varepsilon_1}{(1-v_{12}v_{21})} + \frac{v_{12}\varepsilon_2}{(1-v_{12}v_{21})} \quad (20a)$$

$$283 \quad \bar{\varepsilon}_2 = \frac{v_{21}\varepsilon_2}{(1-v_{12}v_{21})} + \frac{\varepsilon_1}{(1-v_{12}v_{21})} \quad (20b)$$

284 The constitutive law of material relates stresses and uniaxial strains as given by equation (18).

285

286 **OPTIMIZATION BASED GRADIENT DESCENT METHOD**

287 An alternative and efficient procedure to the conventional trial and error method is used for solving the
 288 system of equilibrium and compatibility equations in CA-SMM. Gradient descent method is a first-order
 289 iterative optimization algorithm for finding the minimum of a multi-variable function. To solve for the local
 290 minimum of a function, the subsequent iterations take steps in a direction negative to the gradient of the
 291 function at the current point. The solution algorithm is described in detail in the following sections.

292

293 **Primary Variables**

294 The primary variables are the variables that are varied numerically until the objective functions are set to
 295 zero. In the proposed algorithm, the primary variables are T_x , $\varepsilon_{2s,j}$, $\varepsilon_{1,i}$, and $\gamma_{12,i}$ ($j = 2,3,4$ and $i = 1,2,3,4$).
 296 $\varepsilon_{2s,1}$ of panel 1 is fixed for each step and is incremented until a concrete failure strain of -0.0035. The
 297 primary variable $\varepsilon_{2s,j}$ is varied until the shear stresses $F_{CASMM}(j)$ ($j=2,3,4$) of Eq. 21 are in agreement. The
 298 equilibrium Eq. 2- 3 are summed and subtracted to get the set of objective functions $F_{CASMM}(i + 8)$ and
 299 $F_{CASMM}(i + 12)$, whose primary variables are chosen as $\varepsilon_{1,i}$ and $\gamma_{12,i}$, respectively.

300

301 **Residual Equations and Objective function**

302 The set of equations of the model that has to be solved are developed from the equilibrium and compatibility
 303 conditions as explained in earlier sections. This set of equations that has to be solved are called residual
 304 equations as given in Eq. 21.

$$305 \begin{bmatrix} F_{CASMM}(1) \\ F_{CASMM}(j) \\ F_{CASMM}(i+8) \\ F_{CASMM}(i+12) \end{bmatrix} = \begin{bmatrix} \tau_{lt,1} - q_1/t_{d,1} \\ \tau_{lt,j} - q_j/t_{d,j} \\ (\rho_l f_l + \rho_t f_t)_i - ((\sigma_{l,i} + \sigma_{t,i}) - (\sigma_{2c,i} + \sigma_{1c,i})) \\ (\rho_l f_l - \rho_t f_t)_i - ((\sigma_{l,i} - \sigma_{t,i}) - (\sigma_{2c,i} - \sigma_{1c,i}) \cos 2\alpha_i + 2\tau_{12c,i} \sin 2\alpha_i) \end{bmatrix} \quad (21)$$

306 The above set of equations are compactly represented as $\mathbf{f}(\mathbf{x}) = 0$.

307 where \mathbf{x} is a vector of primary variables taken as $\mathbf{x} = \{T_x, \varepsilon_{2s,j}, \varepsilon_{1,i}, \gamma_{12,i}\}$. (where $j = 2,3,4$ and $i = 1,2,3,4$). In
 308 conventional way of solving, the function $\mathbf{f}(\mathbf{x})$ is solved by trial and error way of varying primary variables. It
 309 is very tedious and time consuming. In the present study, the set of equations of the model are solved by
 310 adopting an optimisation technique (Gradient descent method). Instead by directly solving for $\mathbf{f}(\mathbf{x}) = 0$, we
 311 will minimise the objective function “ J ”. The objective function “ J ” is the norm of the function $\mathbf{f}(\mathbf{x})$, as defined
 312 in Eq. 22.

$$313 \quad J = \frac{1}{2} (\mathbf{f}^T(\mathbf{x}) \cdot \mathbf{f}(\mathbf{x})) \quad (22)$$

314 The scalar output given by the objective function at every step is called a residue. The residue is zero only when
 315 each of the residual functions $f_1(\mathbf{x}), f_2(\mathbf{x}) \dots f_{12}(\mathbf{x})$ is zero. The value of primary variables gets updated for
 316 each step as per gradient descent method as given in Eq. 23.

$$317 \quad \mathbf{x}^+ = \mathbf{x}^- - \gamma \frac{\partial J}{\partial \mathbf{x}} \quad (23)$$

318 where γ is chosen as a small incremental decimal value such that $J(\mathbf{x}^+) < J(\mathbf{x}^-)$.

319 The characteristic of residue (J) at a fixed value of $\overline{\varepsilon}_{2s,1}$ for specimen tested by Klus (1968) is shown in
 320 Fig. 10, till the objective function reaches a tolerable value. The tolerance for Klus specimen has been set
 321 a value of $1e^{-3}$ after 5700 steps (Fig. 10). By moving towards the minimum of the objective function (J)

322 at each step, the residue (J) decreases. The optimal minimum solution within the tolerant limits is obtained
323 by minimising the objective function.

324

325 **Solution procedure**

326 The proposed solution algorithm is explained in Fig. 11. The solution algorithm is executed using a program
327 developed and executed in the software MATLAB. The geometry of the member cross-section, the
328 equivalent longitudinal and transverse reinforcement in each panel, the mechanical properties for the
329 concrete and steel, the ratios of the internal acting forces to the torsional moment (N_x/T_x , V_y/T_x , V_z/T_x)
330 and the initial strain $\varepsilon_{2s,1}$, are known or assumed to start with. The unknown variables T_x , $\varepsilon_{2s,j}$, $\varepsilon_{1,i}$, and
331 $\gamma_{12,i}$ ($j = 2,3,4$ and $i = 1,2,3,4$) are determined by solving the nonlinear system of twelve equations $\mathbf{f}(\mathbf{x}) =$
332 0 . For these system of equations, the residue of the objective function (J) should be within an acceptable
333 tolerance. This is formulated as a nonlinear least-squares problem, where F_{CA-SMM} , Eq. (21) are the residual
334 equations.

335

336 **EXPERIMENTAL VALIDATION**

337 The proposed solution algorithm is validated using experimental data obtained from the literature. Prakash
338 et al. (2010, 2012) conducted experiments on RC columns subjected to torsion. Li (2013) tested square
339 columns with torsion and axial loads. Columns tested by Prakash and Belarbi (2010) and Li et al. (2013)
340 are denoted as Missouri columns. Rahal and Collins (1993) and Klus (1968) tested RC beams under
341 combined torsion and shear loading. The data of following RC members are used in validation of the CA-
342 SMM model proposed in this study: Missouri-1 (Pure Torsion); Missouri 2 (Torsion + Axial); one RC
343 square girder of Greene (Pure Torsion); two beams tested by Rahal and Collins (Torsion + Shear + Axial)
344 and three beams tested by Klus (one in Pure Torsion and two in Torsion + Shear). The details of all these
345 specimens are given in Table 2. Cross sections of specimens are shown in Fig. 12.

346

347 **Torque – Twist Behavior:**

348 The torque-twist behavior of the specimens under different load combinations is shown in Fig. 13. The
349 behavior is linear until cracking. The stiffness reduces considerably after the peak torque. The peak torque
350 and the corresponding twist are captured reasonably well by the CA-SMM. The proposed model predicted
351 the peak torque and twist more accurately for the specimen of Missouri, Rahal, and Collins while the results
352 of CA-STM are close to experimental peak values of Greene's and Klus specimen. However, it can be
353 observed from the Table 3 that the predictions in the peak torque and peak twist predictions of CASTM and
354 CASMM are very close. The observed behavior until cracking is similar to the torsional response of plain
355 concrete elements as observed by Karayannis and Chalioris (2013). Comparison of predictions is provided
356 in Table 3 and Table 4. Table 3 presents the comparison of values of peak torque and twist values. Table 4
357 presents the comparison of values of ultimate torque and corresponding ultimate twist values. It is evident
358 that the response predicted by the CA-SMM is better in the post-cracking regime and close to the
359 experimental peak values. It is observed that due to consideration of bi-axial stress effects, CA-SMM
360 predicts the ultimate torque values with fair accuracy. The ultimate twist values predicted by the CA-SMM
361 are close to experimental values. Specimens considered for analysis had the following failure progression:
362 shear cracking followed by yielding of transverse reinforcement and the longitudinal reinforcement
363 respectively. All the specimens finally failed by crushing of the concrete under diagonal compression. The
364 same failure progression was observed in the predictions of CA-SMM. The strain distribution in the steel
365 for the specimens is shown in Figs. [14-15]. The parametric study also depicts that the effect of transverse
366 steel on torsional behavior is very significant when compared to any other sectional parameters.

367

368 **Distribution of Strains in Reinforcement:**

369 Predictions of behavior at the local level, i.e. the distribution of strains in reinforcement are analyzed using
370 CA-SMM. Variation of strain in longitudinal and of transverse steel reinforcement with change in applied
371 torque are presented in Figs. 14 &15. It is worth mentioning that the strains predicted by the model are
372 smeared strains. The strains are calculated as an average of all the strains smeared across the number of
373 cracks. Before the onset of cracking in the concrete, the contribution from reinforcement is negligible. After
374 cracking, steel reinforcement gets engaged and starts contributing to the load resistance. Moreover, the

375 transverse reinforcement is known to be a prime contributor in resisting shear, and torsional loads and the
376 same is reflected in the predictions (Figs. 14,15). It can be observed that at any given loading level, the
377 strains in the transverse steel reinforcement is higher than that of strains in the longitudinal steel. Due to
378 unavailability of experimental data pertaining to the longitudinal and transverse strains, only the analytical
379 predictions are presented in the Fig. [14-15]. When the section is subjected to the combined loading of
380 torsion and shear as shown in the direction as represented in Fig. 4, the shear flow due to torsion and shear
381 gets added up in panel 3 and gets subtracted in panel 1. The shear flow in the panels 2 and 4 are only due
382 to torsion and are not affected by the applied shear in Y-direction. It is due to this difference in the shear
383 flow that the strains are different in each of the panels for the specimen that are loaded with torsion and
384 shear (Fig. 15). The strains predicted by the model are observed to be increasing smoothly with an increase
385 in the level of torsional loading. Steel in the transverse direction is the key component of resisting shear
386 and torsion. It is expected typically that the strains in the transverse direction increase till the loading
387 reaches peak value and decreases after that (Ganganagoudar et al. 2016, Prakash et al. 2012). The model
388 is capable of capturing the same trend of strain variations in accordance with the expectation, that in Fig.
389 15 the transverse strains were increasing smoothly till the peak load is reached and decreased after that.

390

391 **The interaction between torsion and shear loads**

392 The torsion and shear loads are distributed as shear stresses at the element level. Therefore, the presence of
393 any external shear loads directly influences the shear flow (q_i) of the cross-section. The presence of shear
394 load either increases or decreases the shear flow in the panels depending on its direction of application. The
395 effect of shear load and torsion on shear flow has been quantified through Eq. (5). The developed algorithm
396 has been used for developing these interaction diagrams of torsion and shear. Fig. 16 depicts the validation
397 of predicted interaction with that of the experimental data of specimens tested by Rahal and Collins and
398 Klus. The results predicted by the algorithm are in good agreement with the experimental results.

399

400 **Parametric studies using CA-SMM**

401 The effect of transverse reinforcement ratio (ρ_t), longitudinal reinforcement ratio (ρ_l) and concrete strength
402 (f_{ck}) on the behavior of specimens are investigated by carrying out a detailed parametric study and shown
403 in Fig. 16. The torsion shear interaction curves are plotted for the Rahal and Collins series 2 specimen by
404 varying the parameters (ρ_l, ρ_t and f_{ck}). Torsion (T) and shear (V) interaction curves are presented in Fig.
405 16. Transverse reinforcement is a key element in resisting the shear loads. Therefore, the increase in
406 transverse reinforcement ratio directly increases the torsional capacity of the specimen. The parametric
407 study of varying concrete compressive strength and longitudinal reinforcement ratio for predicting the
408 torsion shear interaction is also presented in Fig. 16. The variation in torsional capacity with respect to the
409 variation of longitudinal reinforcement is observed to be marginal and insignificant.

410

411 **SUMMARY AND CONCLUSIONS**

412 A robust algorithm is used in this study for predicting the behavior of RC members subjected to different
413 combinations of torsion, shear and axial loads. The set of equations of CA-SMM are employed by modeling
414 the geometry of section as an assembly of four shear panels. The accuracy in predictions can be improved
415 by increasing the number of panels and by establishing compatibility conditions among the panels, but this
416 occurs at the cost of a significant increase in computation time. Also, the inclusion of bending effects
417 (Ewida and McMullen 1981, Rahal 2007) and prestress effects (Karayannis et al. 2000) would also be
418 interesting. The bending effects can be included by altering the longitudinal strain variable in the solution
419 algorithm and is scope for future work. It is also to be noticed that the constitutive laws adopted in the
420 model are derived based on 2-dimensional flat panels. Since torsion is a 3-dimensional problem, it causes
421 the walls of the member to warp. However, the constitutive laws for warped 3-dimensional elements are
422 not established yet. Currently researchers (Labib et al., 2017) are focusing in the direction to establish the
423 constitutive laws of concrete based on 3-dimensional panels. It is referred to future work that the results
424 can be refined accurately by adopting constitutive laws that are developed based on a 3-dimensional panel.
425 Based on the results presented in this study, the following major conclusions can be drawn:

- 426 1. An improved analytical model is proposed for predicting the response of the RC rectangular members
427 using softened membrane model at the element level analysis. The predictions from the analytical
428 model were in agreement with the experimental results.
- 429 2. For combined shear and torsional loading, the inclusion of Poisson's effect and strain gradient effect
430 resulted in improved torque twist predictions and strain variations in the reinforcement.
- 431 3. Transverse reinforcement plays a key role in improving the overall torque – twist performance of RC
432 members under combined torsion and shear loading. It is observed that the reinforcements in panel 3
433 (torsion and shear as additive) experienced higher strain levels than the other individual panels.
- 434 4. A detailed parametric investigation considering the effect of concrete strength and various steel
435 reinforcement ratio under combined shear and torsion loading was carried out. Results indicate that the
436 transverse reinforcement plays a major role in the load resistance when compared to longitudinal
437 reinforcement ratio and concrete strength under all combinations of torsion and shear loading.

438 **Acknowledgements**

439 This analytical work is carried out as part of the project funded by SERB, Department of Science and
440 Technology, India. Grant No. SB/S3/CEE/0060/2013 and FAST center of excellence for sustainable
441 development at IIT Hyderabad. Their financial support is gratefully acknowledged.

442

443 **Notations:**

444 *The notations used in the paper are:*

A_l	The total cross-section area of longitudinal steel bars
A_t	The cross-section area of transverse steel bar
A_o	The core area of the idealized cross-section
B	Variable as defined in the constitutive relation of steel bar
b	Breadth of the actual cross-section
b_o	Breadth of the idealised cross-section
E_c	Modulus of elasticity of concrete
E_s	Modulus of elasticity of steel

$f_{l,i}, f_{t,i}$	Stress in Longitudinal steel and transverse steel
f_y	Yield strength of steel bar
f'_c	Cylinder compressive strength of concrete
f_{cr}	Cracking stress of concrete
H_i	A variable to calculate shear flow depth
h	Depth of the actual cross-section
h_o	Depth of the idealized cross-section
$K_{2c,i}$	Ratio of average compressive stress to peak compressive stress in concrete struts
P_o	Perimeter of the idealized cross-section
q_i	Shear flow force in i^{th} panel
r_o	Radius or perpendicular distance from centre to centre of shear flow region
s	Spacing of transverse steel bars
T_x	Applied Torsion with respect to X-direction
$t_{d,i}$	Shear flow depth of i^{th} panel
V_y, V_z	Applied Shear force in Y and Z directions
α_i	Cracking angle of i^{th} panel of RC element
β_i	Deviation angle of i^{th} panel
$\varepsilon_{l,i}, \varepsilon_{t,i}$	Strain along longitudinal and transverse directions
$\overline{\varepsilon}_{l,i}, \overline{\varepsilon}_{t,i}$	Smeared uniaxial strain in L and T directions respectively
$\varepsilon_{1,i}, \varepsilon_{2,i}$	Principle tensile strain and Principle compressive strains
$\overline{\varepsilon}_{2s,i}, \overline{\varepsilon}_{1s,i}$	Smeared uniaxial strain in 1 and 2 directions respectively at centre of shear flow zone.
$\overline{\varepsilon}_{2s,l}, \overline{\varepsilon}_{1s,l}$	Smeared uniaxial strain in 1 and 2 directions respectively at top surface of strut.
$\gamma_{12,i}$	Shear strain in 1 and 2 coordinate system
ρ_l, ρ_t	Ratio of Longitudinal steel and transverse steel
Ψ_i	Curvature of strut
θ	Twist per unit length of the member
ζ_i	Softening co-efficient of concrete in compression
v_{12}, v_{21}	Hsu/Zhu ratios
$\sigma_{l,i}$	Longitudinal Normal stress in i^{th} panel in RC element

$\sigma_{t,i}$	Transverse Normal stress in i^{th} panel in RC element
$\sigma_{2c,i}, \sigma_{1c,i}$	Smearred Normal stresses on concrete element in directions 1 and 2
$\tau_{lt,i}$	Shear stress in i^{th} panel in RC element
$\tau_{12c,i}$	Smearred Shear stress on concrete element in 1 and 2 coordinate system

445

446 **References:**

447

448 Belarbi, A., Prakash, S.S., and Silva, P.F. (2010). "Incorporation of decoupled damage index models in the
449 performance-based evaluation of RC circular and square bridge columns under combined loadings", *ACI*
450 *Special Publication-SP271*, Vol. 271, 2010, Pages 79-102

451 Chalioris, C. E. (2007). "Analytical model for the torsional behavior of reinforced concrete beams
452 retrofitted with FRP materials". *Engineering Structures*, 29(12), 3263-3276.

453 Chalioris, C. E., and Karayannis, C. G. (2013). "Experimental investigation of RC beams with rectangular
454 spiral reinforcement in torsion". *Engineering Structures*, 56, 286-297

455 Collins, M.P. and Mitchell, D. (1991), "Prestressed Concrete Structures", Response Publications, Canada.

456 Deifalla, A. (2015). "Torsional behavior of rectangular and flanged concrete beams with FRP
457 reinforcements". *Journal of Structural Engineering, ASCE*, 141(12), p.04015068.

458

459 Ewida, A. A., and McMullen, AE. (1982). "Concrete members under combined torsion and shear." *Journal*
460 *of the Structural Division, ASCE*, 108.4: 911-928.

461

462 Ewida, A. A., and A. E. McMullen. (1981). "Torsion–shear–flexure interaction in reinforced concrete
463 members." *Magazine of Concrete Research* 33.115 113-122.

464

465 Ganganagoudar A, Mondal, TG., and Prakash, S.S., (2016). "Analytical and Finite Element Studies on
466 Behavior of FRP Strengthened Beams under Torsion" *Composite Structures*, Volume 153, 1 October 2016,
467 Pages 876–885.

468 Ganganagoudar A, Mondal, TG., and Prakash, SS., (2016). "Improved Softened Membrane Model for
469 Reinforced Concrete Circular Bridge Columns under Torsion" *Journal of Bridge Engineering, ASCE*, Vol.
470 21, Issue 7 (July 2016), Pages 1-12. DOI: 10.1061/(ASCE)BE.1943-5592.0000907.

471 Greene GG., and Belarbi, A., (2009). "Model for Reinforced Concrete Members under Torsion, Bending
472 and Shear. I: Theory". *Journal of Engineering Mechanics* 135, ASCE, No. 9, 961-969.

473

474 Greene GG., and Belarbi, A., (2009). "Model for Reinforced Concrete Members under Torsion, Bending
475 and Shear. II: Model Application and Validation", *Journal of Engineering Mechanics* 135, ASCE, No.9,
476 970-977.

477

478 Hsu, T. T., and Zhu, R. R., (2002). "Softened membrane model for reinforced concrete elements in shear."
479 *ACI Structural Journal.*, 99(4), 460–469.

480

481 Hsu, T. T. C., (1993). "Unified Theory of Reinforced Concrete", CRC Press, Florida, 313 pp.

482

483 Jeng, C. H., and Hsu, T. T., (2009). "A softened membrane model for torsion in reinforced concrete
484 members." *Engineering Structures Journal*, 31(9), 1944–1954.

485 Jeng, C.H., (2014). "Unified softened membrane model for torsion in hollow and solid reinforced concrete
486 members: modeling precracking and postcracking behavior." *Journal of Structural Engineering*,
487 *ASCE*, 141(10), p. 04014243.

488 Karayannis, Chris G., and Constantin E. Chalioris. (2000). "Strength of prestressed concrete beams in
489 torsion." *Structural Engineering and Mechanics* 10.2, 165-180.

490

491 Klus, J., (1968). "Ultimate Strength of Reinforced Concrete Beams in Combined Torsion and Shear," *ACI*
492 *Journal Proceedings*, V. 65, No. 3, pp. 210-216.

493

494 Lampert, P. and Thürlimann, B., (1969). "Torsion-Bending Tests of Reinforced Concrete Beams," *Report*
495 *No. 6506-3*, Intitut für Baustatik, ETH, Zurich, 116 pp., 1969.

496 Li, Q., (2012), "Performance of RC Bridge Columns under Cyclic Combined Loading including Torsion".
497 *Ph.D. thesis* Department of Civil Engineering, University of Houston, 374 pages.

498 Li, Q. and Belarbi A., (2013), "Damage assessment of square RC bridge columns subjected to torsion
499 combined with axial compression, flexure, and shear." *KSCE Journal of Civil Engineering*, Volume 17,
500 Issue 3, pp 530–539.

501 MATLAB. [Computersoftware]. MathWorks, Natick, MA.

502

503 Mondal, T. G., and Prakash, S. S., (2015a). "Effect of tension stiffening on the behavior of reinforced
504 concrete circular columns under torsion." *Engineering. Structures Journal.*, 92, 186–195.

505

506 Mondal, T. G., and Prakash, S. S., (2015b). "Nonlinear finite-element analysis of RC bridge columns under
507 torsion with and without axial compression." *Journal of. Bridge Engineering, ASCE.*,
508 10.1061/(ASCE)BE.1943 -5592.0000798, 04015037.

509

510 Mondal, T. G., and Prakash, S. S., (2015), "Effect of tension stiffening on the behavior of square RC
511 columns under torsion." *Struct. Eng. Mech. J* 54.3, 501-520.

512

513 Mondal, T.G. and Prakash, S.S., (2015). "Improved softened truss model for RC circular columns under
514 combined torsion and axial compression". *Magazine of Concrete Research*, 67(16), pp.855-866.

515

516 Mondal, T. G., Kothamuthyala, S. R, Prakash, S.S., (2017). "Hysteresis modeling of reinforced concrete
517 columns under pure cyclic torsional loading." *Structural engineering and mechanics*, 64(1), 11-21.

518 Mullapudi, T.R. and Ayoub, A., (2010). "Modeling of the seismic behavior of shear-critical reinforced
519 concrete columns." *Engineering Structures*, 32(11), pp. 3601-3615.

520 Mullapudi, T.R.S., and Ayoub, A., (2013). "Analysis of reinforced concrete columns subjected to combined
521 axial, flexure, shear, and torsional loads." *Journal of Structural Engineering, ASCE*, 139(4), pp. 561-573.

522

523 Onsongo, W. M., (1978). "The Diagonal Compression Field Theory for Reinforced Concrete Beams
524 Subjected to Combined Torsion, Flexure and Axial Loads," *Ph.D. Dissertation*, Department of Civil
525 Engineering, University of Toronto, Canada, 246 pp.

526

527 Prakash, S. S., Li, Q., and Belarbi, A., (2012). "Behavior of circular and square RC bridge columns under
528 combined loading including torsion." *ACI Structural Journal.*, 109(3), 317–328.

529

530 Prakash, SS., and Belarbi, A., (2010). "Towards damage-based design approach for RC bridge columns
531 under combined loadings using damage index models," *Journal of Earthquake Engineering*, Taylor &
532 Francis Group Journals, Vol. 14, No. 3, pages 363 – 389.

533 Prakash, S.S., Belarbi, A., and You, Y.M., (2010). "Seismic performance of circular RC columns subjected
534 to axial, bending, and torsion with low and moderate shear," *Engineering Structures*, Elsevier, Vol. 32, No.
535 1, 2010, Pages 46-59.

536 Rahal, K.N., (1993). "The Behavior of Reinforced Concrete Beams Subjected to Combined Shear and
537 Torsion," *Ph.D. Thesis*, Department of Civil Engineering, University of Toronto.

538 Rahal, K. L., & Collins, M. P., "Analysis of sections subjected to combined shear and torsion-a theoretical
539 model." *ACI Structural Journal* 1995, 459-459.

540 Rahal, Khaldoun N. (2007). "Combined torsion and bending in reinforced and prestressed concrete beams
541 using simplified method for combined stress-resultants." *ACI structural journal* 104.4 , 402.

542 Labib, Moheb, Yashar Moslehy, and Ashraf Ayoub. (2017). "Softening coefficient of reinforced concrete
543 elements subjected to three-dimensional loads." *Magazine of Concrete Research*.

544

545 Silva, J. R, Horowitz, B, & Bernardo, L. F. (2017). "Efficient analysis of beam sections using softened truss
546 model." *ACI Structural Journal*, 114(3) 2017, 765.

547

548 Tirasit, P., and Kawashima, K., (2007). "Seismic performance of square reinforced concrete columns under
549 combined cyclic flexural and torsional loadings." *Journal of Earthquake Engineering*, 11(3), 425–452.

550

551 Vecchio, F. J., and Collins, M., (1986). "The modified compression-field theory for reinforced concrete
552 elements subjected to shear." *ACI Structural Journal*, 83(2), 219–231.

553

554 Zhang, L.X.B. and Hsu, T.T., (1998). "Behavior and analysis of 100 MPa concrete membrane
555 elements". *Journal of Structural Engineering, ASCE*, 124(1), pp.24-34.

556

557 Zhu, R. R., and Hsu, T. T. (2002). "Poisson effect in reinforced concrete membrane elements." *ACI*
558 *Structural Journal*,, 99(5), 631–640.

Table 1: Comparison between CA-STM and CA-SMM

Details	CA-STM	CA-SMM
Theory	Rotating angle theory	Fixed angle theory
Crack Direction	Cracking is assumed along principal coordinate of the concrete element	Cracking is assumed along Principal Coordinates of RC Element
Poisson's Effect	Not considered	Included in the formulation
Strain Gradient effect	Considered only for principal compression	Considered for both principal compression and principal tension.
Post Peak Behavior	Cannot predict accurately	Predictions are better than CA-STM
Post-Cracking Stiffness	Cannot predict accurately	Predictions are better than CA-STM
The contribution of Concrete in Shear	Shear stress contribution from the concrete element is not considered.	Shear stress contribution from the concrete element is considered.
Solution procedure	Iterative trial and error	Optimisation of functional residue (Gradient descent method)
Computation time	Very large	Significantly less(few seconds)

Table 1: Specimen Details

Specimen ID	Rahal-Collins Series-1	Rahal-Collins Series-2	Greene – Box Girder	Klus specimen		Missouri Columns	
				I	II	I	II
Cross-section type	Rectangle	Rectangle	Square	Rectangle	Rectangle	Square	Square
Section dimension (m x m)	0.30 X 0.60	0.34 X 0.64	0.76 X 0.76	0.2 X 0.3	0.2 X 0.3	0.56 X 0.56	0.56 X 0.56
Hollow core area (m x m)	-	-	0.50 X 0.50	-	-	-	-
Effective Column height (m)	1.66	1.66	3.66	1	1	3.35	3.35
Cylinder strength (MPa)	28.4	28.4	45	27	27	34.6	34.5
Long. Reinf. Ratio (%)	1.27	1.27	0.63	1.48	1.48	2.1	2.1
Trans. Reinf. Ratio (%)	0.75	0.75	0.95	0.08	0.08	1.32	1.32
Longitudinal bar yield strength (MPa)	354	354	446	439	439	512	512
Transverse bar Yield strength (MPa)	328	328	446	270	270	454	454
Axial Force (kN)	160	160	0	0	0	0	668
Elastic modulus of steel (MPa)	200000	200000	226000	200000	200000	200000	200000
T/V ratios	1500 mm	1500 mm	0	0	656 mm & 281 mm*	0	0

*The presented T/V ratios were that of those used in validation, out of various Klus specimen of Klus 1968.

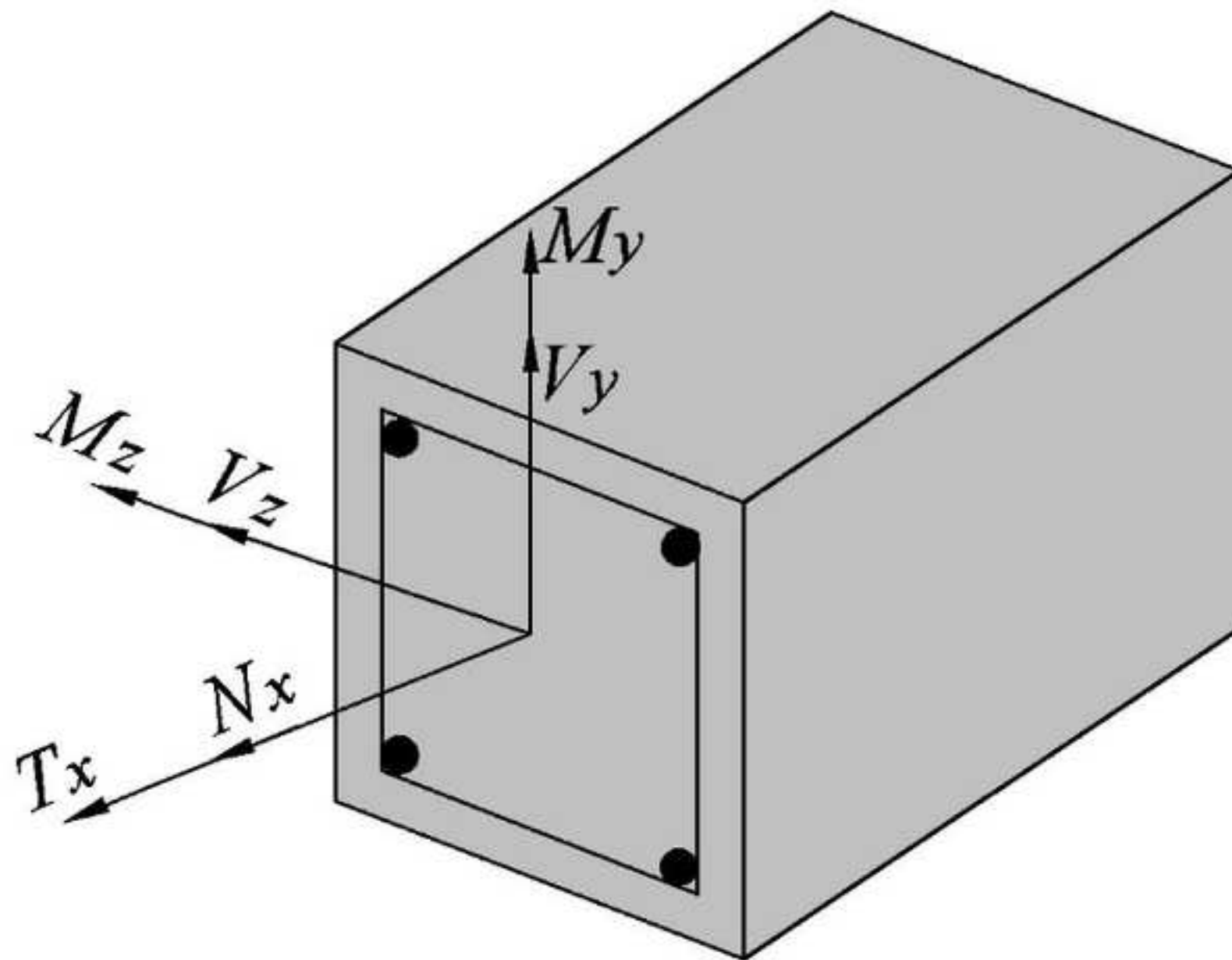
Table 1: Comparison of Predictions with Experimental Data (at Peak)

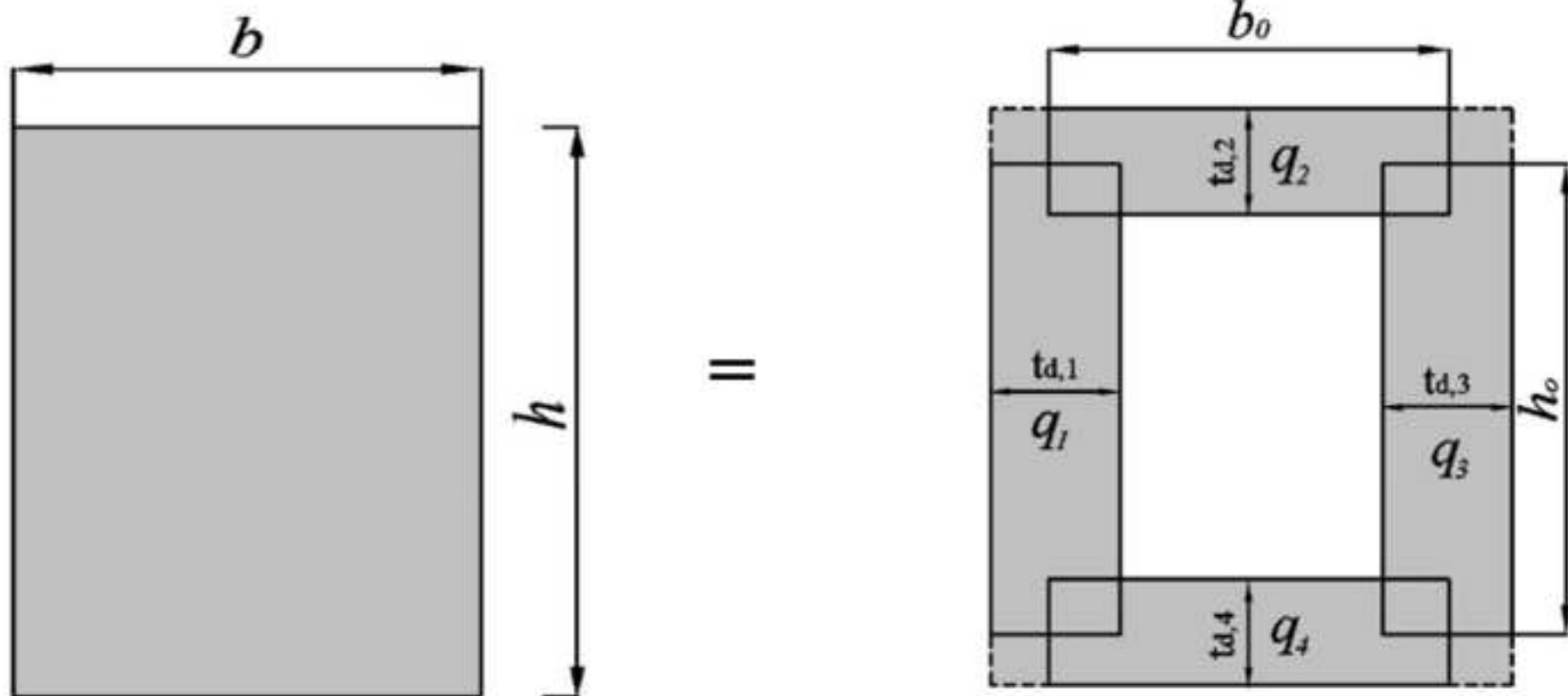
Parameter/ Specimen ID	Peak Torque (KN-m)				Peak twist (degrees)			
	Exp. (T_{exp})	CA- STM	CA- SMM (T_{calc})	T_{exp}/T_{calc}	Exp. (θ_{exp})	CA- STM	CA- SMM (θ_{calc})	$\theta_{exp}/\theta_{calc}$
Missouri specimen								
Series I	330.1	322.6	353.4	0.94	6.3	4.1	7.4	0.85
Series II	324.9	323.4	357	0.91	6.3	4.1	7.3	0.86
Rahal and Collins specimen								
Series 1	141.0	114.0	117.5	1.20	4.2	2.4	3.5	1.20
Series 2	134	145.7	144.8	0.92	2.4	2.2	3.5	0.68
Greene specimen								
Greene	428.0	402.0	444.0	0.96	1.0	1.0	1.4	0.71
Klus specimen*								
Series I (Pure Torsion)	14.5	14.0	15.0	0.96	2.0	2.3	2.0	1.00
Series II (T/V = 656 mm)	12.8	13.5	14.0	0.91	1.8	2	1.9	0.94
Series II (T/V = 281 mm)	11.8	11.8	11.2	1.05	1.5	1.7	1.2	1.25

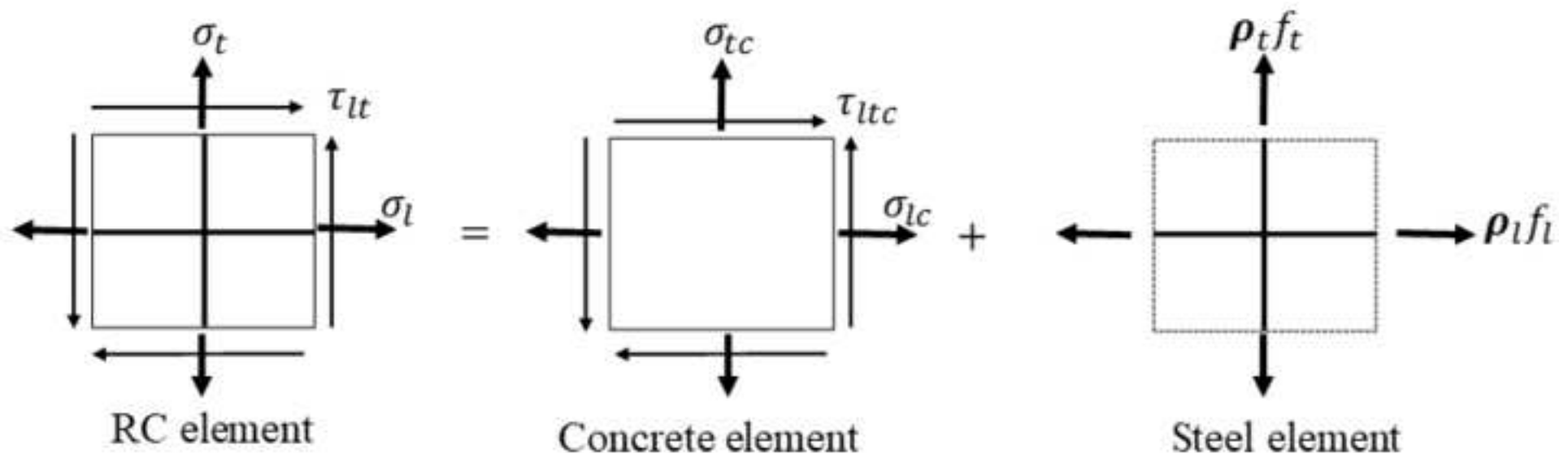
*The presented T/V ratios were that of those used in validation, out of various Klus specimen of Klus 1968.

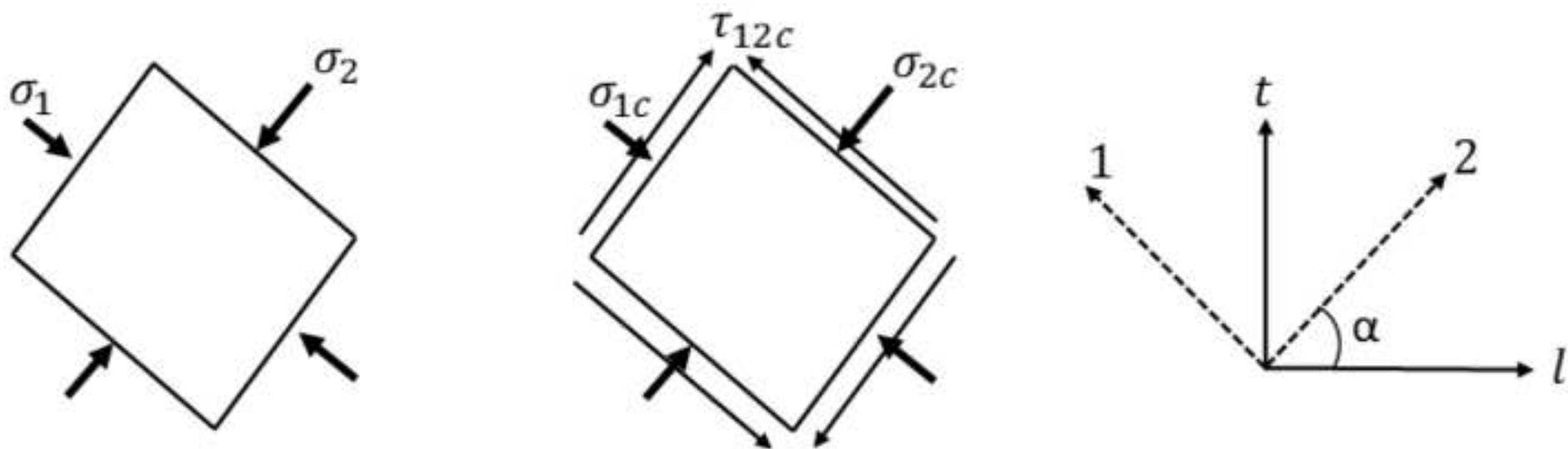
Table 1: Comparison of Predictions with Experimental Data (at ultimate)

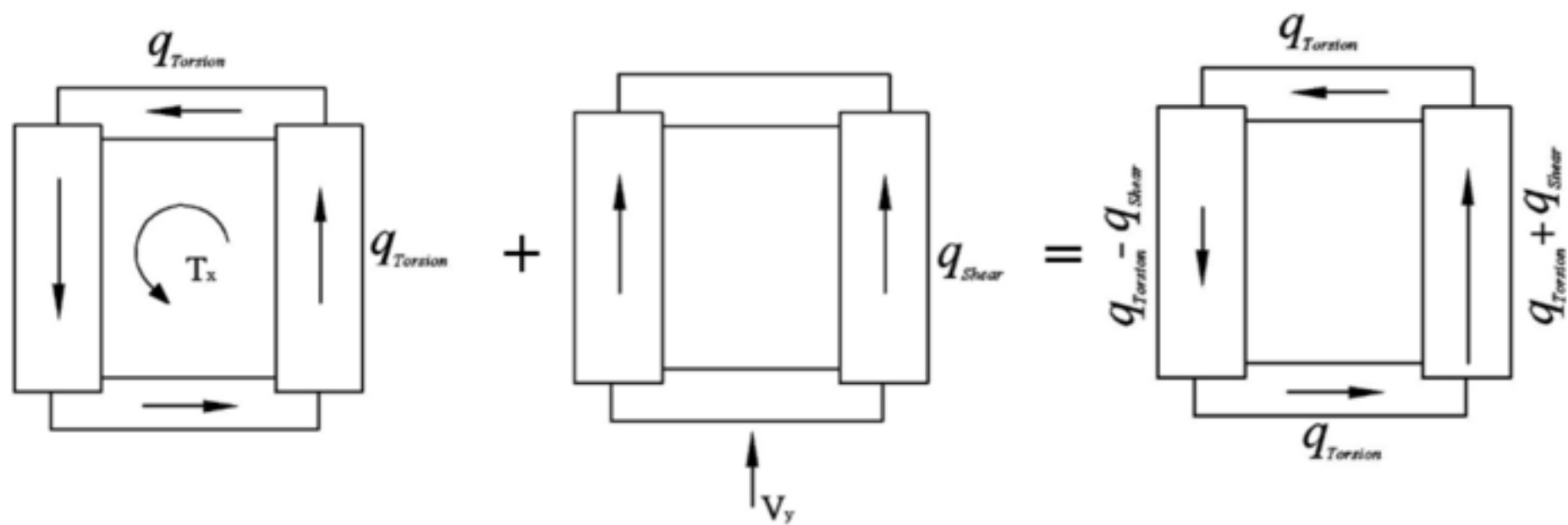
Parameter/ Specimen ID	Ultimate Torque (KN-m)				Ultimate twist (degrees)			
	Exp. ($T_{u,exp}$)	CA- STM	CA-SMM ($T_{u,calc}$)	$T_{u,exp}/T_{u,calc}$	Exp. ($\theta_{u,exp}$)	CA- STM	CA- SMM ($\theta_{u,calc}$)	$\theta_{exp}/\theta_{calc}$
Missouri specimen								
Series I	300.2	294.7	353.0	0.85	9.7	5.4	7.4	1.31
Series II	295.0	303.0	357.0	0.82	9.7	5.3	7.2	1.34
Rahal and Collins specimen								
Series 1	131.0	113.0	116.0	1.13	4.9	2.4	4.1	1.19
Series 2	123.0	145.0	144.0	0.85	4.4	2.5	3.9	1.13
Greene specimen								
Greene	354.0	394.0	440.0	0.80	1.4	1.5	1.9	0.76

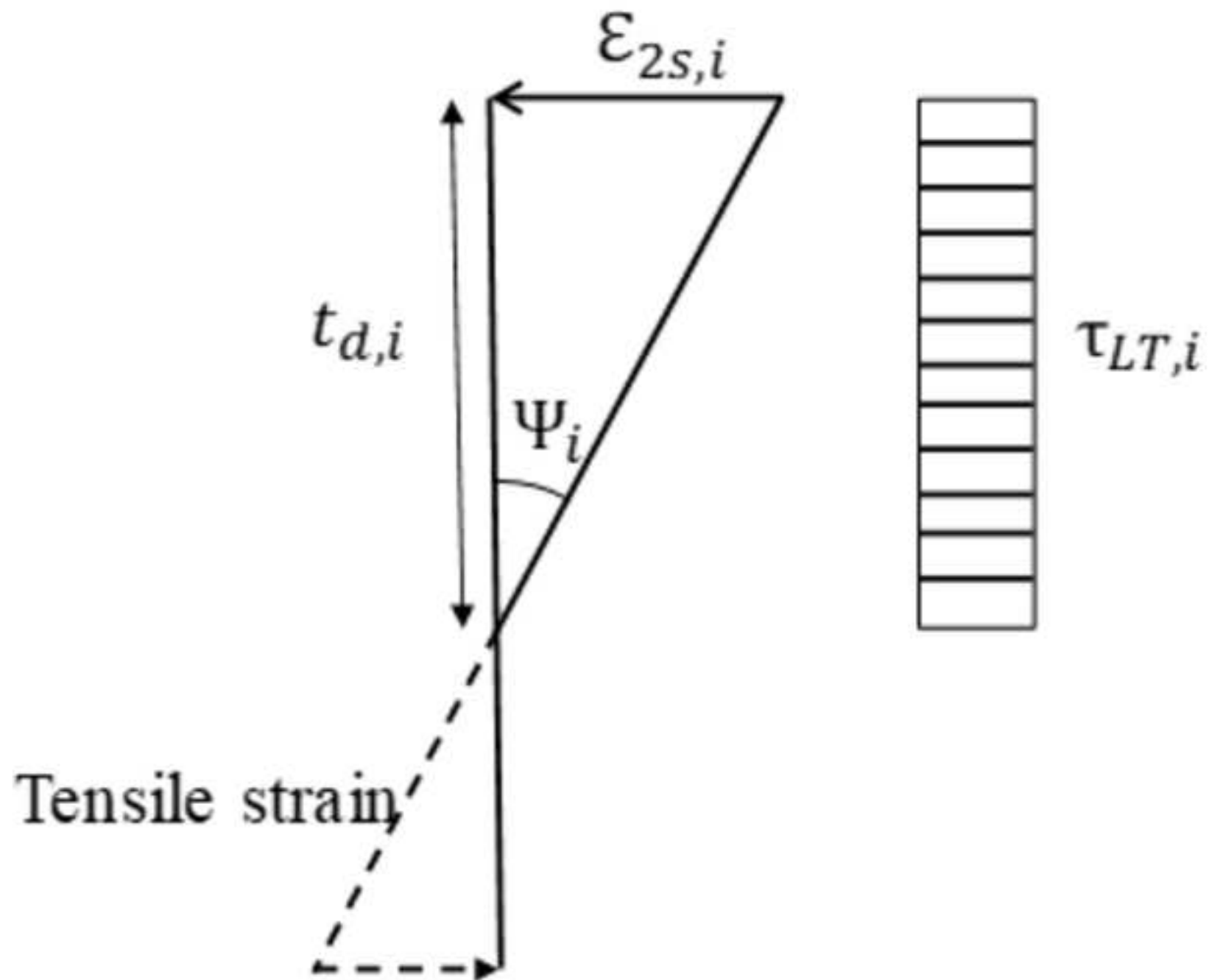


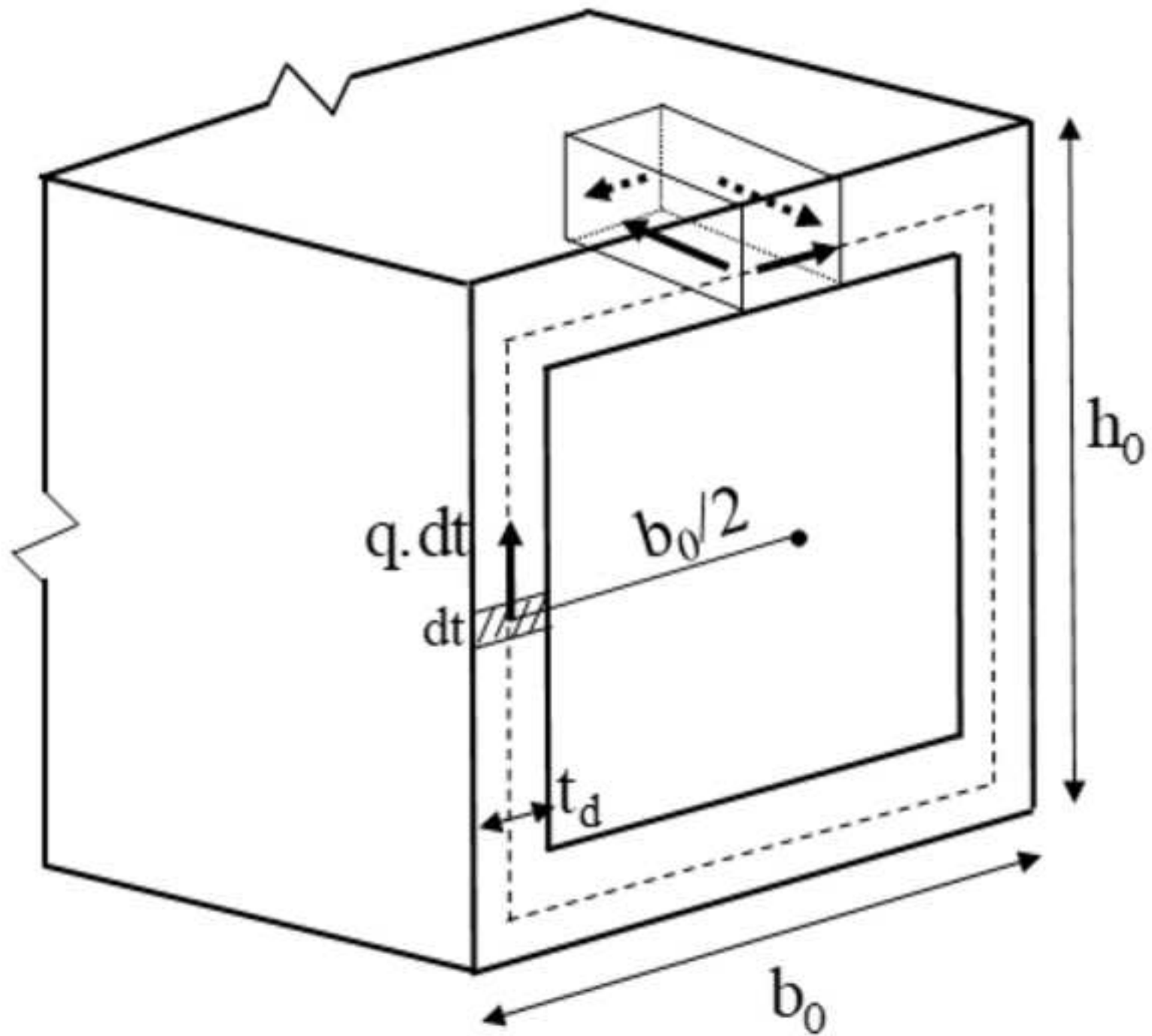


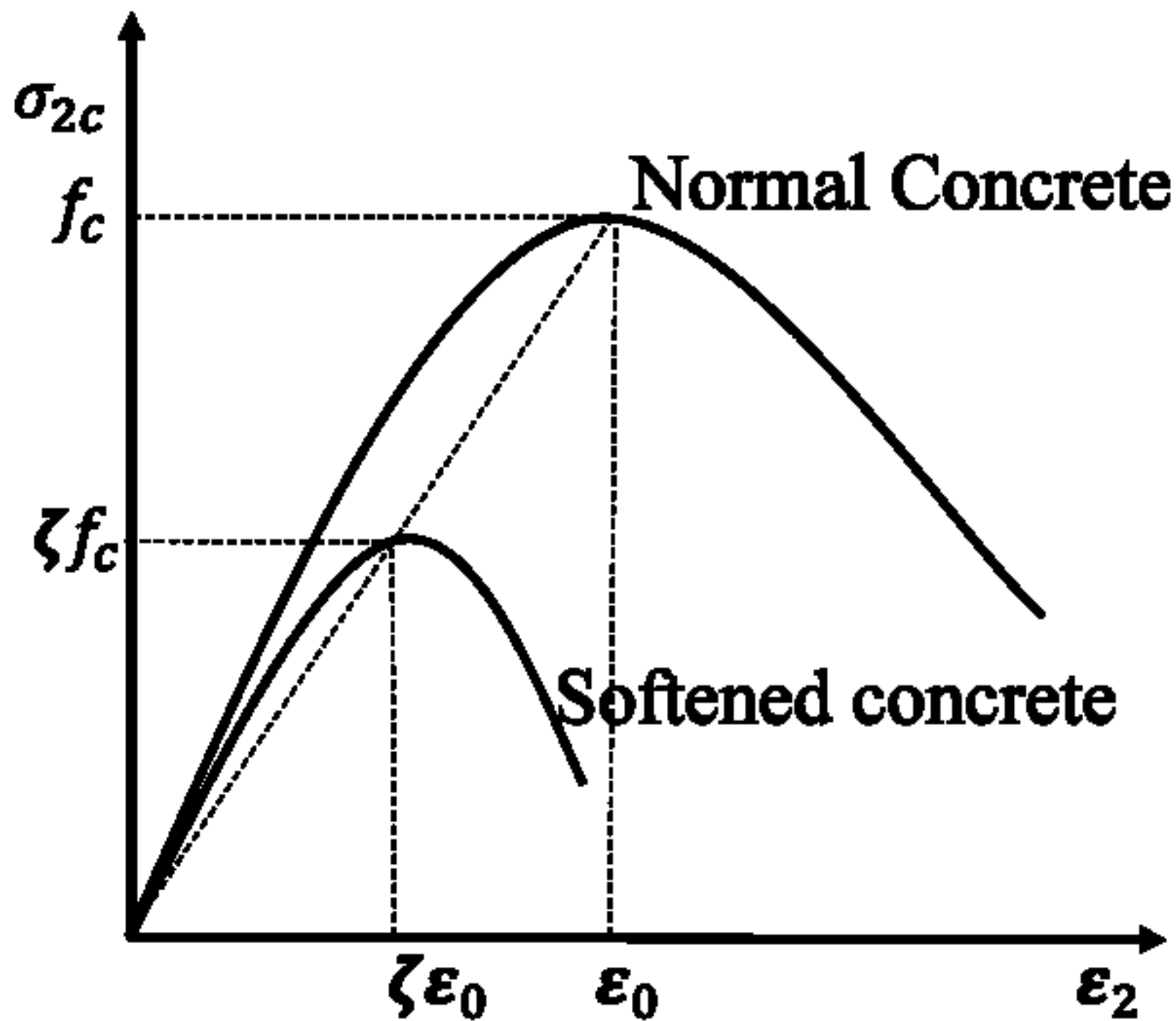


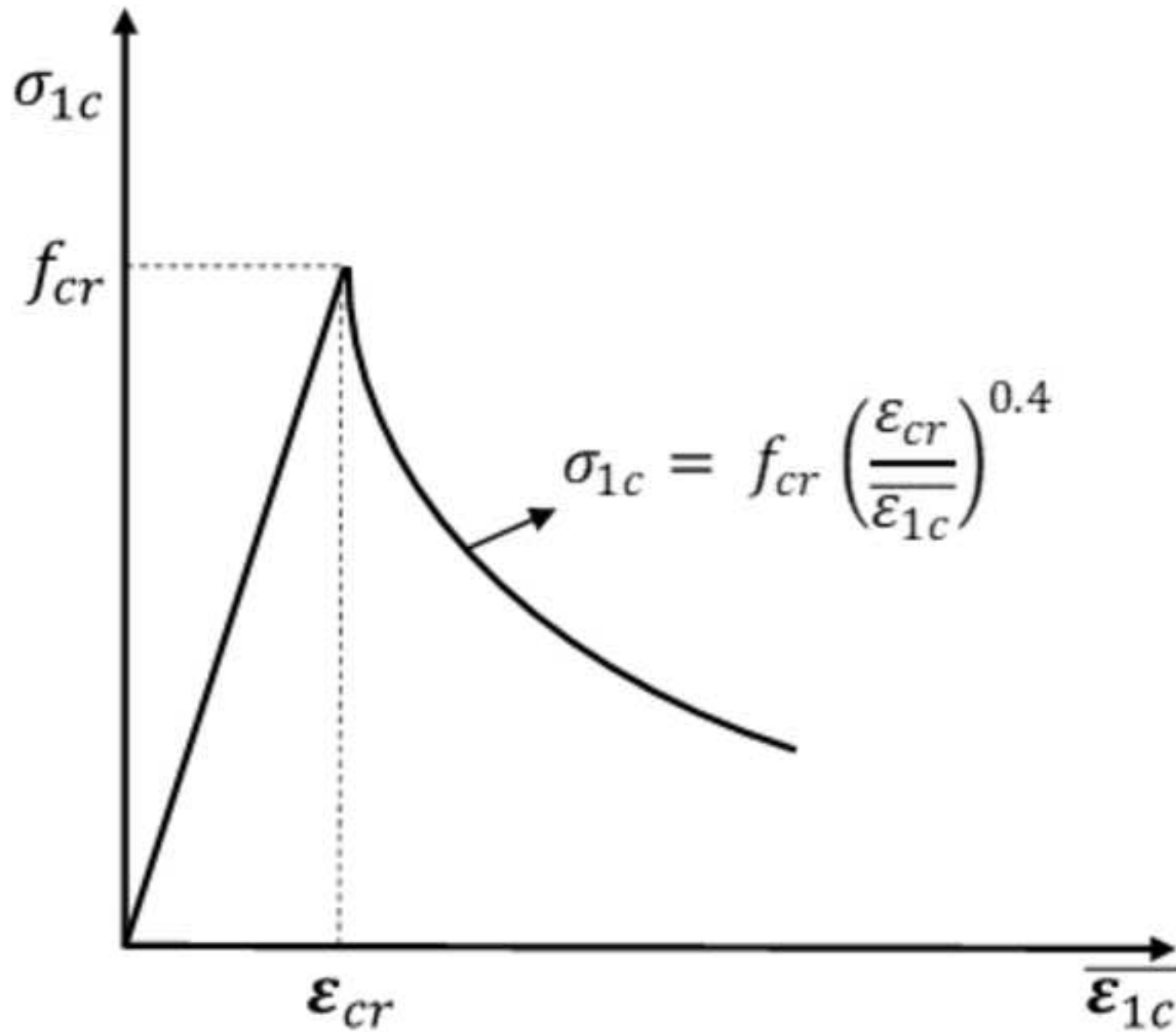


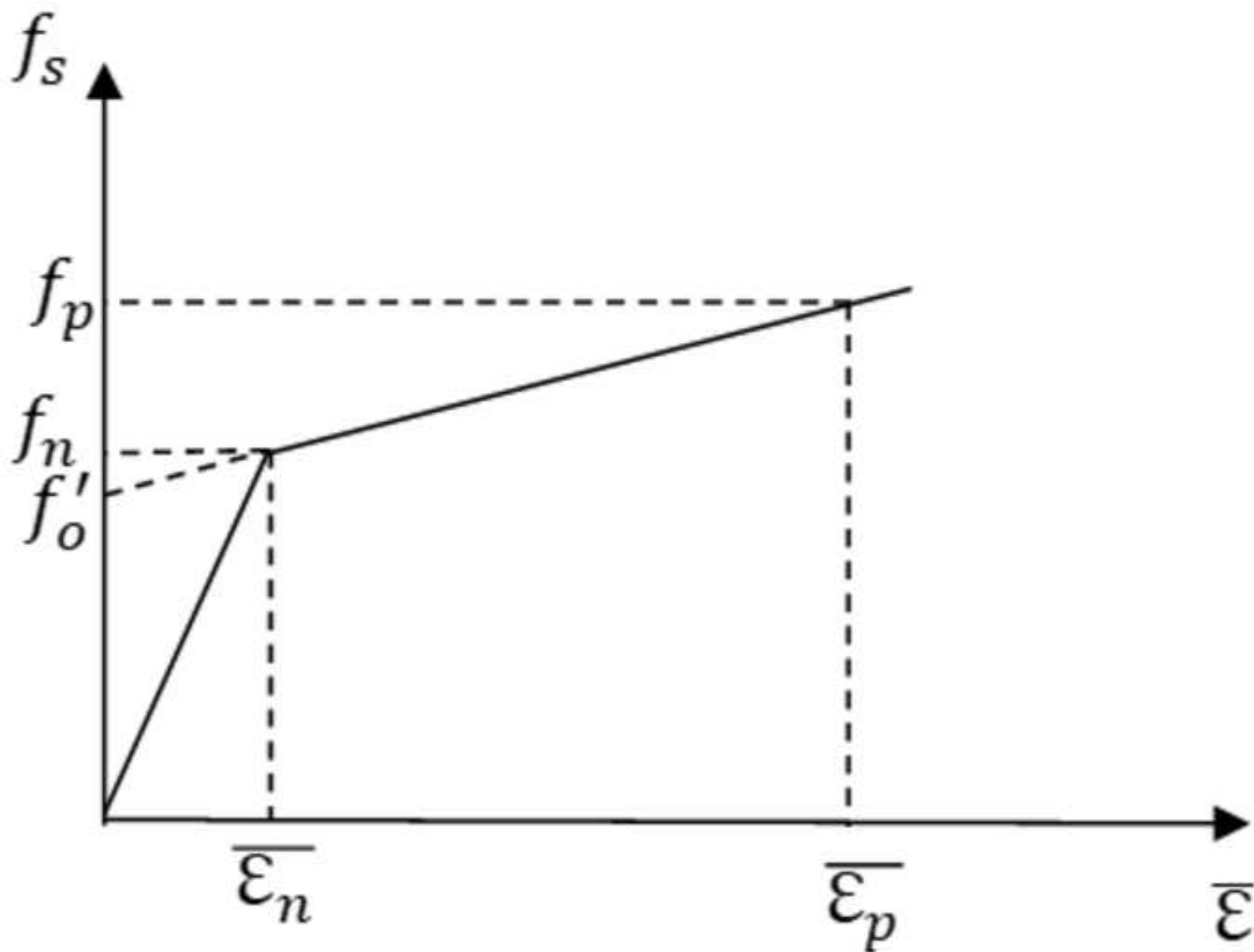


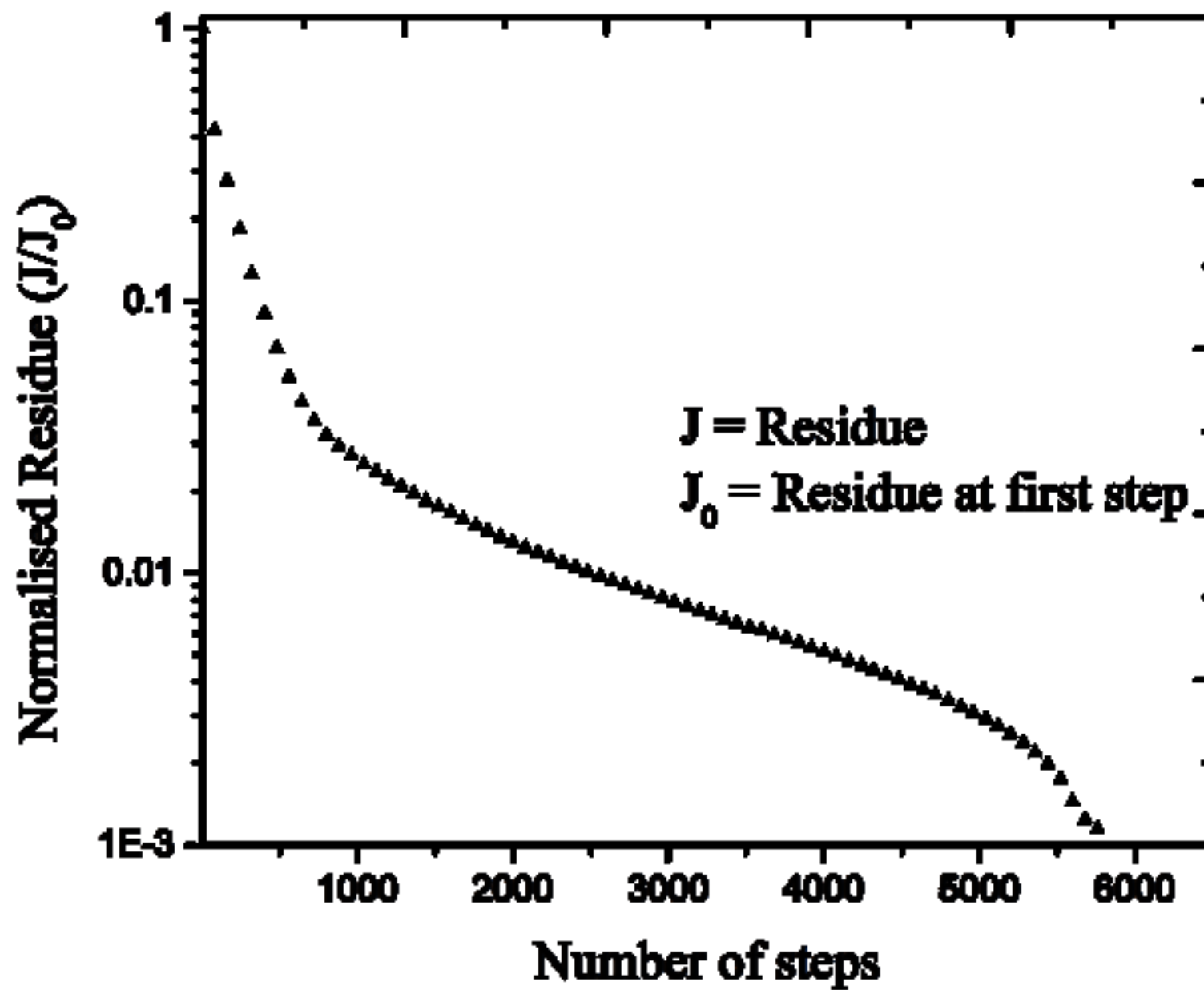


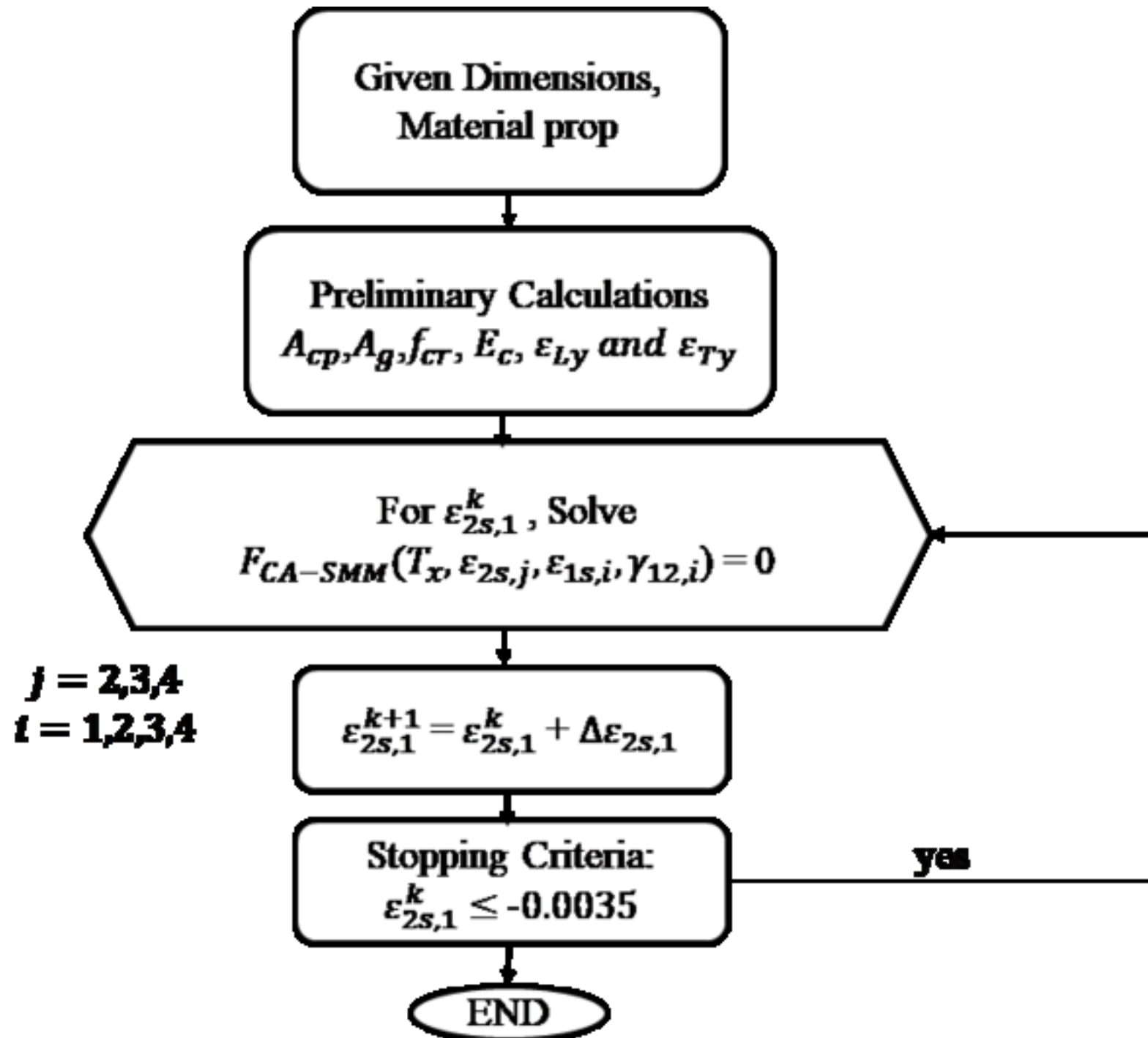


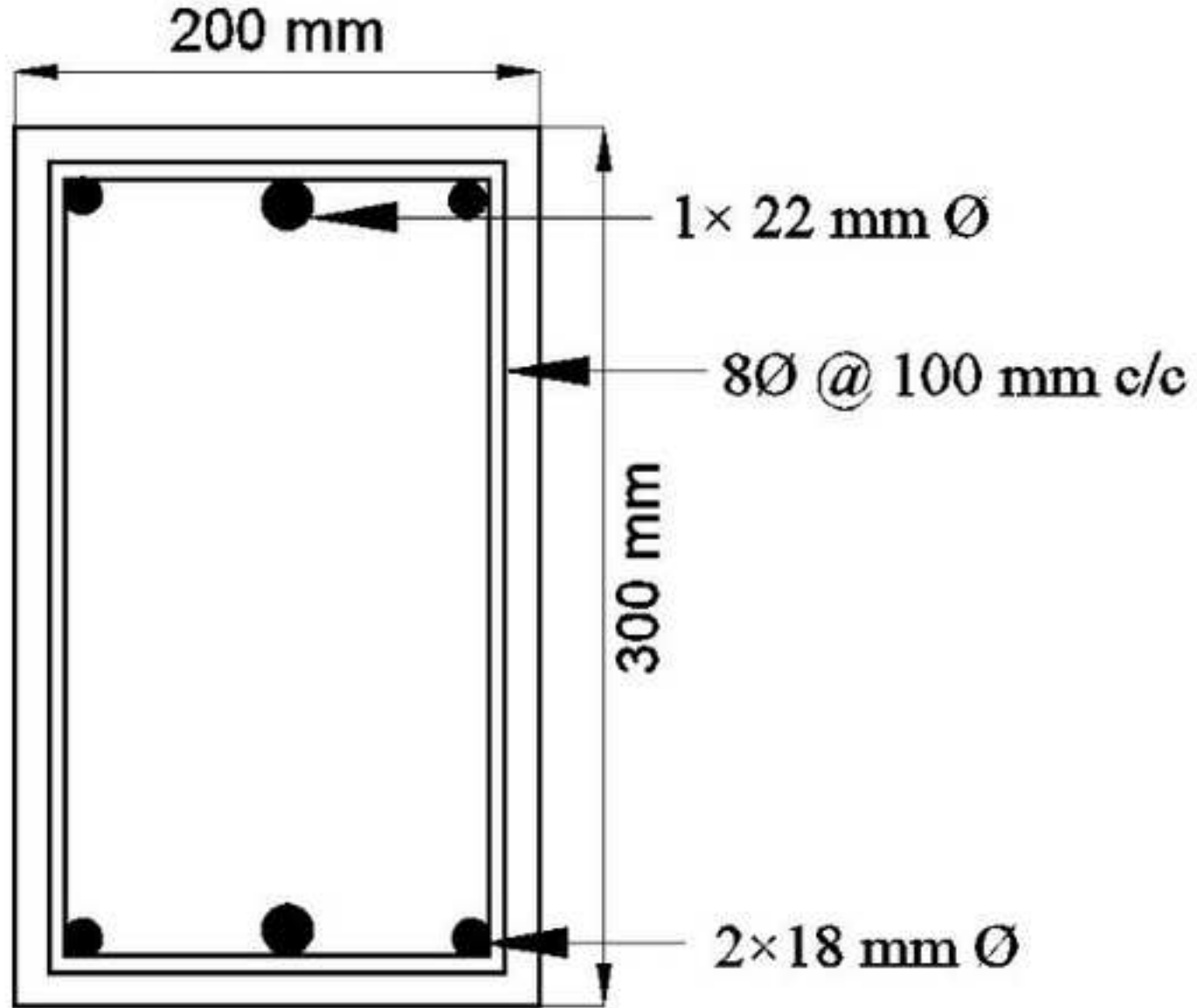


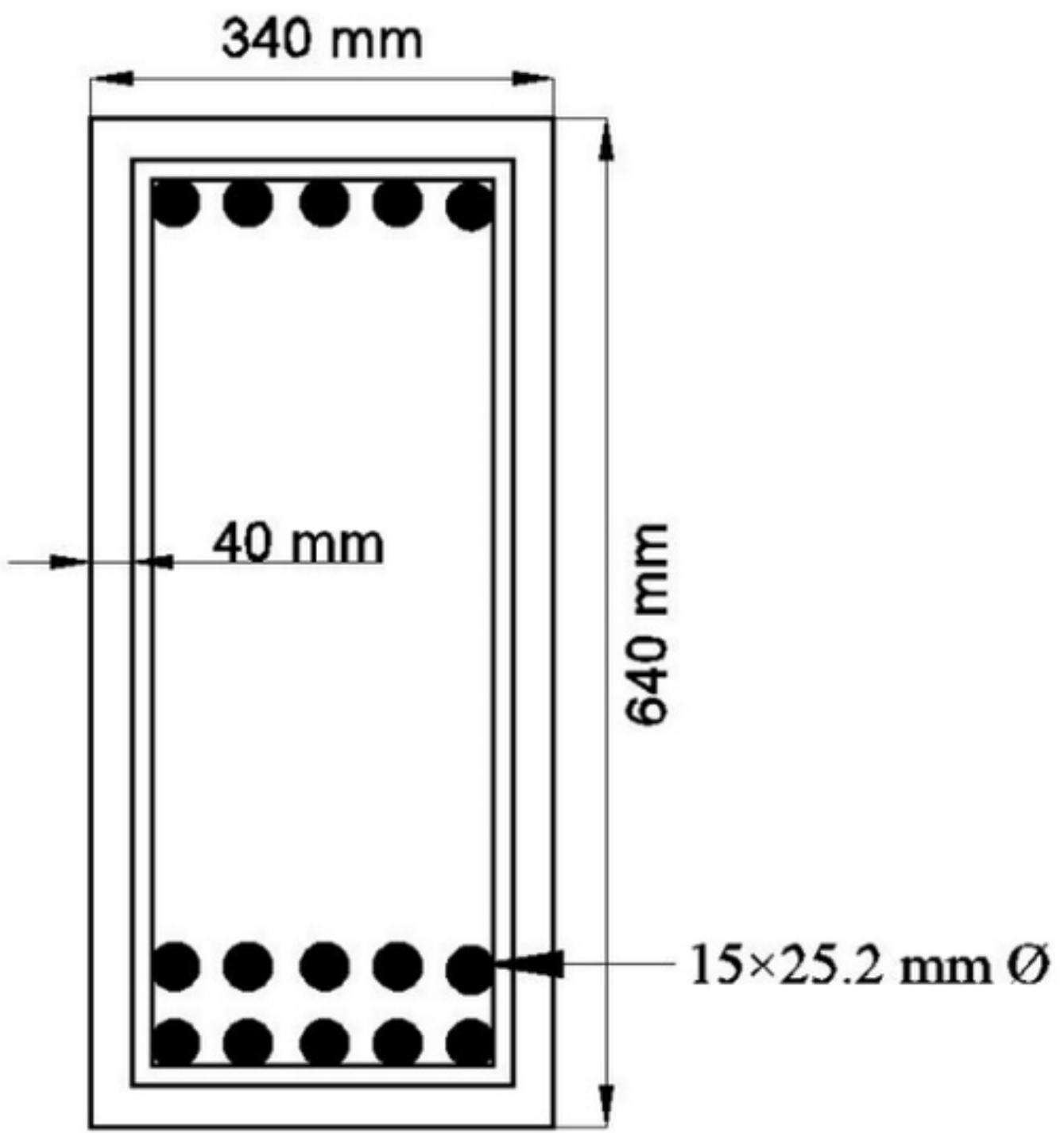


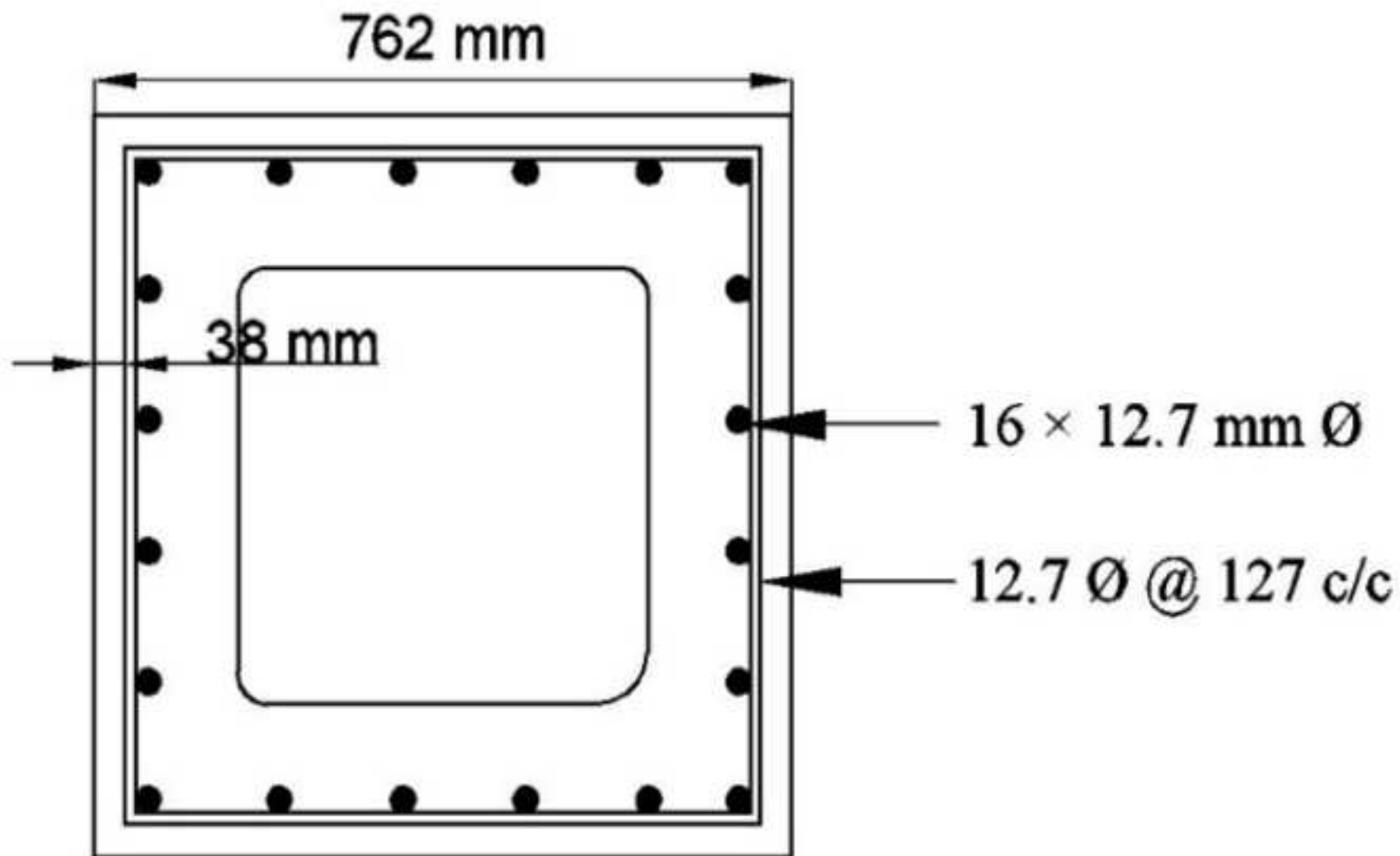


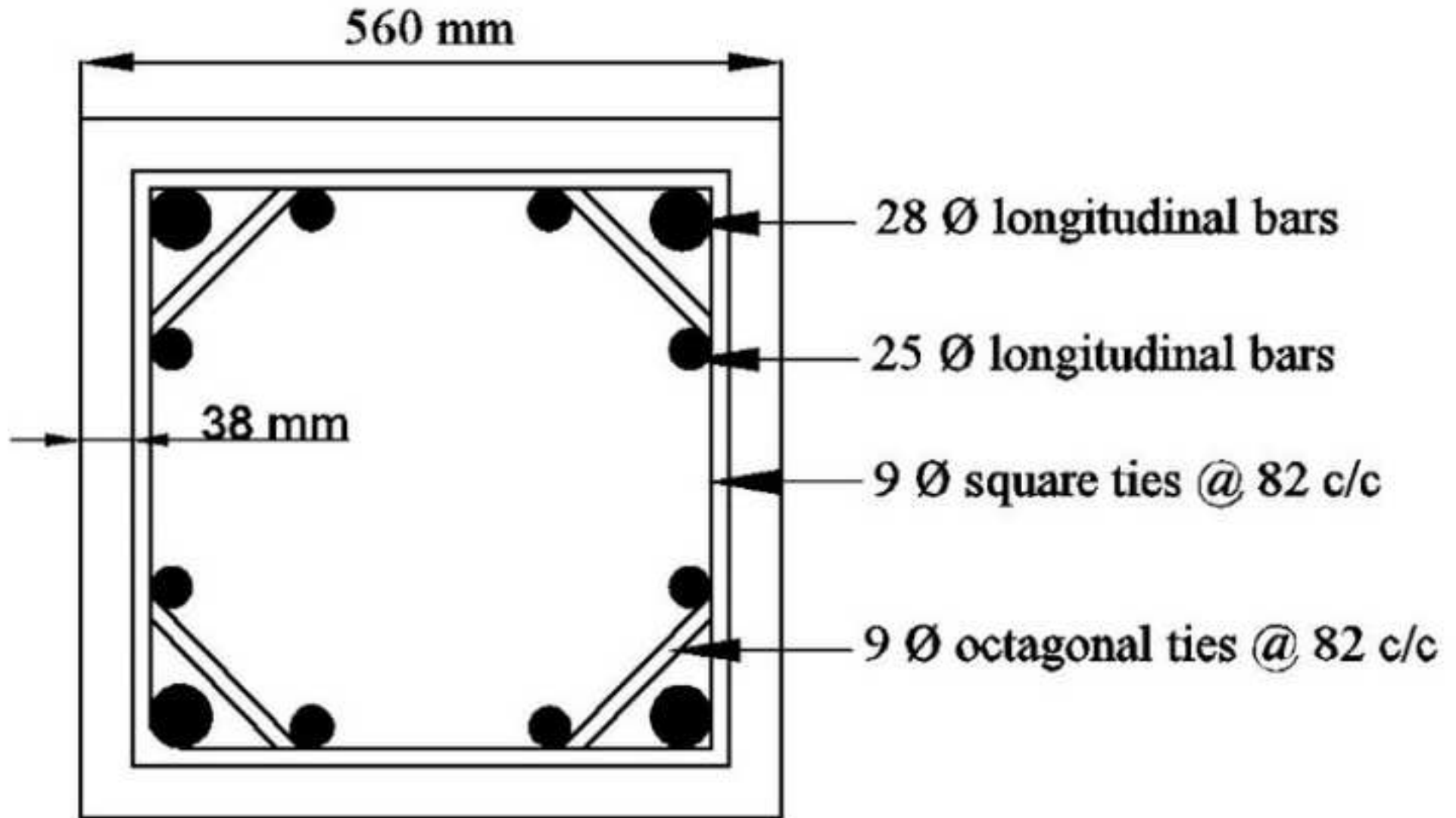


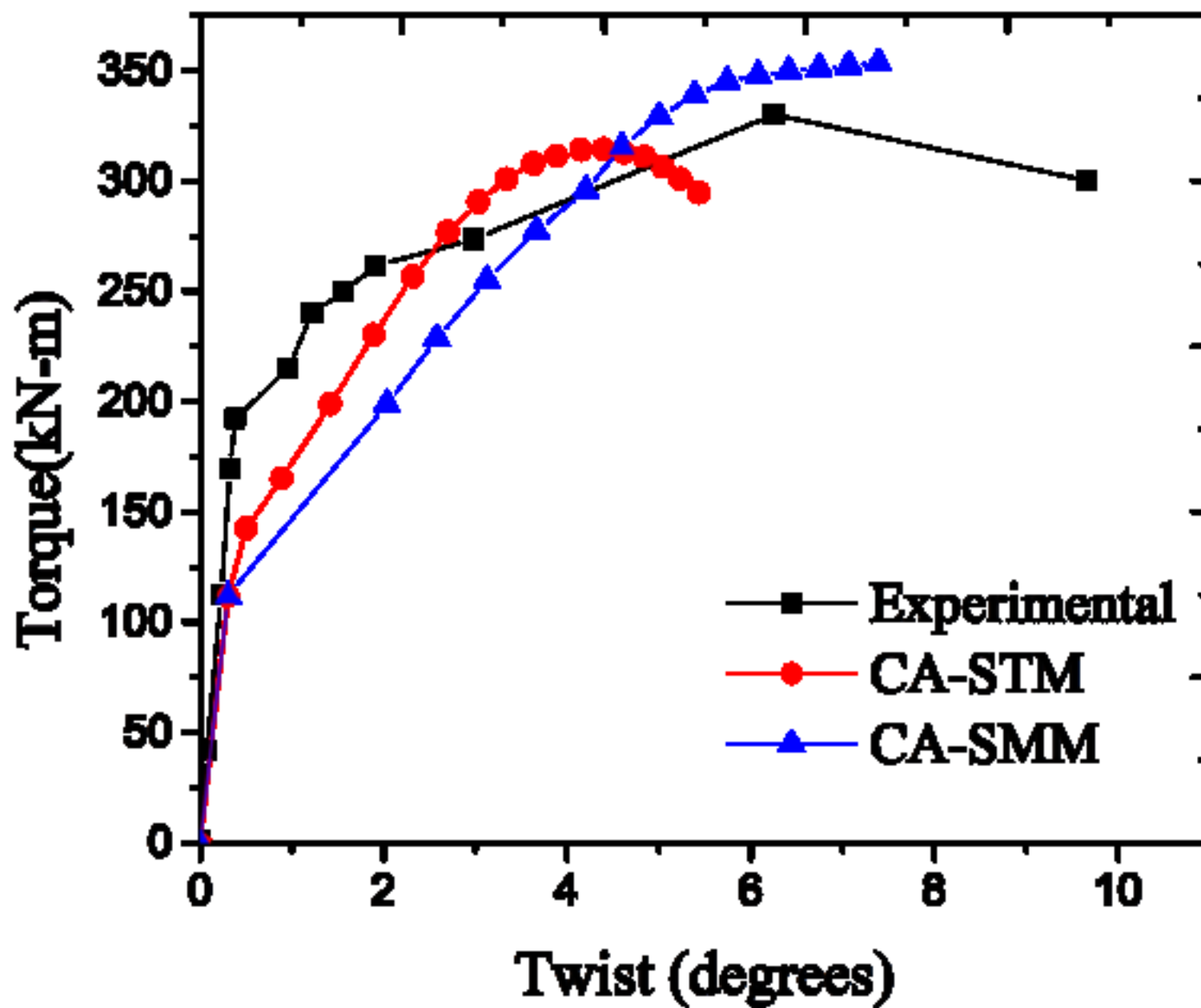


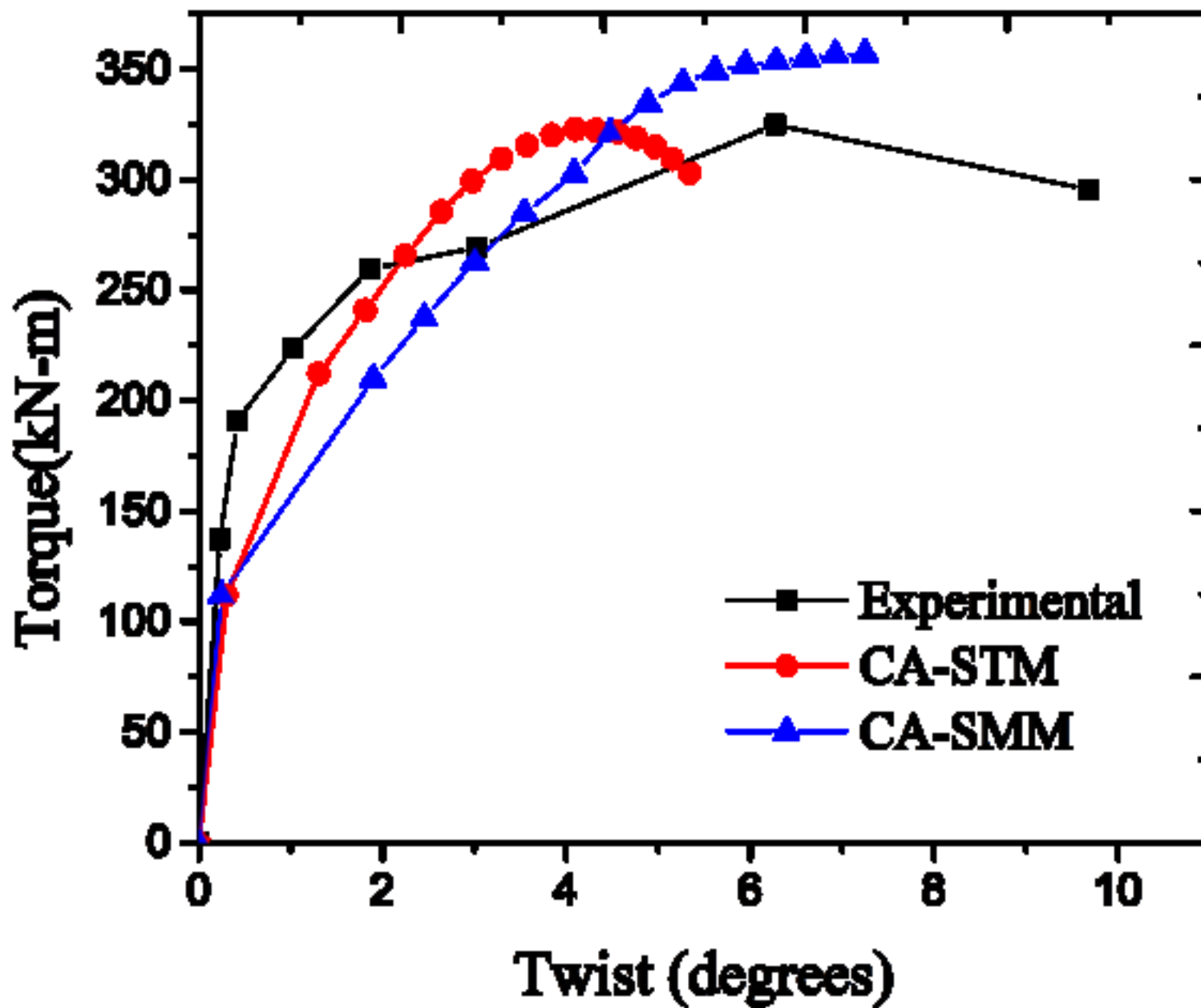


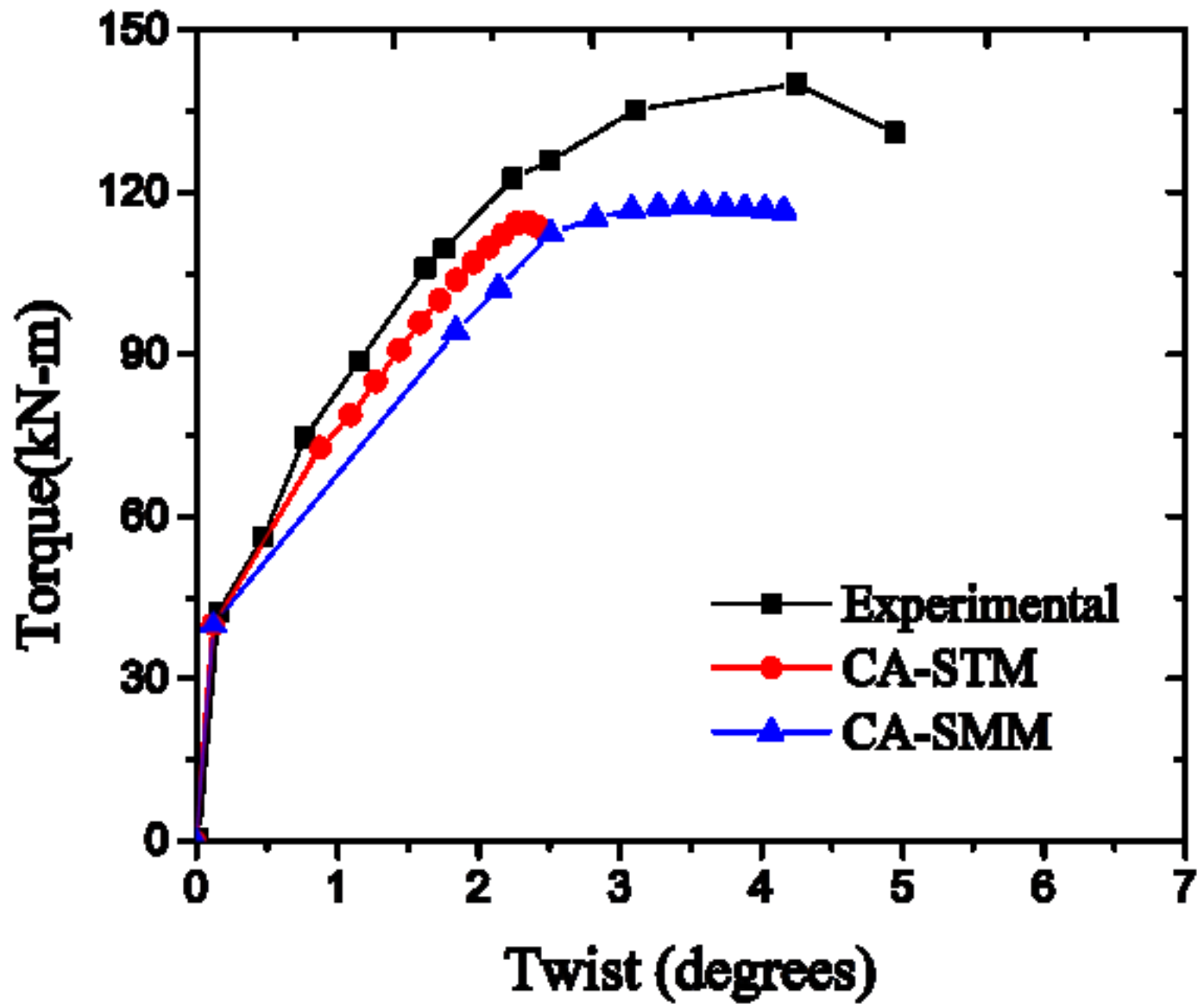


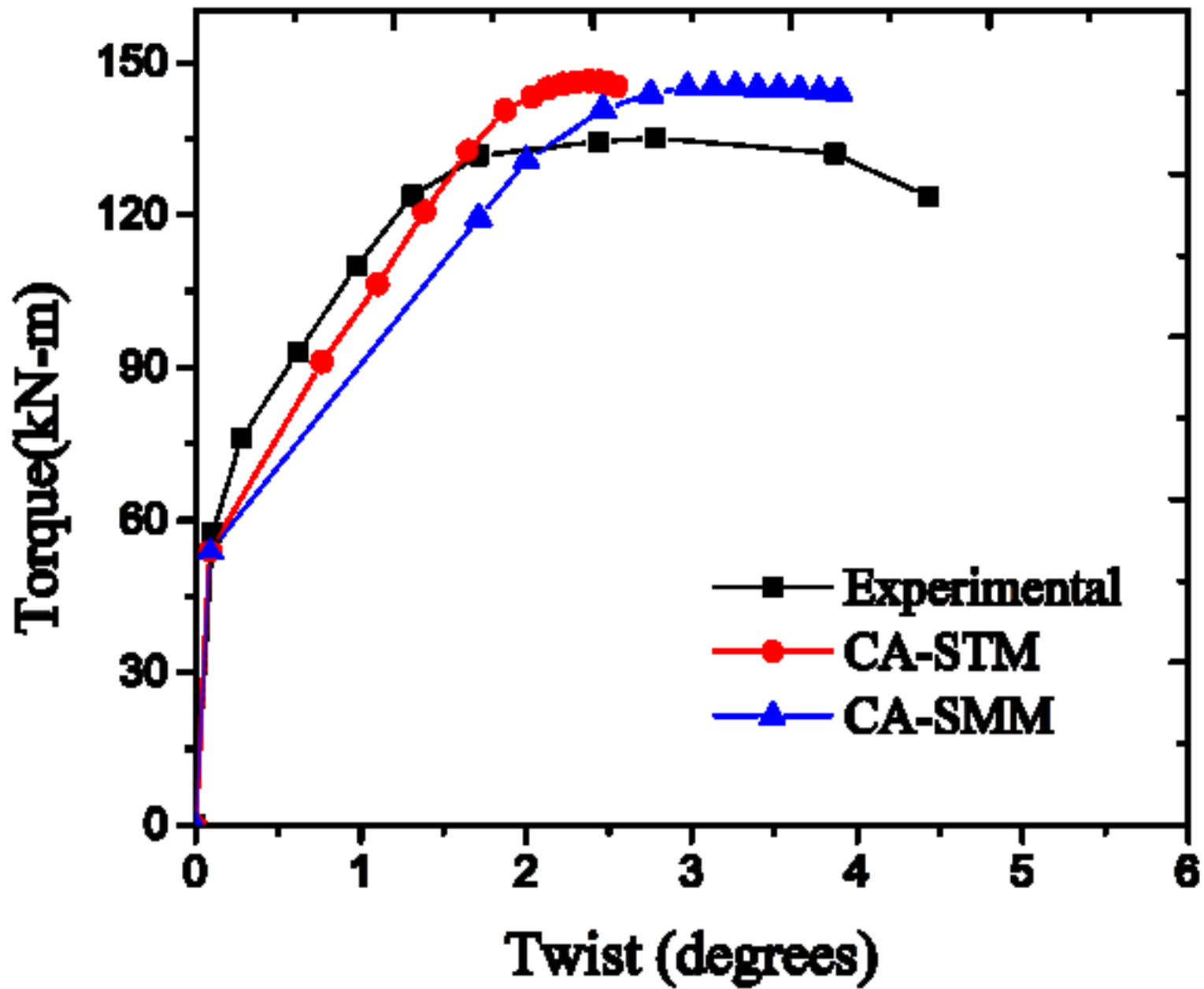


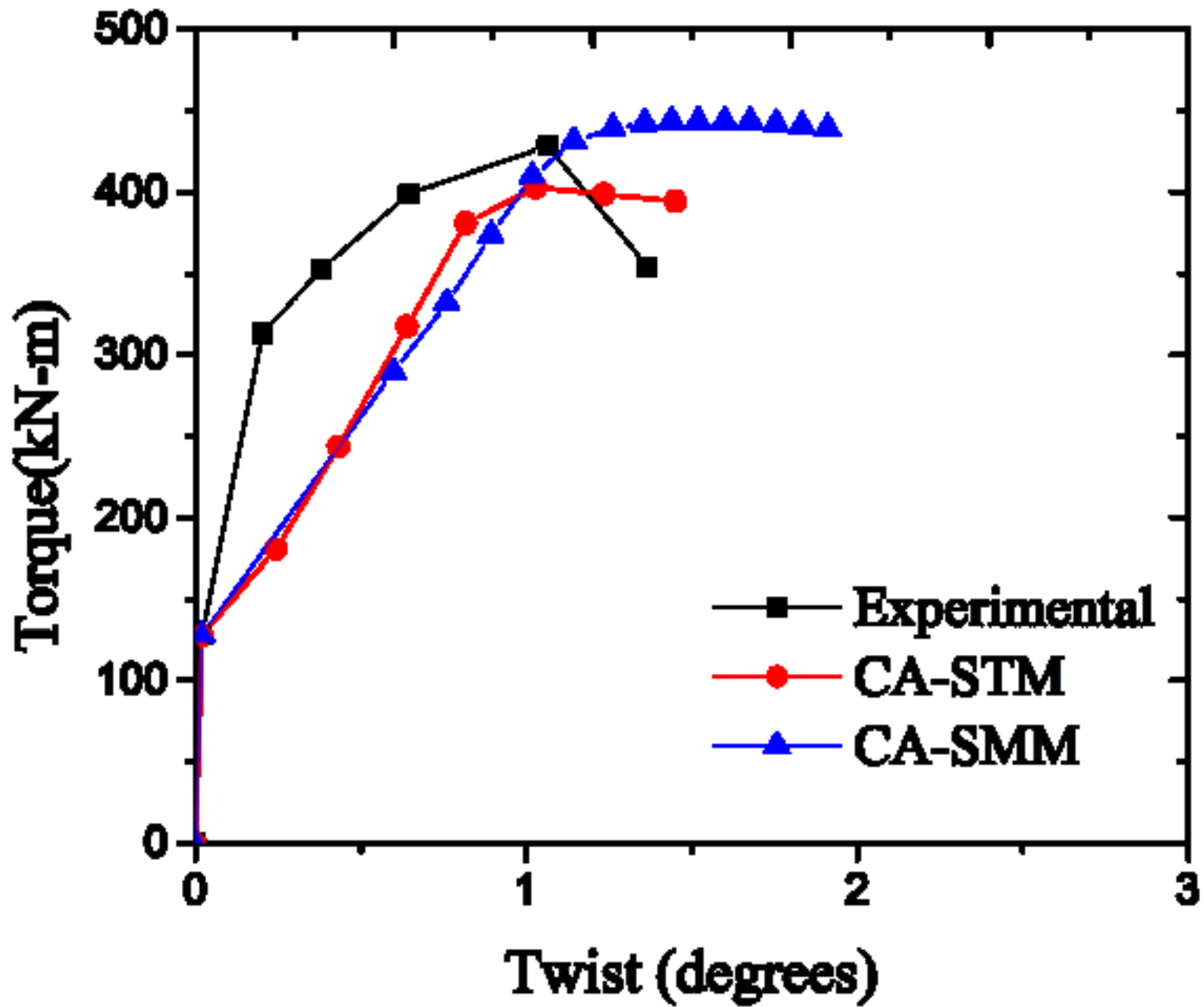


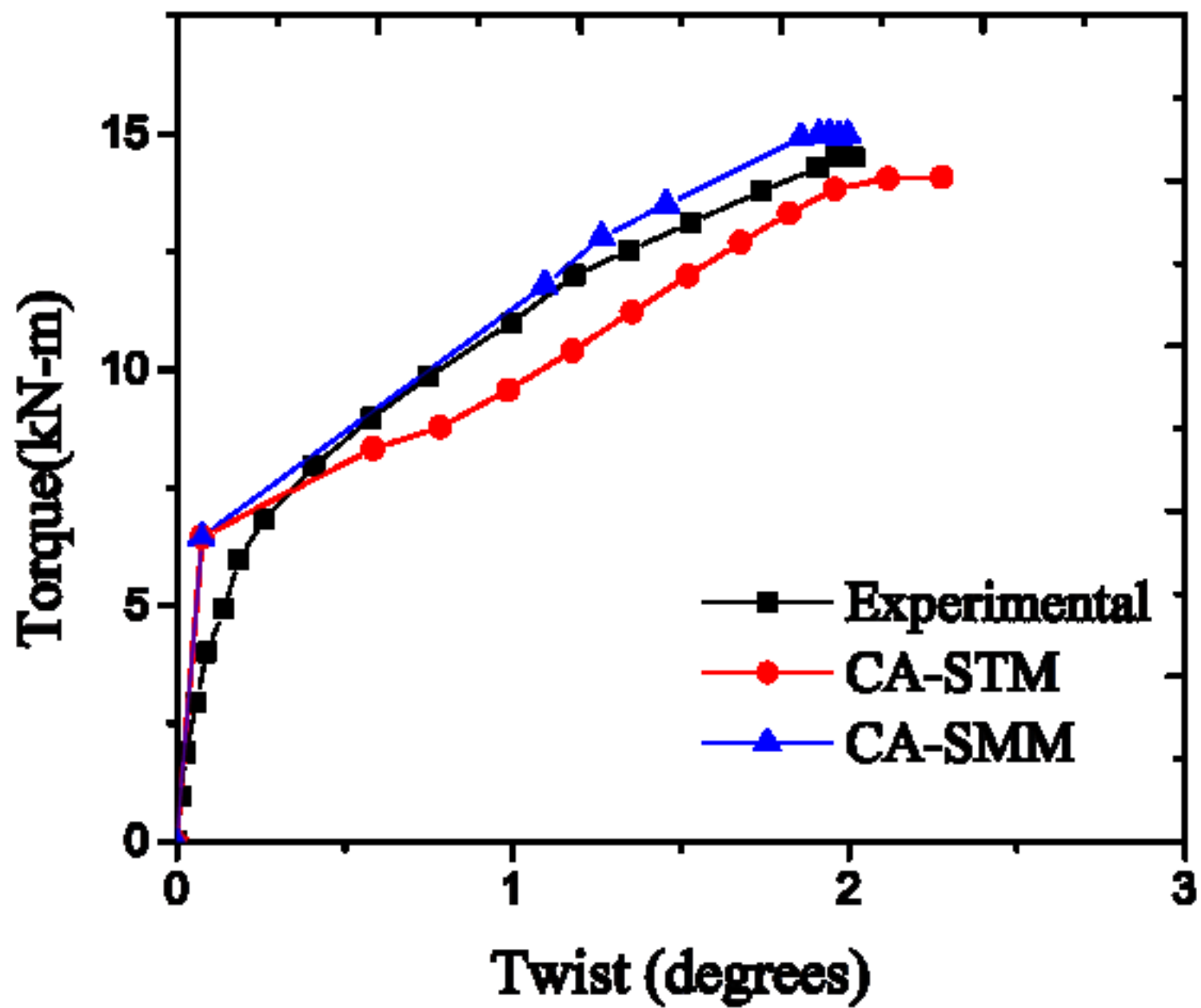


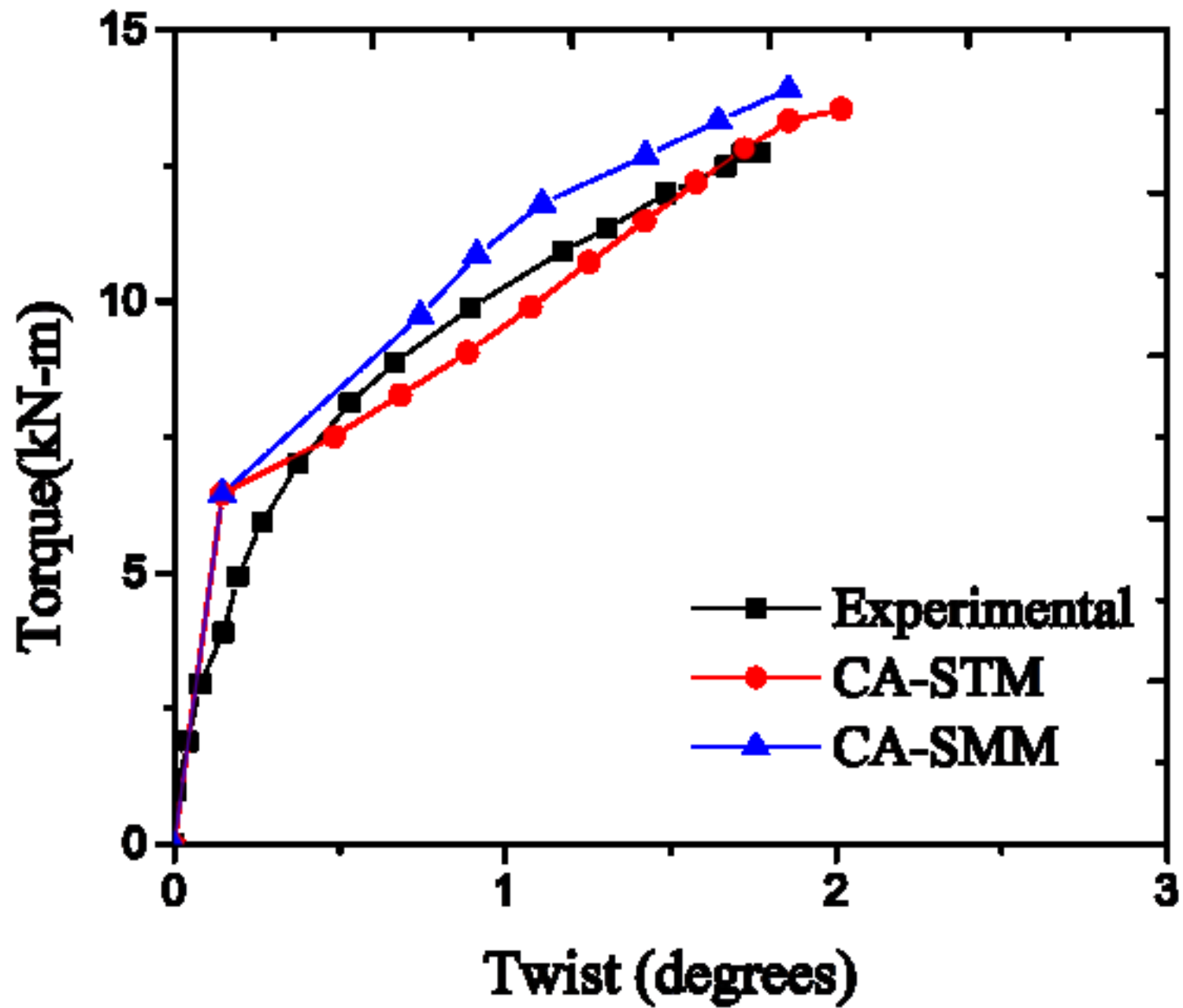


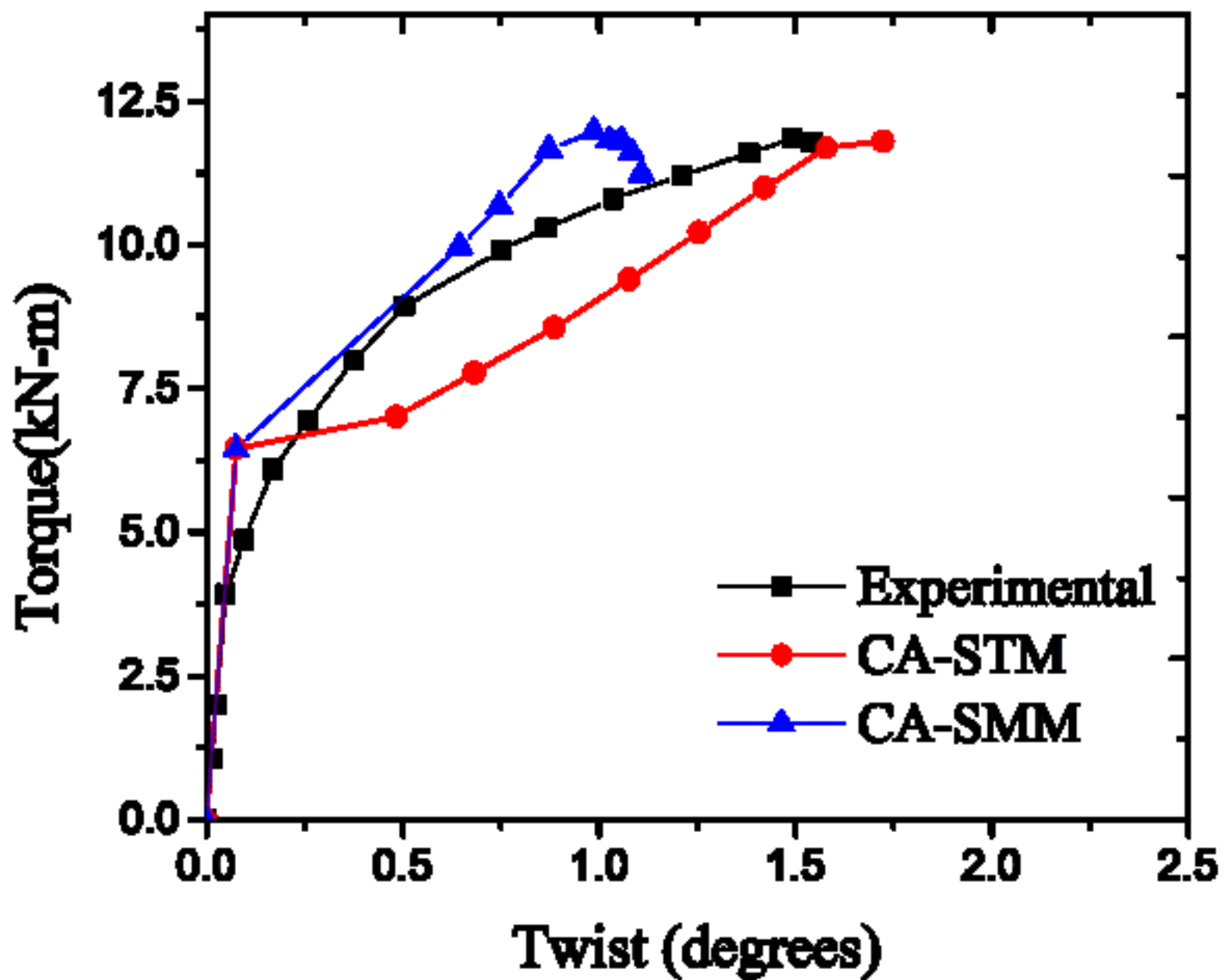


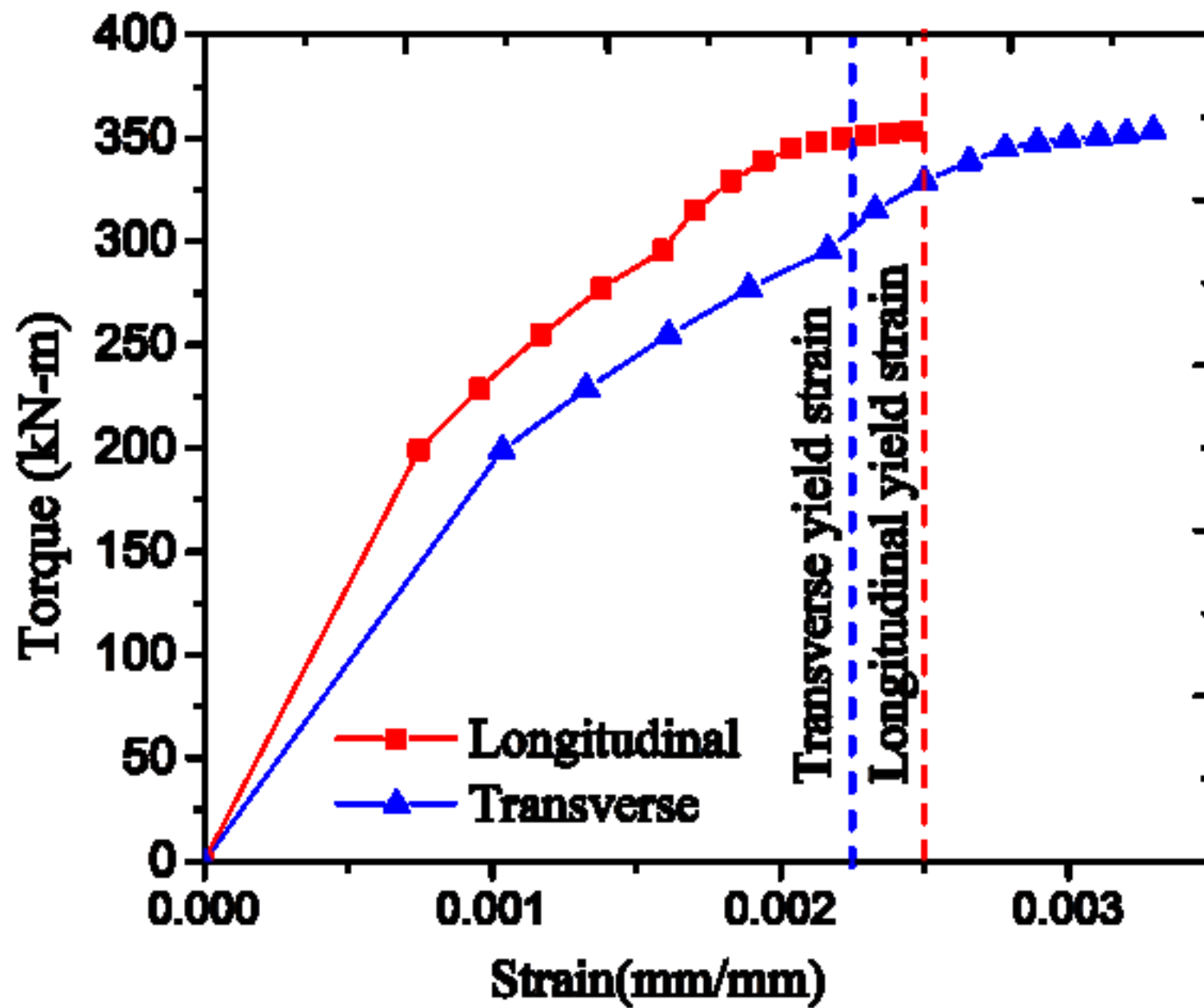


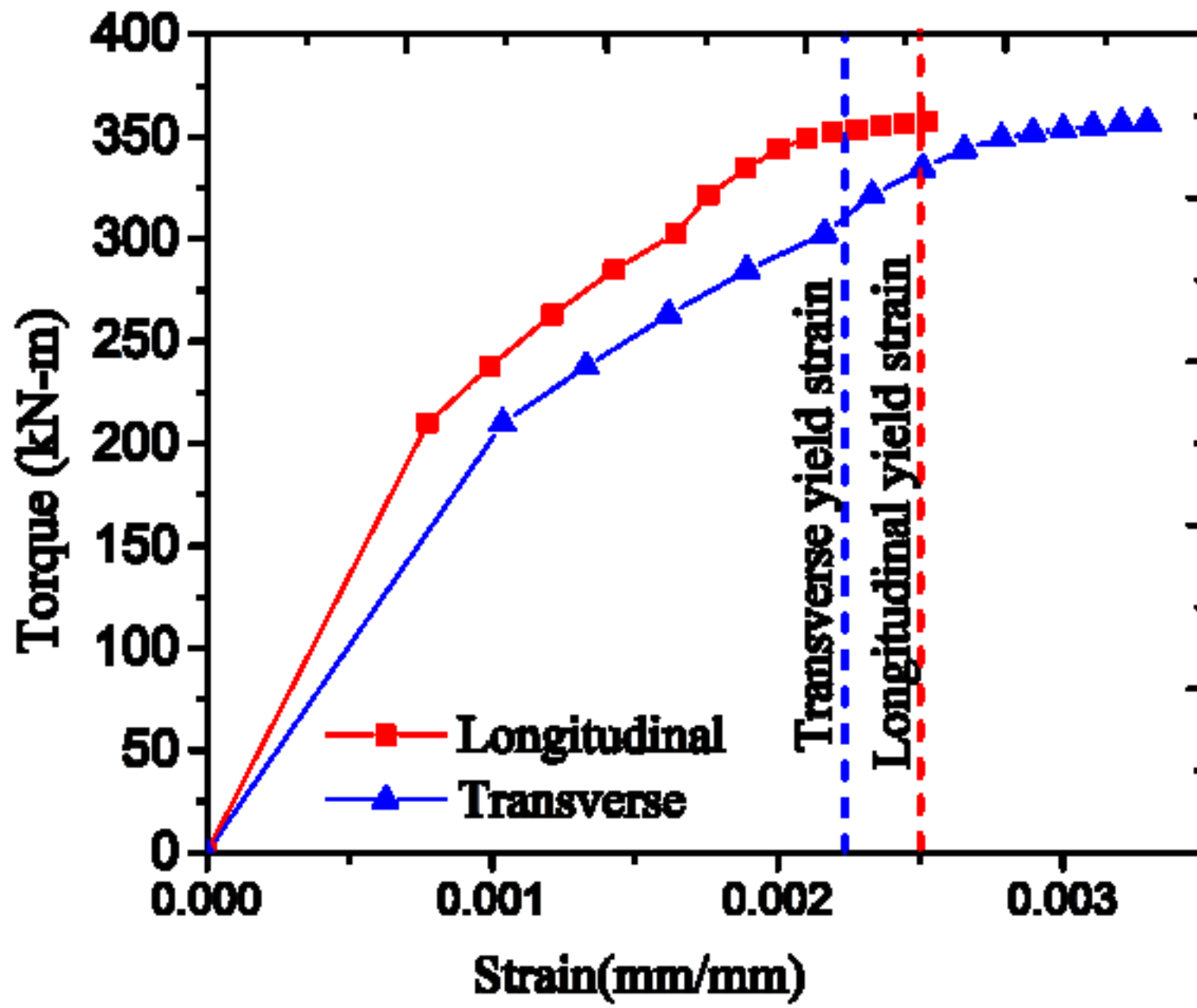


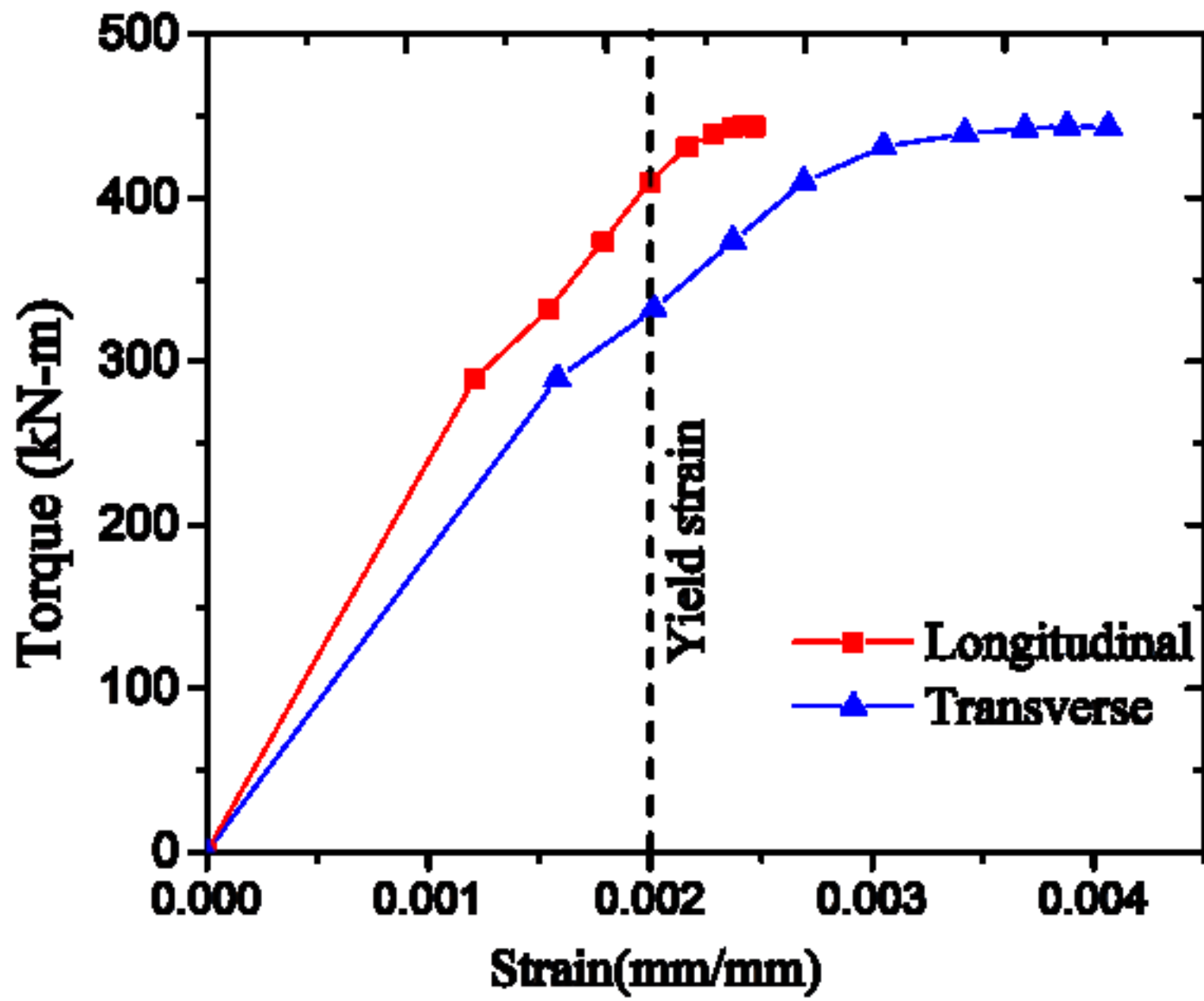


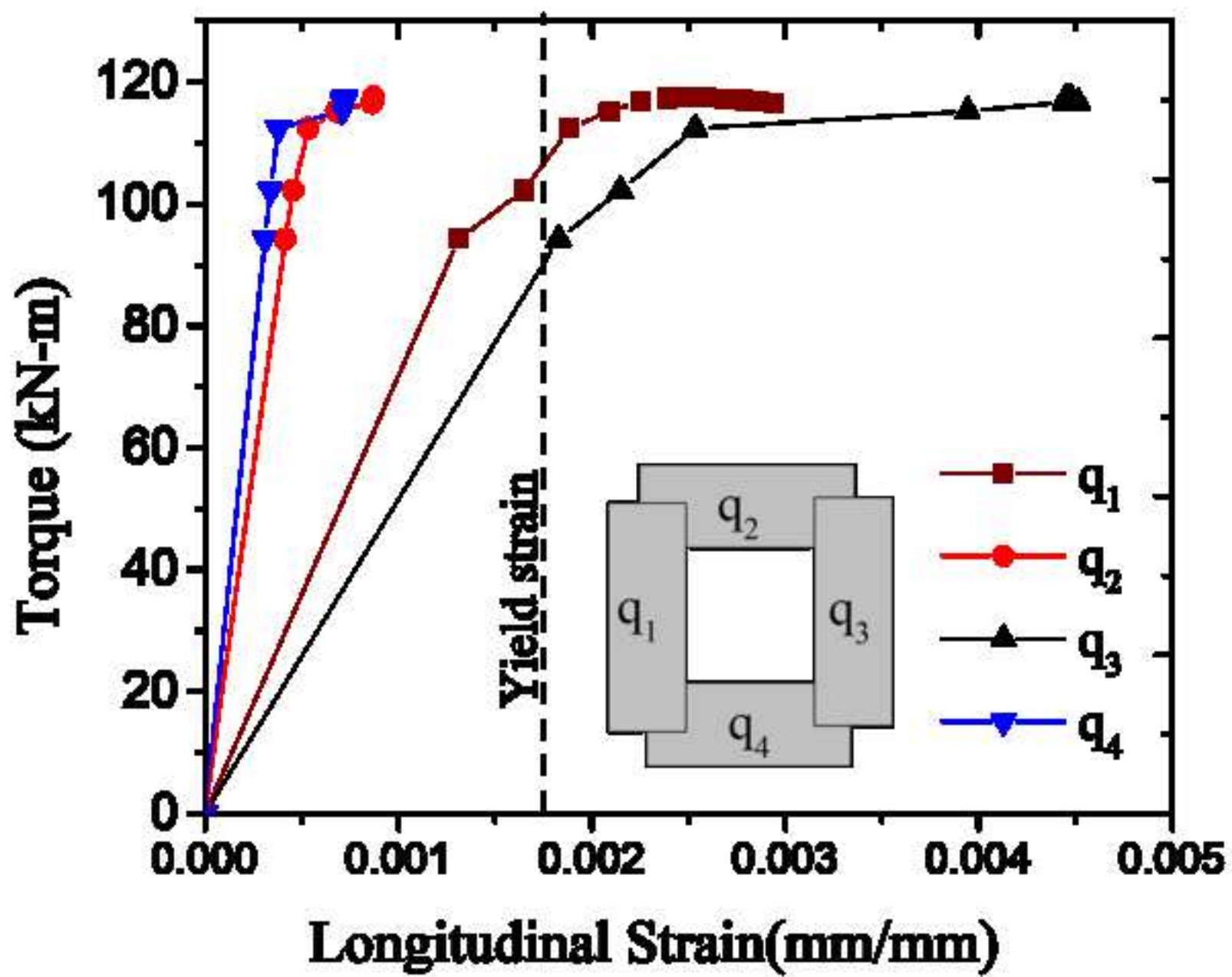


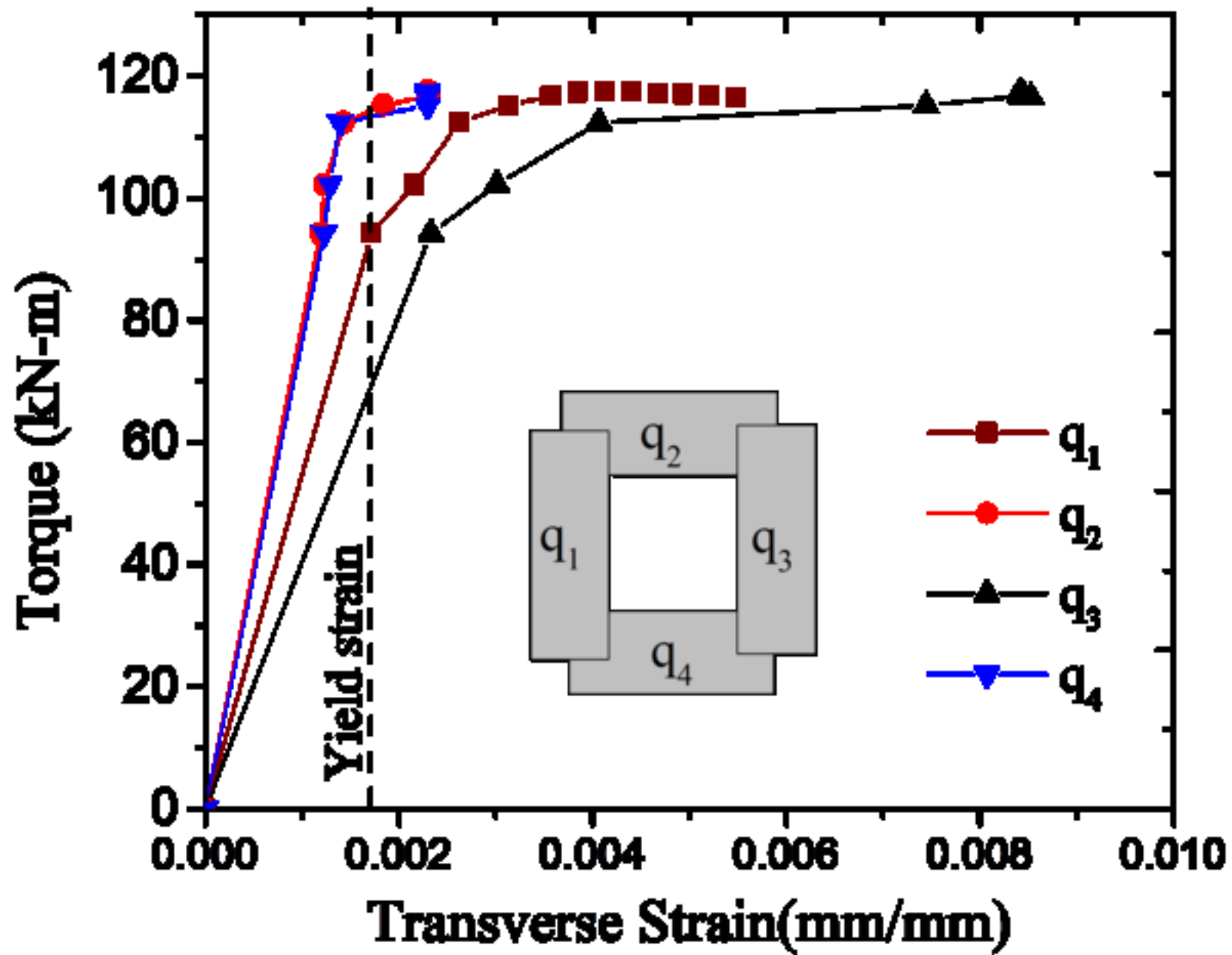


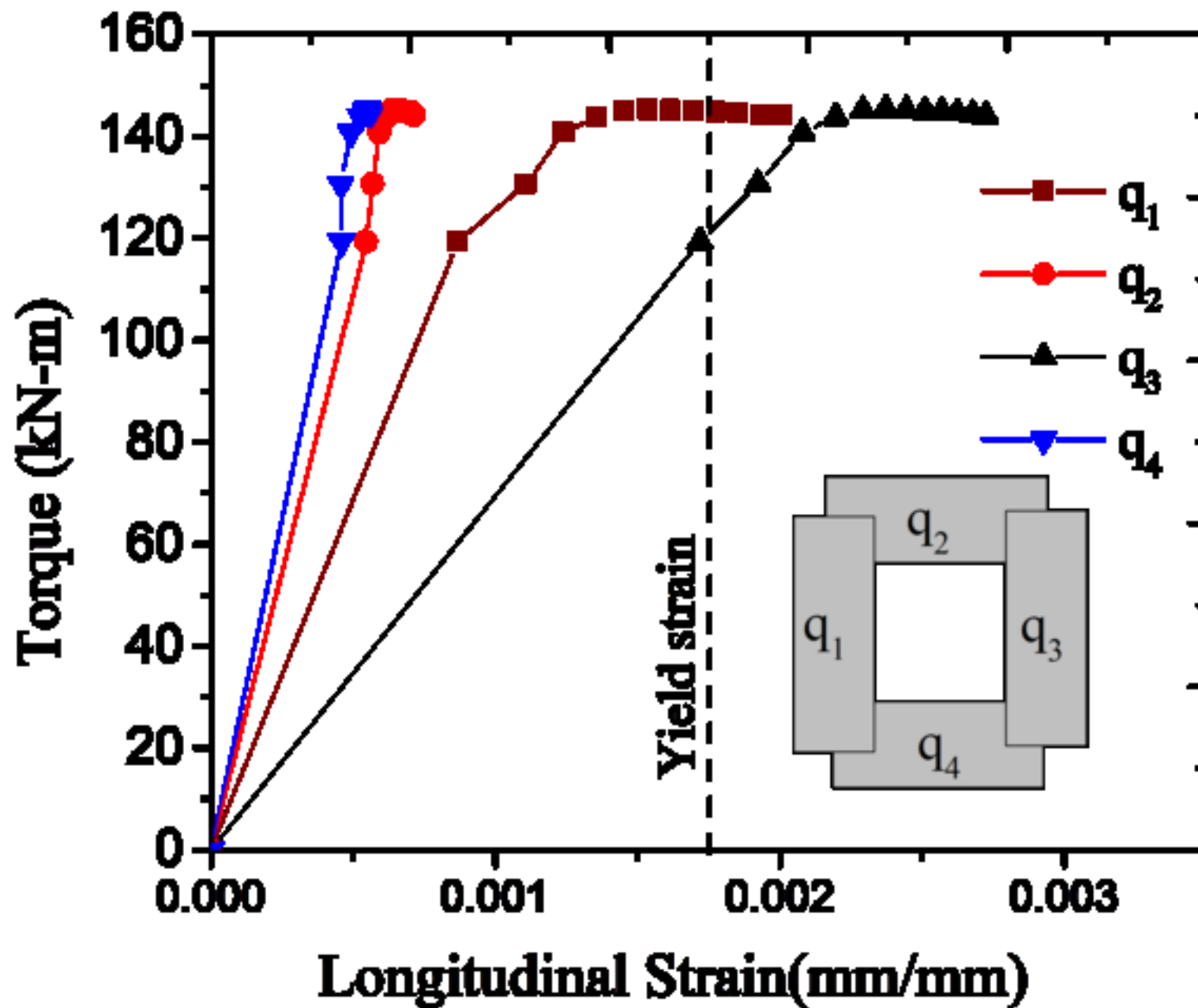


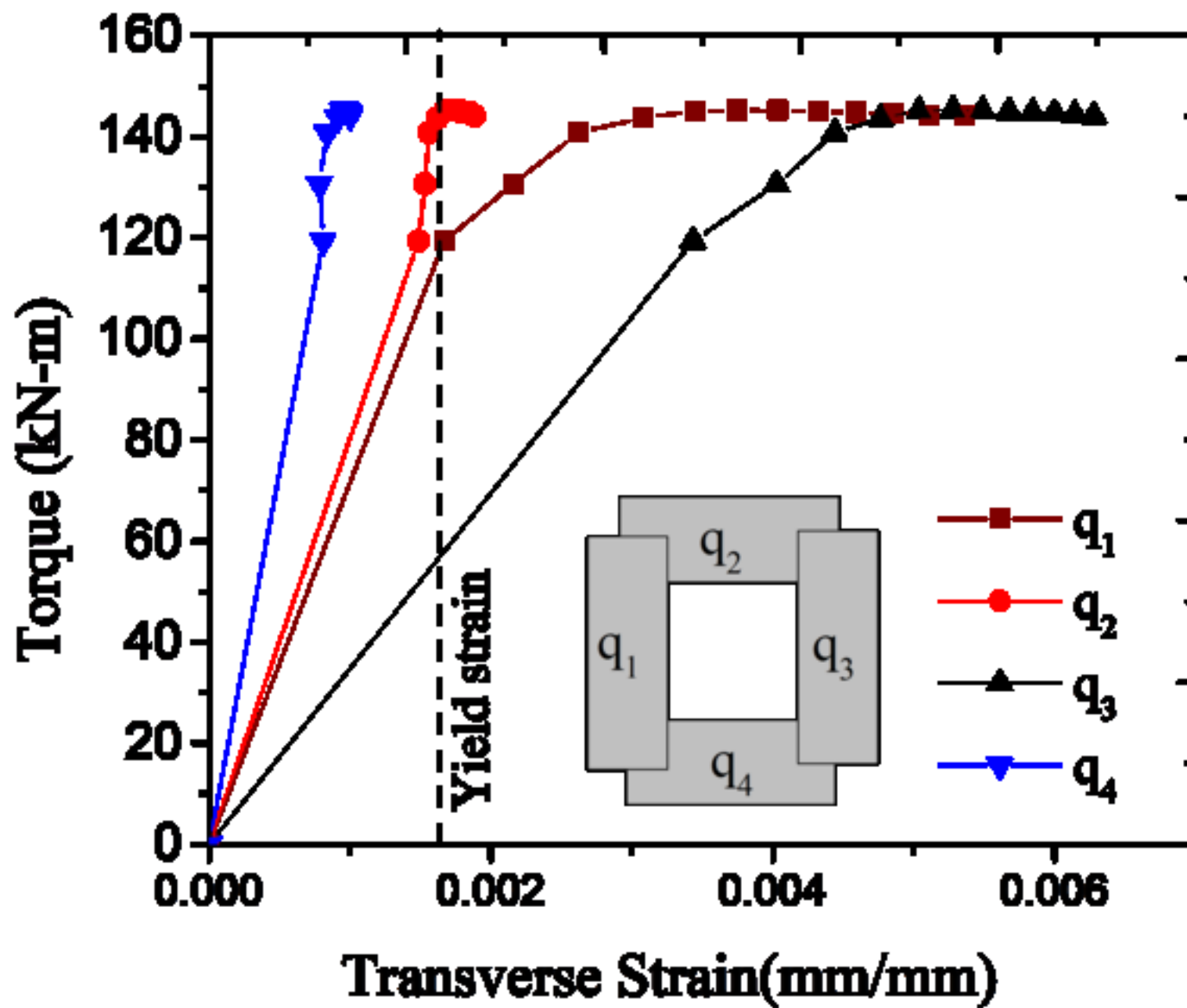


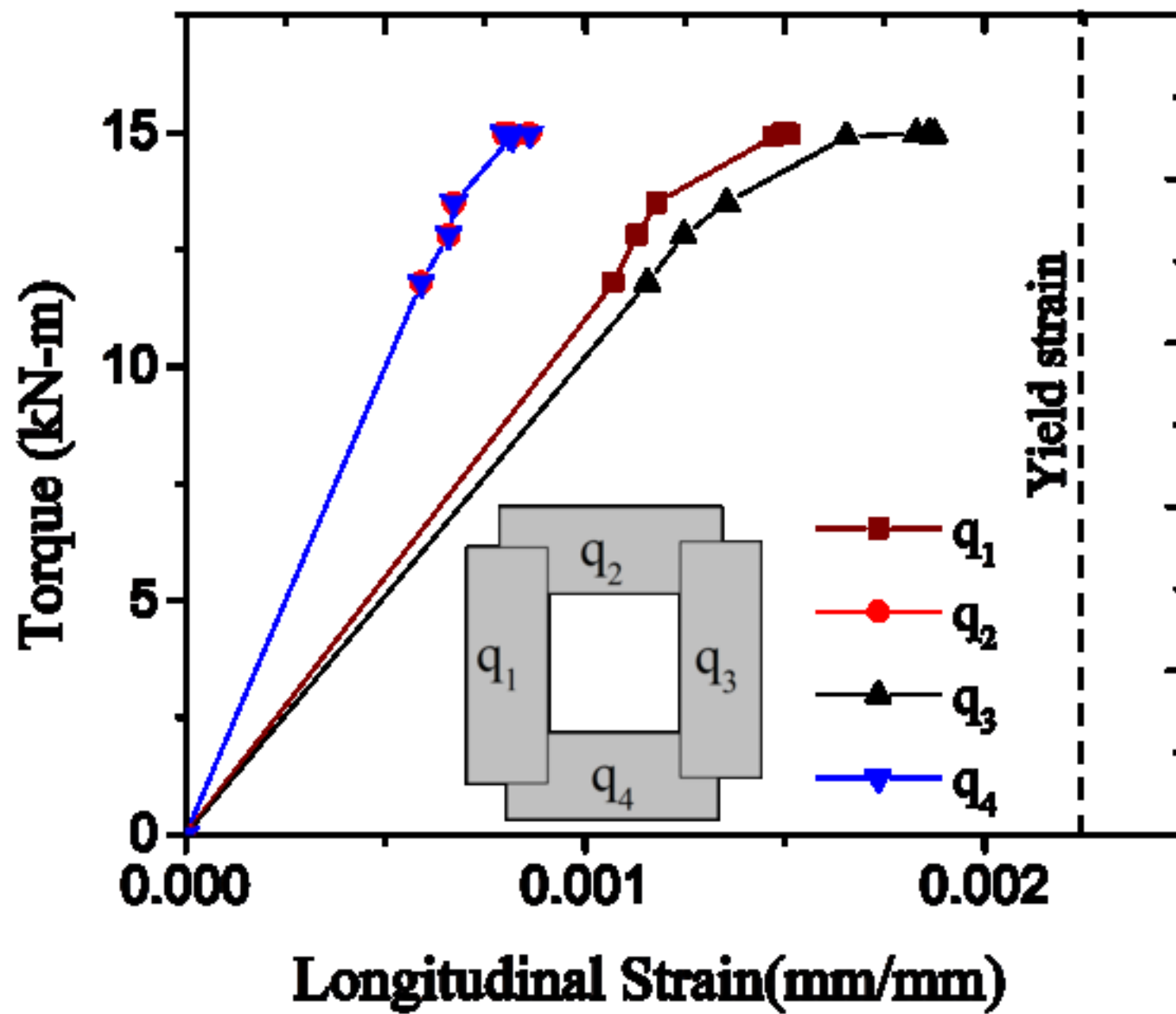


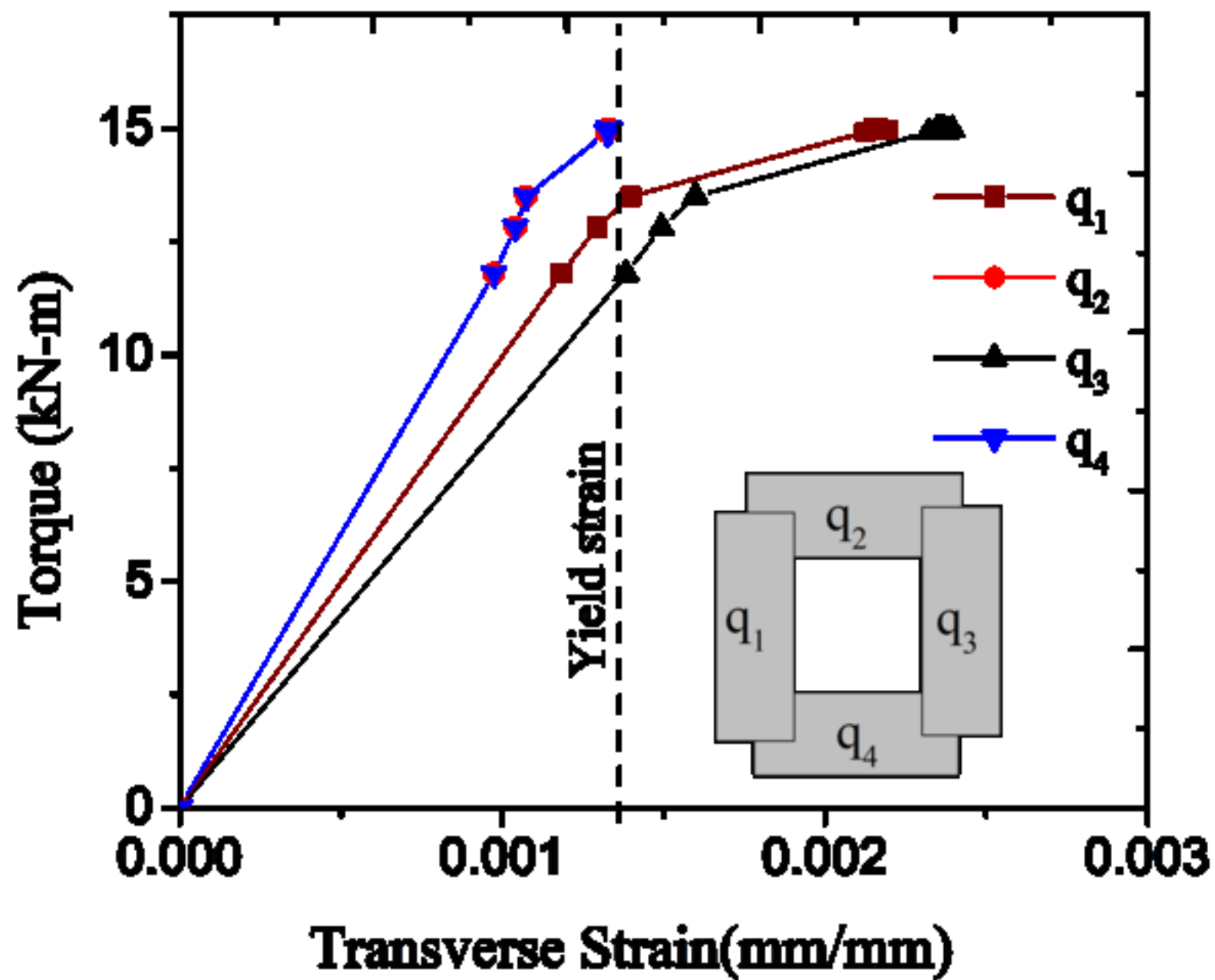


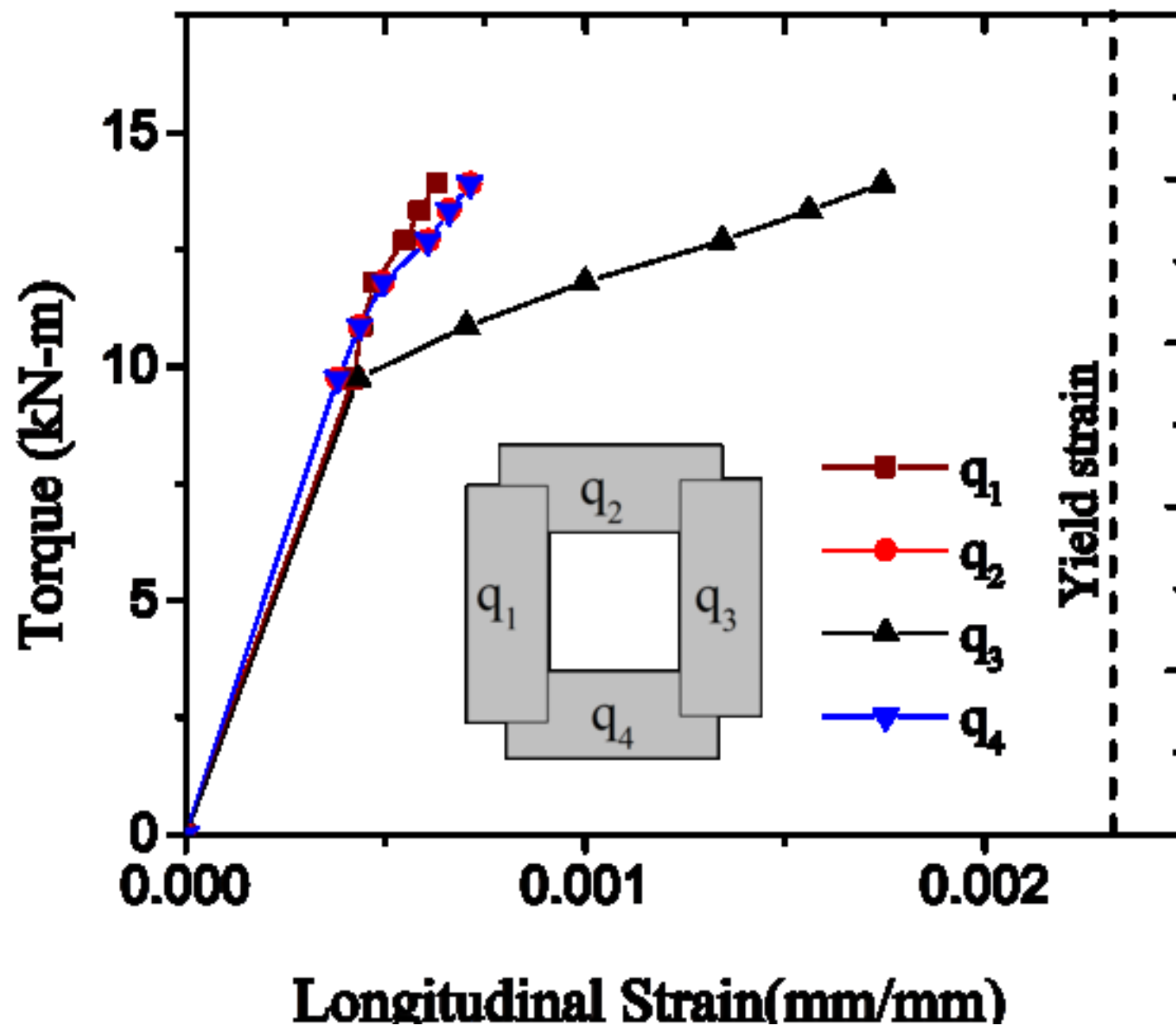


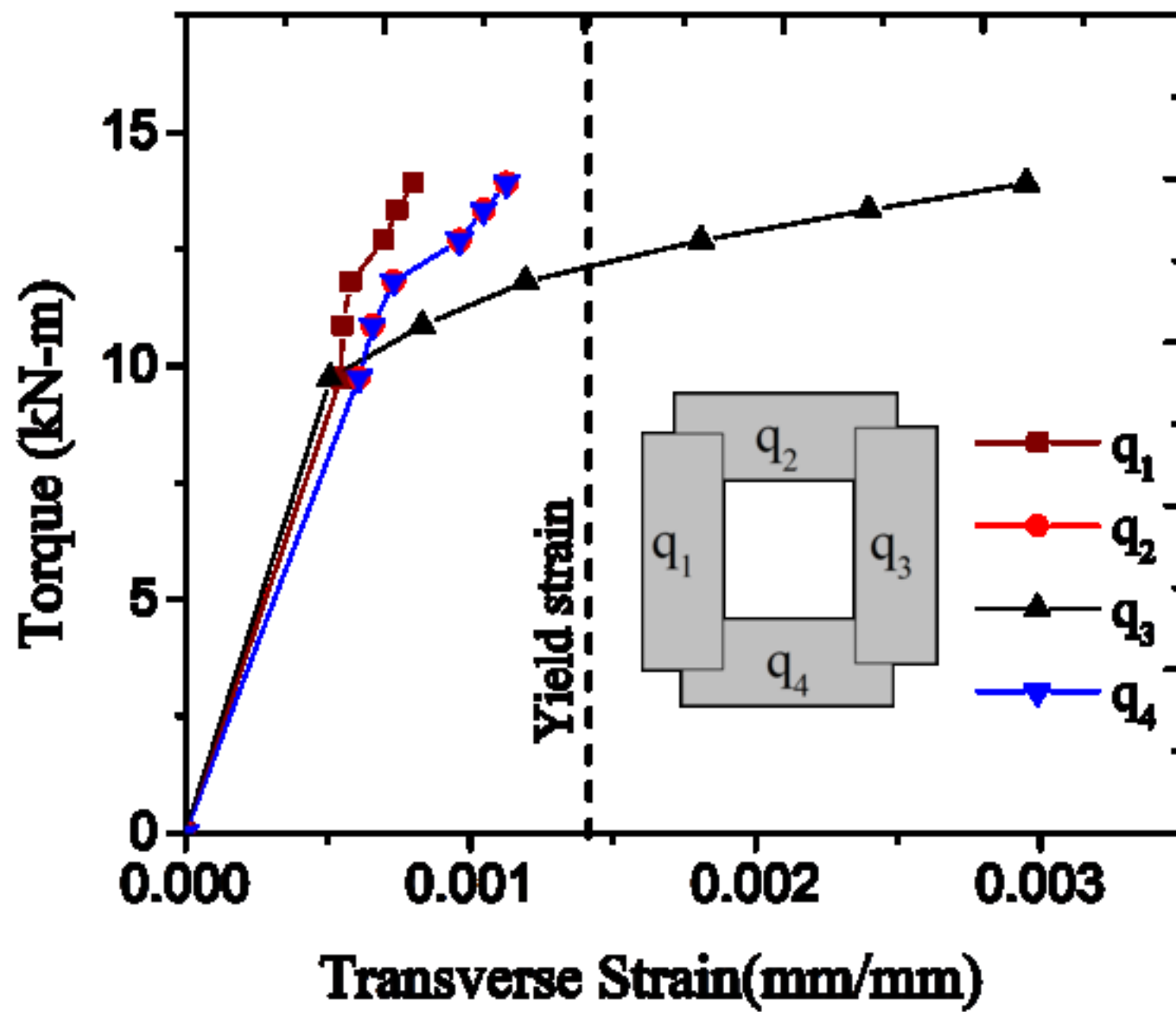


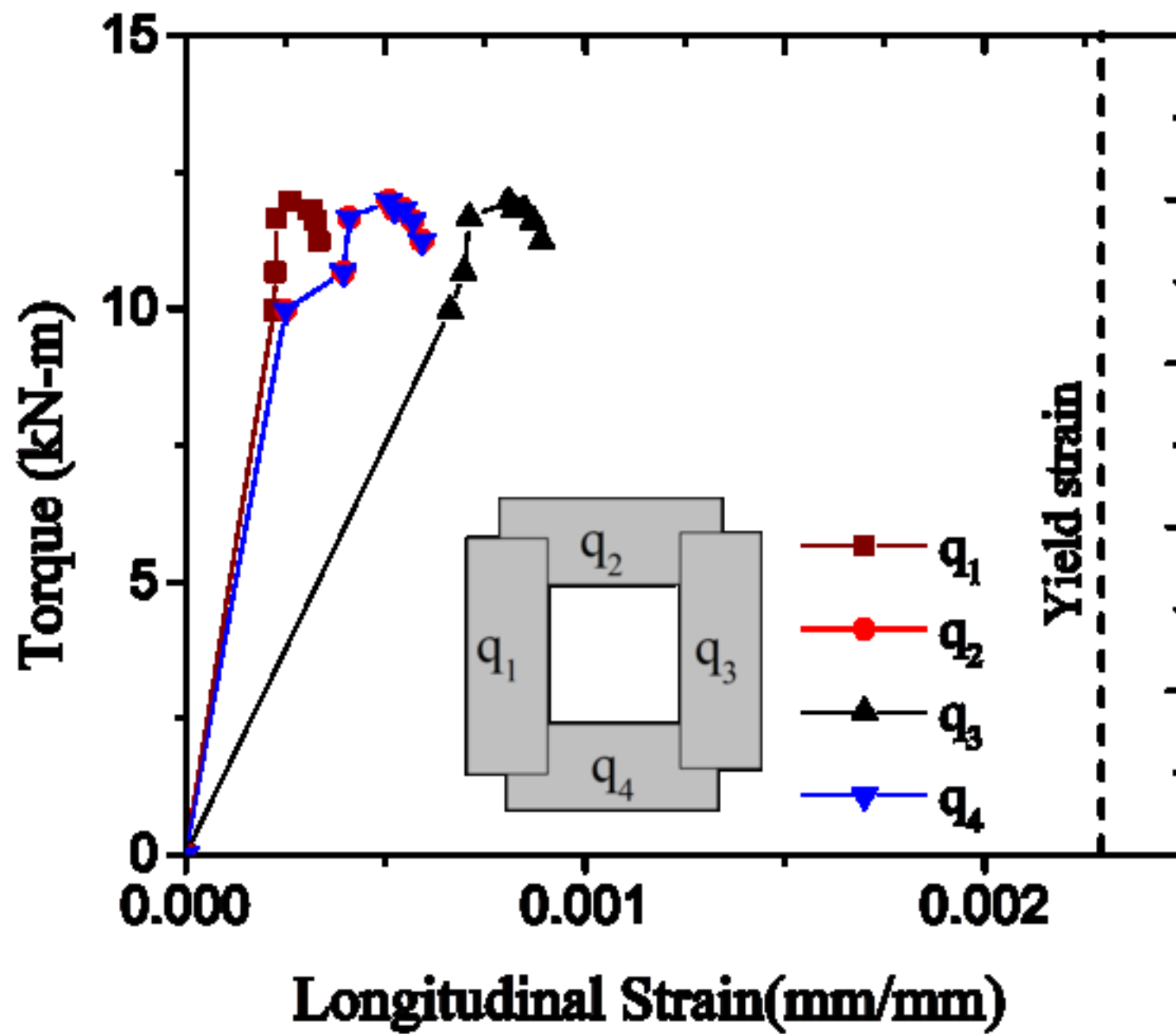


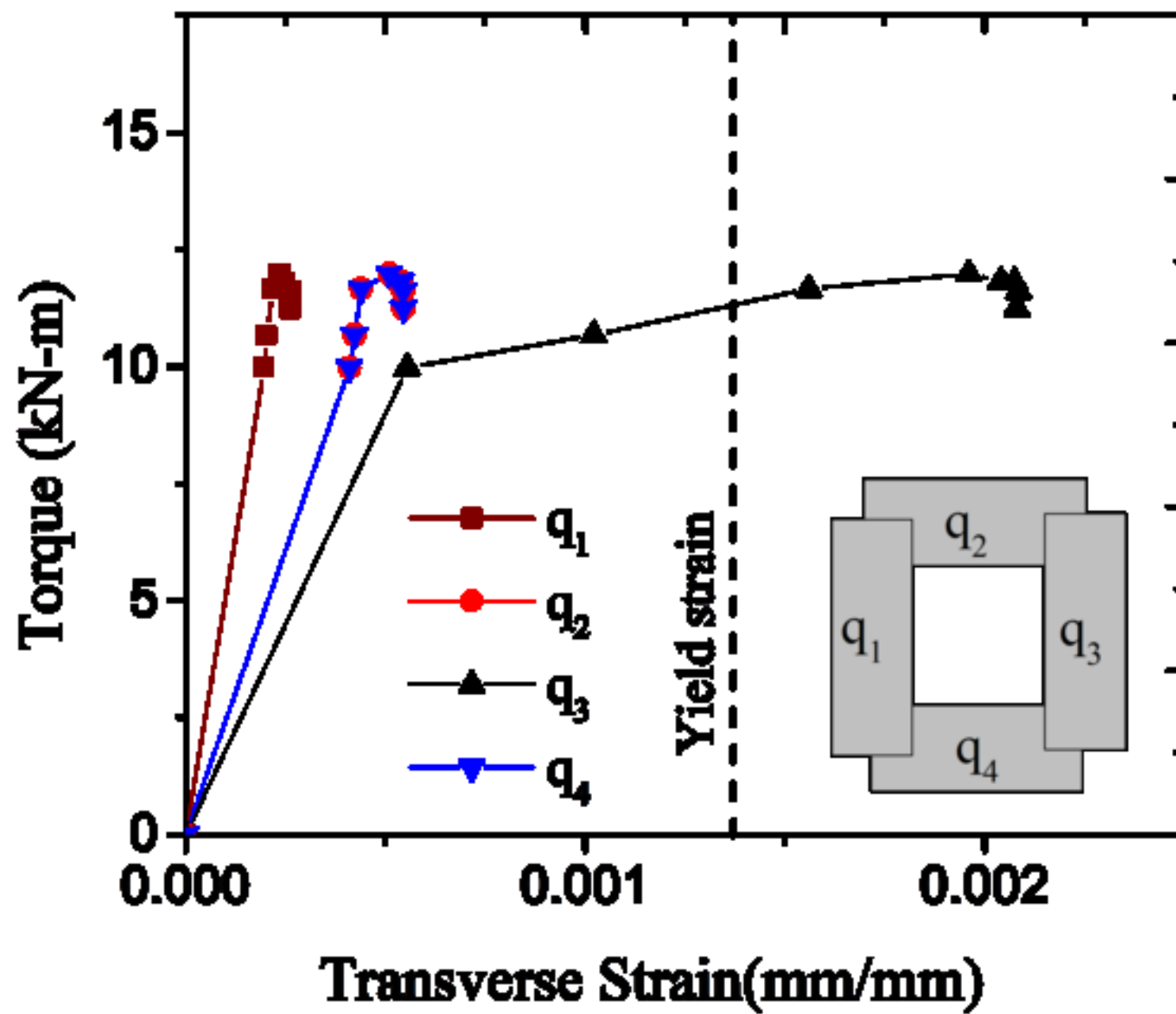


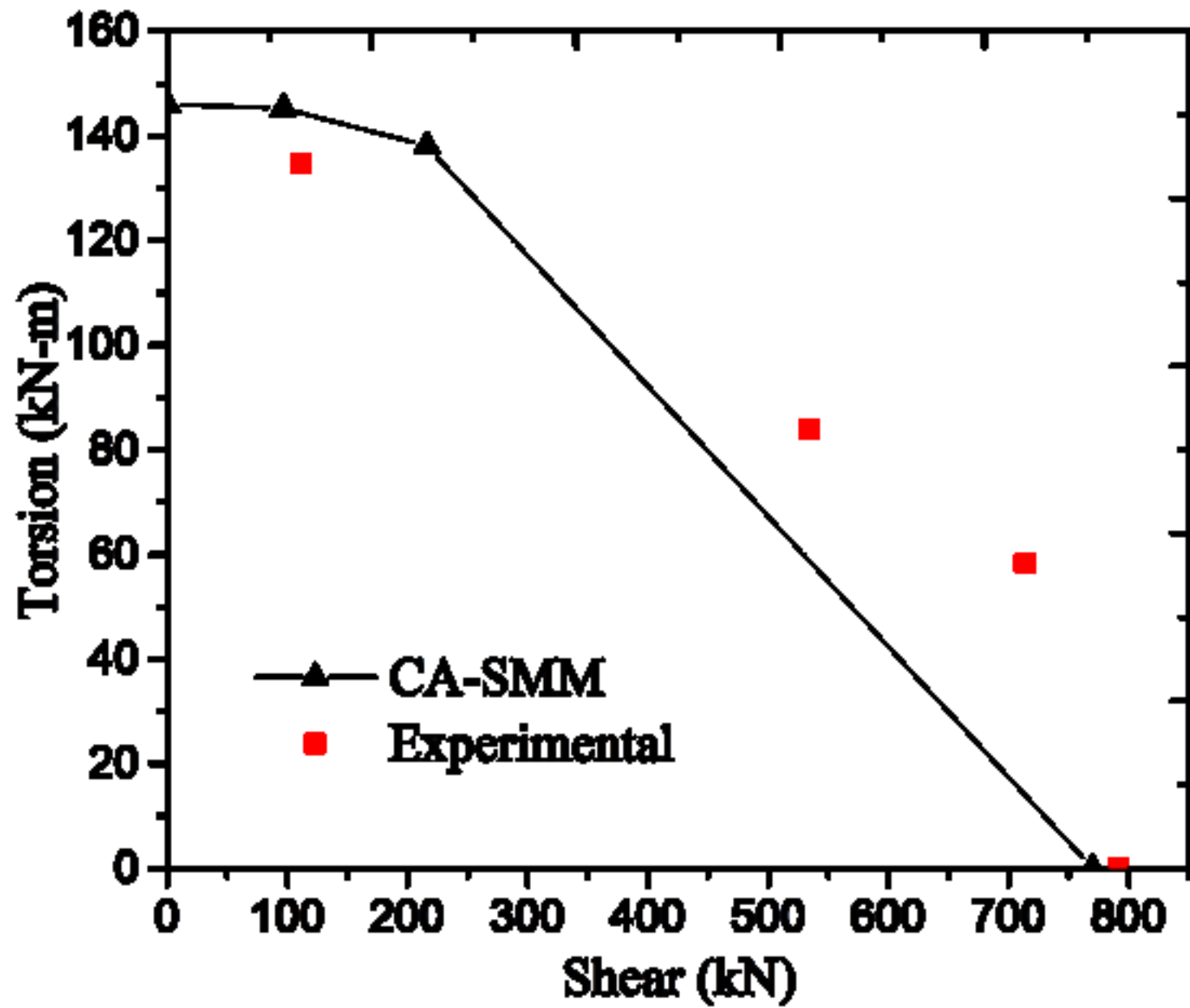


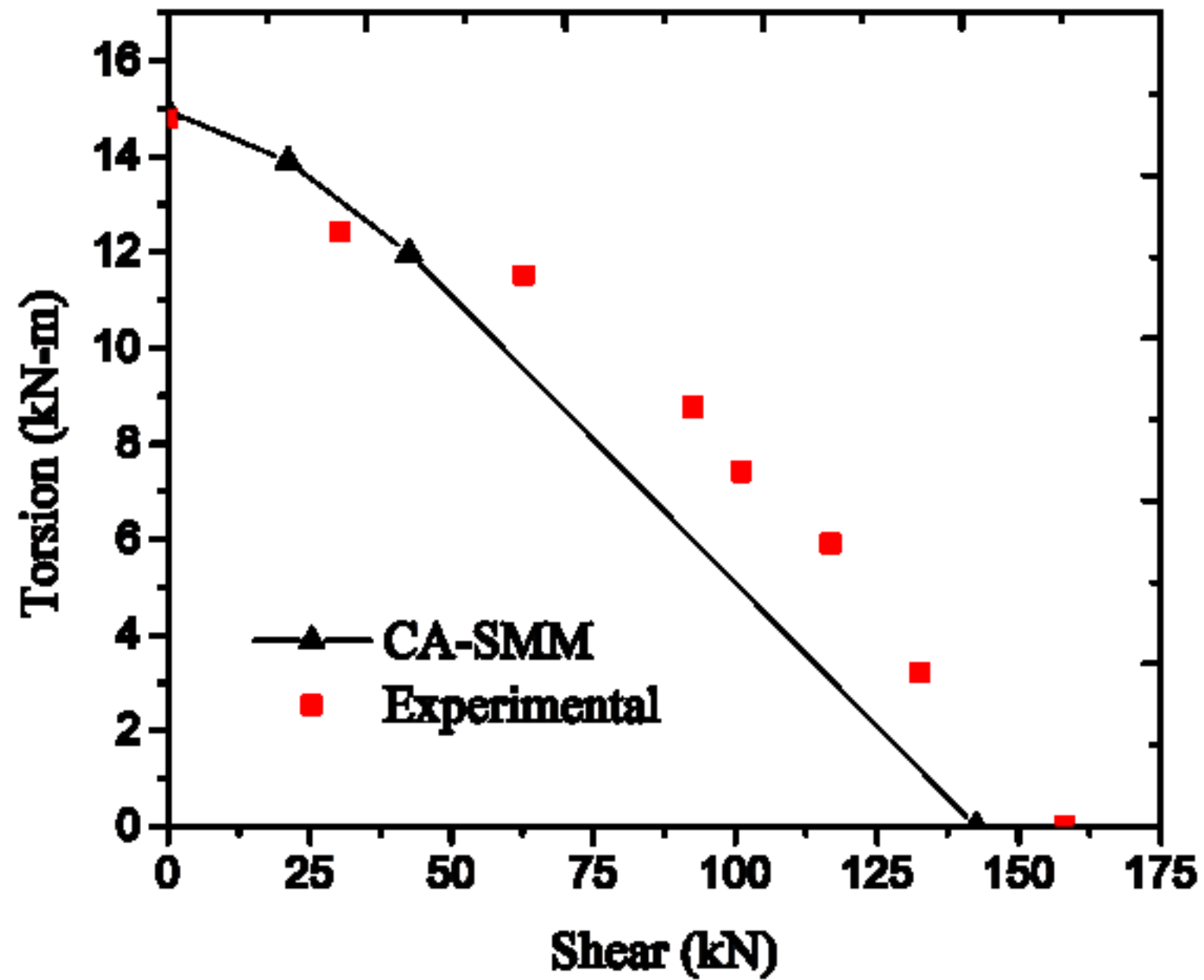


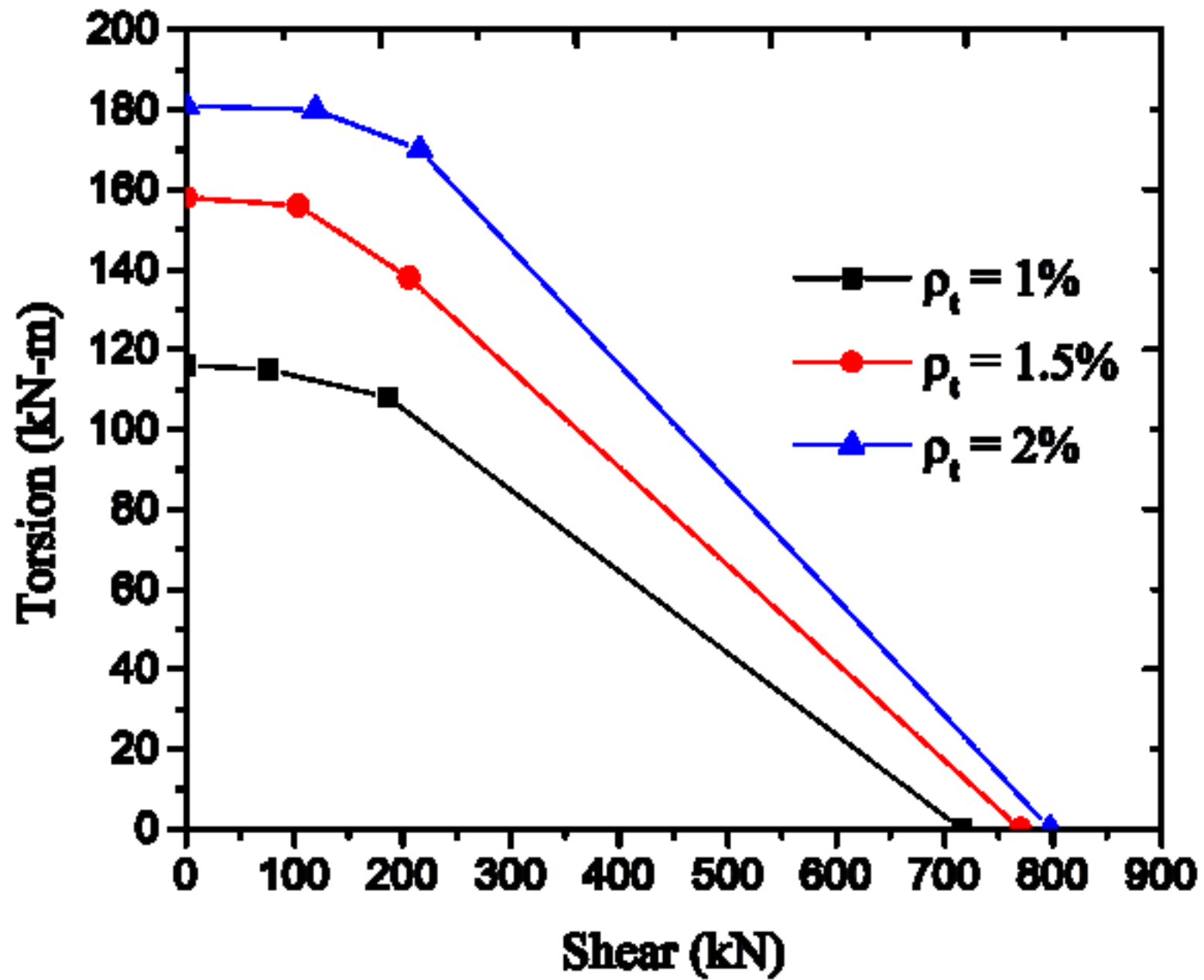


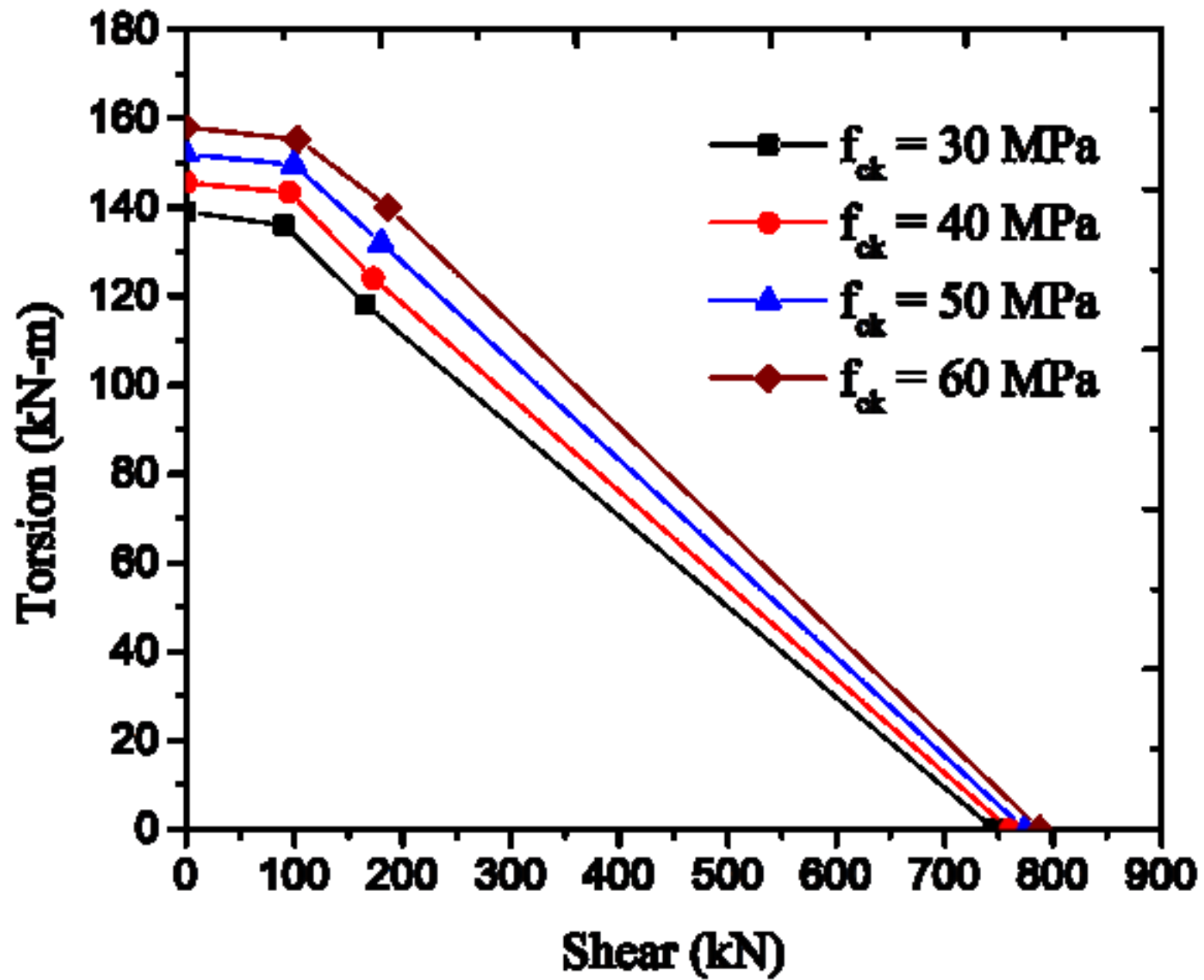












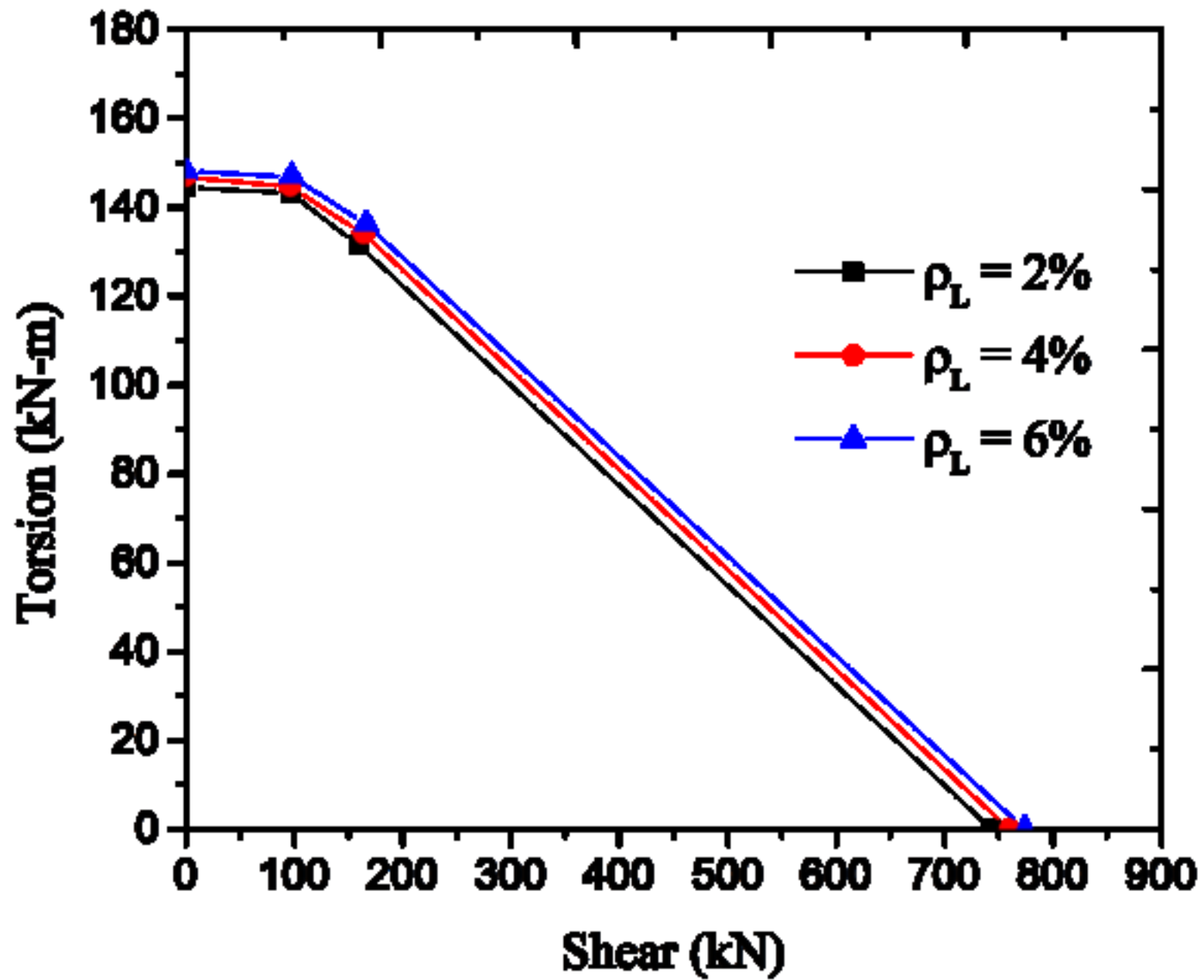


Figure Caption List

Figure 1: Cross-section of a member subjected to combined loading

Figure 2: Idealisation of the cross-section

Figure 3: Membrane Element Description

3a : Membrane element

3b : Principal planes and Coordinate system

Figure 4: Distribution of Shear and Torsion Loads

Figure 5: Stress and strain distribution in the shear flow zone

Figure 6: Distribution of Shear stresses due to Torsion

Figure 7: Concrete Compression behavior (Jeng 2009, Ganganagoudar et al. 2016)

Figure 8: Tension behavior of concrete

Figure 9: Smeared stress-strain behavior of steel

Figure 10: Showing the convergence of the Gradient descent method at a fixed value of $\overline{\varepsilon}_{2s,1}$ for Klus specimen.

Figure 11: Solution algorithm

Figure 12: Cross Section details of Specimen used in Validation

Figure 13: Torque-Twist Predictions

13a: Missouri Column I (Pure Torsion)

13b: Missouri Column II (Torsion + Axial)

13c: Rahal and Collins Series 1 (T/V = 1500 mm)

13d: Rahal and Collins Series 2 (T/V = 1500 mm)

13e: Greene's specimen (Pure Torsion)

13f: Klus (Pure Torsion)

13g: Klus (T/V = 656 mm)

13h: Klus (T/V = 281 mm)

Figure 14: Strain Variation among Specimen

14a: Missouri column I

14b: Missouri column II

14c: Greene's Box Girder Specimen

Figure 15: Longitudinal and Transverse strain variations of specimen

15a: Rahal Collins series 1

15b: Rahal Collins series 1

15c: Rahal Collins series 2

15d: Rahal Collins series 2

15e: Klus (Pure Torsion)

15f: Klus (Pure Torsion)

15g: Klus ($T/V = 656$ mm)

15h: Klus ($T/V = 656$ mm)

15i: Klus ($T/V = 281$ mm)

15j: Klus ($T/V = 281$ mm)

Figure 16: Torsion-Shear Interaction

16a: Rahal Collins series 2

16b: Klus Specimen

Figure 17: Parametric Study – Rahal Collins series 2

17a: Effect of Variation of Transverse Reinforcement Ratio

17b: Effect of Variation of Concrete Compressive Strength

17c: Effect of Variation of Longitudinal Reinforcement Ratio

The undersigned, with the consent of all authors, hereby transfers, to the extent that there is copyright to be transferred, the exclusive copyright interest in the above-cited manuscript (subsequently called the "work") in this and all subsequent editions of the work (to include closures and errata), and in derivatives, translations, or ancillaries, in English and in foreign translations, in all formats and media of expression now known or later developed, including electronic, to the American Society of Civil Engineers subject to the following:

- The undersigned author and all coauthors retain the right to revise, adapt, prepare derivative works, present orally, or distribute the work, provided that all such use is for the personal noncommercial benefit of the author(s) and is consistent with any prior contractual agreement between the undersigned and/or coauthors and their employer(s).
- No proprietary right other than copyright is claimed by ASCE.
- If the manuscript is not accepted for publication by ASCE or is withdrawn by the author prior to publication (online or in print), or if the author opts for open-access publishing during production (journals only), this transfer will be null and void.
- Authors may post a PDF of the ASCE-published version of their work on their employers' **Intranet** with password protection. The following statement must appear with the work: "This material may be downloaded for personal use only. Any other use requires prior permission of the American Society of Civil Engineers."
- Authors may post the **final draft** of their work on open, unrestricted Internet sites or deposit it in an institutional repository when the draft contains a link to the published version at www.ascelibrary.org. Final draft means the version submitted to ASCE after peer review and prior to copyediting or other ASCE production activities; it does not include the copyedited version, the page proof, a PDF, or full-text HTML of the published version.

Exceptions to the Copyright Transfer policy exist in the following circumstances. Check the appropriate box below to indicate whether you are claiming an exception.

U.S. GOVERNMENT EMPLOYEES: Work prepared by U.S. Government employees in their official capacities is not subject to copyright in the United States. Such authors must place their work in the public domain, meaning that it can be freely copied, republished, or redistributed. In order for the work to be placed in the public domain, ALL AUTHORS must be official U.S. Government employees. If at least one author is not a U.S. Government employee, copyright must be transferred to ASCE by that author.

CROWN GOVERNMENT COPYRIGHT: Whereby a work is prepared by officers of the Crown Government in their official capacities, the Crown Government reserves its own copyright under national law. If ALL AUTHORS on the manuscript are Crown Government employees, copyright cannot be transferred to ASCE; however, ASCE is given the following nonexclusive rights: (1) to use, print, and/or publish in any language and any format, print and electronic, the above-mentioned work or any part thereof, provided that the name of the author and the Crown Government affiliation is clearly indicated; (2) to grant the same rights to others to print or publish the work; and (3) to collect royalty fees. ALL AUTHORS must be official Crown Government employees in order to claim this exemption in its entirety. If at least one author is not a Crown Government employee, copyright must be transferred to ASCE by that author.

WORK-FOR-HIRE: Privately employed authors who have prepared works in their official capacity as employees must also transfer copyright to ASCE; however, their employer retains the rights to revise, adapt, prepare derivative works, publish, reprint, reproduce, and distribute the work provided that such use is for the promotion of its business enterprise and does not imply the endorsement of ASCE. In this instance, an authorized agent from the authors' employer must sign the form below.

U.S. GOVERNMENT CONTRACTORS: Work prepared by authors under a contract for the U.S. Government (e.g., U.S. Government labs) may or may not be subject to copyright transfer. Authors must refer to their contractor agreement. For works that qualify as U.S. Government works by a contractor, ASCE acknowledges that the U.S. Government retains a nonexclusive, paid-up, irrevocable, worldwide license to publish or reproduce this work for U.S. Government purposes only. This policy DOES NOT apply to work created with U.S. Government grants.

I, the corresponding author, acting with consent of all authors listed on the manuscript, hereby transfer copyright or claim exemption to transfer copyright of the work as indicated above to the American Society of Civil Engineers.

SURIYA PRAKASH

Print Name of Author or Agent



Signature of Author or Agent

15, April, 2018

Date

More information regarding the policies of ASCE can be found at <http://www.asce.org/authorsandeditors>.

ASCE Authorship, Originality, and Copyright Transfer Agreement

Publication Title: MS STENG-6964-

Manuscript Title: Optimization-Based Improved Softened Membrane Model for Rectangular Reinforced Concrete Members Under Combined Shear and Torsion

Author(s) - Names, postal addresses, and e-mail addresses of all authors

Srinasha Reddy Kotnamuthyala Graduate Student, Email: ce15mech11023@iit.ac.in Department of Civil Engineering, IIT Hyderabad, India

Nikesh Thammishetti, Ph.D. Candidate, Email: ce16resch11005@iit.ac.in Department of Civil Engineering, IIT Hyderabad, India

Suriya Prakash S, Associate Professor and Corresponding Author, Email: suriyap@iit.ac.in Department of Civil Engineering, IIT Hyderabad, India

Chandrika Prakash Vyasarayam, Associate Professor, Email: vcp@iit.ac.in Department of Mechanical and Aerospace Engineering, IIT Hyderabad, India

I. Authorship Responsibility

To protect the integrity of authorship, only people who have significantly contributed to the research or project and manuscript preparation shall be listed as coauthors. The corresponding author attests to the fact that anyone named as a coauthor has seen the final version of the manuscript and has agreed to its submission for publication. Deceased persons who meet the criteria for coauthorship shall be included, with a footnote reporting date of death. No fictitious name shall be given as an author or coauthor. An author who submits a manuscript for publication accepts responsibility for having properly included all, and only, qualified coauthors.

I, the corresponding author, confirm that the authors listed on the manuscript are aware of their authorship status and qualify to be authors on the manuscript according to the guidelines above.

SURIYA PRAKASH

15, April 2018

Print Name

Signature

Date

II. Originality of Content

ASCE respects the copyright ownership of other publishers. ASCE requires authors to obtain permission from the copyright holder to reproduce any material that (1) they did not create themselves and/or (2) has been previously published, to include the authors' own work for which copyright was transferred to an entity other than ASCE. Each author has a responsibility to identify materials that require permission by including a citation in the figure or table caption or in extracted text. Materials re-used from an open access repository or in the public domain must still include a citation and URL, if applicable. At the time of submission, authors must provide verification that the copyright owner will permit re-use by a commercial publisher in print and electronic forms with worldwide distribution. For Conference Proceeding manuscripts submitted through the ASCE online submission system, authors are asked to verify that they have permission to re-use content where applicable. Written permissions are not required at submission but must be provided to ASCE if requested. Regardless of acceptance, no manuscript or part of a manuscript will be published by ASCE without proper verification of all necessary permissions to re-use. ASCE accepts no responsibility for verifying permissions provided by the author. Any breach of copyright will result in retraction of the published manuscript.

I, the corresponding author, confirm that all of the content, figures (drawings, charts, photographs, etc.), and tables in the submitted work are either original work created by the authors listed on the manuscript or work for which permission to re-use has been obtained from the creator. For any figures, tables, or text blocks exceeding 100 words from a journal article or 500 words from a book, written permission from the copyright holder has been obtained and supplied with the submission.

SURIYA PRAKASH

15, April, 2018

Print name

Signature

Date

III. Copyright Transfer

ASCE requires that authors or their agents assign copyright to ASCE for all original content published by ASCE. The author(s) warrant(s) that the above-cited manuscript is the original work of the author(s) and has never been published in its present form.

Dear Editor,

Thank you for reviewing and providing us with the opportunity to revise our manuscript (MS STENG-6964). We appreciate the careful review, complimentary comments, and constructive suggestions to improve our work. We believe that the manuscript is significantly improved by incorporating the suggestions.

Following this letter are the point-by-point response to reviewers' comments, including how and where the text has been modified. The revision has been developed, and each author has approved the final form of this revision. We hope that you find our responses satisfactory and that the manuscript is now acceptable for publication.

Thank you for your consideration.

Sincerely,

S. Suriya Prakash, Ph.D.
Associate Professor
Department of Civil Engineering
Indian Institute of Technology, Hyderabad
Sangareddy, Telangana, India
Email: suriyap@iith.ac.in

Response to Reviewer's Comments

Optimization Based Improved Softened Membrane Model for Rectangular Reinforced Concrete Members under Combined Shear and Torsion

(Manuscript Number: MS STENG-6964)

We are very much thankful to the reviewers for their deep and thorough review. We have revised the manuscript in the light of their useful suggestions and comments. We hope our revision has improved the manuscript to a level of their satisfaction. Number wise answers to their specific comments/suggestions/queries are as follows.

Response to Reviewer #1 Comments

General Comment: The paper entitled "Optimization-Based Improved Softened Membrane Model for Rectangular Reinforced Concrete Members under Combined Shear and Torsion" contains original contribution to the analytical study of Reinforced Concrete (RC) members under predominant torsion. A Combined Actions Softened Membrane Model (CA-SMM) to evaluate the entire behaviour of RC structural members under torsion, shear and axial load is developed and evaluated. The proposed model adopts an interesting optimization technique (namely gradient descent method) to solve the well-known non-linear equations of the SMM. Although there are several versions of the SMM available in the literature that face successfully the problem of torsion certain utility. Validation of the CA-SMM is achieved using comparisons between analytical and experimental torsional moment versus angle of twist curves. Further, an effort to investigate the interaction between shear and torsion using the developed method as a numerical tool for parametric analysis is attempted. The manuscript is well-structured, and the developed model is adequately presented.

Response: The authors thank the reviewer for the positive feedback on the submitted work. Reviewers suggestions have been included as explained below:

1. *The linear, pre-cracking behavior of the analytical torsional moment versus angle of twist curves illustrated in the diagrams of Fig. 13 presents increased stiffness that is very close to the*

experimentally observed one. However, this is not justified since based on the assumptions of the model (see also line 118) "the concrete member is assumed to act as a truss after cracking." Further, it is claimed that (see also lines 330-332) "...the response predicted by the CA-SMM is better in the post-cracking regime and close to the experimental peak values." Additional comments on these issues and proper clarification are required.

Response: The authors agree with the reviewer's comment that the apparent truss model should lead to less stiff prediction. However, the assumption that the RC member acts as a truss is valid only after cracking. The pre-cracking behavior is known to be linear. The point corresponding to which cracking occurs is calculated from the expressions given by Collins and Mitchell (1991). The information explaining the same has been added in lines 128-131 (Page 3). As the current work focuses more on the truss model based SMM theory, the equations about cracking are not mentioned explicitly in the draft. Those equations are referred to the below references, and the same discussion has been included in the revised manuscript.

References added:

- Collins, M.P., and Mitchell, D. (1991), "Prestressed Concrete Structures," Response Publications, Canada.
- Mondal, TG, and Prakash, SS. (2015) "Effect of tension stiffening on the behavior of square RC columns under torsion." Struct. Eng. Mech. J 54.3 (2015): 501-520.

As suggested by the reviewer, more clarifications on the predictions of model and comparisons with the experimental results are provided.

2. *The results and the concluding remarks derived from the torsional moment versus longitudinal and transverse strain diagrams presented in Fig. 15 are not adequately discussed. The statement reported in line 352 that "... the model is capable of capturing the trend of strain variations in the section accurately" needs further justification and explanation.*

Response: The experimental results pertaining to the variation of longitudinal and transverse strains are not available for all the specimens to compare with the analytical predictions. However, the authors wanted to highlight the variation of the strain distribution in the longitudinal and transverse steel to illustrate the capability of the model in calculating the strains at the local level. Depending upon the loading that the panel is subjected to (Pure torsion/ torsion + shear/ torsion – shear), there are four different strains on four different panels, as depicted in Fig. 15. Transverse

steel reinforcement primarily resists loads of torsion and shear. Hence, as expected, the strains will increase smoothly until peak load and decreases after that. As the experimental data is not available, the authors want to depict with the graphs that the model is predicting the strains as expected from physical behavior. The section on “distribution of strains in reinforcement” has been elaborated in the revised manuscript.

- 3. The interaction between torsion and shear and the use of the developed CA-SMM as a numerical tool for parametric analysis is very briefly presented. It is strongly recommended to enrich these sections. The influence of the axial load on the torsional response is also a parameter that could be further examined to provide useful interaction curves. The articles "Torsion-shear-flexure interaction in reinforced concrete members", "Strength of prestressed concrete beams in torsion" and "Combined torsion and bending in reinforced and prestressed concrete beams using simplified method for combined stress-resultants" could help in this direction since they present and discuss the flexure-torsion and shear-torsion interaction curves with and without axial force of RC members.*

Response: The authors thank the reviewer for the valuable suggestion. All the suggested references are included in the revised manuscript. Major findings from these references are also presented in the revised manuscript.

The key interaction between torsion and shear is due to the change in shear flow (Eq. 5), which depends on the direction of application of the torsion and shear loads. Torsion-shear interaction diagram is shown in Fig. 4 and quantified in equation 5. The current work focuses on the interaction of torsion and shear, and the same has been validated with the available experimental data.

Authors would like to clarify that the developed algorithm considers the effect of the axial load as well. Axial stress is included in the CA-SMM formulation. The interaction between axial stress and the shear stresses occurs at the membrane element level. The presence of axial compression stress increases the capacity of the shear element, and it is reciprocal for axial tensile stress. The same effect will be reflected at member level when the applied loads are torsion or shear. However, including the curvature and flexural effects in the proposed model is scope for further work. Therefore, only the axial load has been included in the algorithm but not the flexure.

4. *The concrete confinement in RC members with a short spacing of stirrups has been proved as a parameter of significant influence on the torsional response. Special stress-strain relationships of softened and confined concrete have been proposed for RC members, such columns with high ratio of transverse reinforcement. The Authors are invited to comment this issue.*

Response: The authors agree with the reviewer that the short spacing of stirrups will have a significant influence on the torsional response due to a possible reduction in softening of the concrete. The confinement of concrete due to the short spacing of stirrups will enhance the torsional performance of RC member. In the current work, the authors have used the close spacing of stirrups only in parametric studies. The transverse reinforcement ratio is increased theoretically, and the predictions are calculated. By keeping the behavior of concrete as a constant help in observing the changes predicted by the model, with the change in the intended parameter, i.e. transverse reinforcement ratio. The authors only want to depict the applicability of the model for parametric study. The confinement effect due to the close spacing of stirrups and its possible effect on the reduction in softening of concrete will be very interesting. More work is needed to understanding the interaction between the confinement and softening effect and is scope for further work.

Response to Reviewer #2 Comments

General Comment: *The authors have presented a very detailed, well-written paper on the topic of the Optimization Based Improved Softened Membrane Model for Rectangular Reinforced Concrete Members under Combined Shear and Torsion.*

Response: The authors would like to thank the reviewer for his appreciation.

1. *The reviewer observes the analytical model results deviation from the experimental results in the non-elastic region of the load curve. Please explain the possible reasons more elaborately.*

Response: The authors agree with the reviewer that the predictions of the model deviate somewhat from the experimental results in the post-peak region. There are various assumptions involved in the model as follows:

1. “Section is modeled as an assembly of four cracked shear panels”. This assumption is essential to distribute the external loads among the shear panels. Though the actual stress state is very complex and the stress is distributed across the cross-section, the above assumption reduces the overall stress state into four different stress states (one stress state on each panel). The predictions can be refined more accurately by modeling the cross section using more number of panels and by establishing the compatibility conditions among the panels. However, this incurs a significant increase of computational time, and development of sophisticated computational tools would be interesting and is scope for future work.
2. Torsion is modeled using Bredt’s thin tube theory. According to which, the externally applied torsion is resisted by the shear flow stresses developed in the region of shear flow depth ‘ t_d ’ and also the stress is assumed to be uniform across the depth. The actual stress state due to torsion is very complicated for rectangular cross-sections. The results can be refined more accurately by including the exact stress state that occurs due to torsion which is very complicated and has not been established precisely for RC members. The authors here, have used the Bredt’s thin tube theory which is the current state of the art concerning the truss models for modeling torsional effects in RC section.

The predictions of the proposed model are reasonably accurate considering the various assumptions and interactions among the parameters (i.e., sectional details, loading levels, spalling). Future work should focus on more refined predictions. The above discussion is included in the revised draft under the sections “Bredt’s thin tube theory” and “Summary and conclusions.”

Response to Reviewer #3 Comments

The authors thank the reviewer for his detailed review and suggestions. His comments were all included as discussed below:

1. *Page 2, Line 4: Omitted work by Onsongo for RC columns, although his paper is listed in the references (note column in the title).*

Response: The additional reference is included as suggested by the reviewer.

2. *Page 2, Line 50: Omitted work by Greene and Belarbi, although their specimen is used in the analysis included in the paper.*

Response: The additional reference is included as suggested by the reviewer.

3. *Page 3, Line 67-70: The paper incorrectly states that the SMMT which has a 2016 reference was the basis (“also extended”) for models that were developed before 2016 and published in 2009. This is not possible.*

Response: It is a typo. The authors only mean that the SMMT has been extended for various cross-sectional shapes and applications that include box girders, circular sections and FRP strengthened specimen. The phrases that created confusion in the timeline has been rephrased in the same section as mentioned below:

“SMM based torsional model was extended to other geometries, and strengthening configuration like box girders (Greene and Belarbi 2009), hollow RC members (Jeng and Hsu 2009), and rectangular sections strengthened with fiber reinforced polymer (FRP) composites (Ganganagoudar et al. 2016) under pure torsion. Ganganagoudar et al. (2016) have also extended the SMM based model for torsion (SMMT) for circular RC beams and validated with the experimental test results.”

4. *Page 3, Line 84: Bidirectional stress effects used here, but not adequately defined until page 3, line 103. Without a definition, the term is ambiguous and could mean a number of things.*

Response: The authors have introduced the Poisson effect and bi-directional stress states at their first usage in the revised draft, at lines 62-65.

5. Page 5, Line 137 to 140: these four equations have been in at least one of the references cited in this paper. Reference should be given to the source.

Response: Included as suggested. The work of Greene and Belarbi 2009 has been referred in this context.

6. Page 6, Line 162 to 165: these four equations have been in at least one of the references cited for this paper. Reference should be given to the source.

Response: Included as suggested. The works of Greene and Belarbi 2009, Rahal and Collins 1995 have been referred in this context.

7. Page 7, Line 181 to 184: these four equations have been in at least one of the references cited in this paper. Reference should be given to the source.

Response: Included as suggested. The work Hsu and Zhu 2002 has been referred in this context.

8. Page 8, Line 191 and 194: Solving equation 11 into equation 12a would result in $t_{d,i}$ equal to negative $t_{d,i}$. Please explain.

Response: The equation is corrected in the revised draft as given below. The shear flow depth ‘ t_d ’ is always positive. Compression strains are taken as negative in the current analysis, therefore negative of negative number gives a positive value for ‘ t_d ’.

$$\psi_i = \frac{-\overline{\varepsilon_{2s,i}}}{t_{d,i}} \quad (11)$$

$$t_{d,i} = \frac{-\overline{\varepsilon_{2s,i}}}{\psi_i} \left(\leq \frac{b_o}{2} \right) \quad (12a)$$

9. Page 8, Line 192: Equations are given to determine t_d . One of the specimens used in the comparison is hollow. None of the equations appear to limit the value of t_d to the actual wall thickness. The calculated t_d could be greater than the wall thickness at low torque (and small curvature).

Response: The authors agree with the reviewer. The shear flow depth t_d is limited to the actual wall thickness of the specimen. The same information has been added in the revised draft by editing Eq. (12a)

$$t_{d,i} = \frac{\overline{\varepsilon}_{2s,i}}{\psi_i} \left(\leq \frac{b_0}{2} \right) \quad (12a)$$

The following phrase has also been added: “ The calculated shear flow depth $t_{d,i}$ should be limited to the thickness of walthe l in the case of the hollow specimen and should be limited to half of the depth of the idealized cross-section $\left(\frac{b_0}{2}\right)$ in the case of solid cross-sections” (lines 207-209) in the revised draft.

10. Page 8, Line 205 to 209: the constituent laws for concrete in compression used in this paper were developed for flat panels. No justification is given in this paper for how the empirical relationships developed for flat panels are appropriate for the warping walls of a member under torsion.

Response: The authors agree with the reviewer that the constitutive laws used in this work are developed based on test results of flat panels which are 2D elements. Torsion is a 3-dimension problem.. The evaluation of constitutive laws for a 3-dimension panel is currently investigated by a very recent publication of researcher Labib et al. 2017 (referred in the revised draft). These constitutive laws for compression and tension based on a warped 3-dimension panel, Poisson effect on these 3-D panels and their application for torsion are not fully established yet. Understanding these aspects are highlighted as scope for future work. The same limitation as pointed out by the reviewer is added in the revised draft (lines 422-427).

Reference added: Labib, Moheb, Yashar Moslehy, and Ashraf Ayoub. (2017). “Softening coefficient of reinforced concrete elements subjected to three-dimensional loads.” *Magazine of Concrete Research*.

11. Page 9, Line 216 to 217: the constituent laws for concrete in tension used in this paper were developed for flat panels. No justification is given in this paper for how the empirical relationships developed for flat panels are appropriate for the warping walls of a member under torsion.

Response: The authors agree with the reviewer that the constitutive laws used in this model are developed based on flat panels which are 2D elements. Torsion is a 3-dimension problem. The same limitation as pointed out by reviewer has been added in the revised draft (lines 422-427).

Reference added: Labib, M, Moslehy, Y and Ayoub A. (2017). “Softening coefficient of reinforced concrete elements subjected to three-dimensional loads”. *Magazine of Concrete Research*.

12. Page 9, Line 226 to 229: these four equations have been in at least one of the references cited in this paper. Reference should be given to the source.

Response: Included as suggested. The previous works of Jeng 2009, and Ganagnagoudar et al. 2016 have been referred in this context.

13. Page 10, Line 237 to 242: the Poisson effect used in this paper were developed for flat panels. No justification is given in this paper for how the empirical relationships developed for flat panels are appropriate for the warping walls of a member under torsion.

Response: Limitations and justification are highlighted in the revised manuscript.

Reference added: Labib, M, Moslehy, Y and Ayoub A. (2017). “Softening coefficient of reinforced concrete elements subjected to three-dimensional loads”. *Magazine of Concrete Research*.

14. Page 11, Line 271: It states that the principal compressive strain in panel 1 is varied from zero to failure. Equation 5a shows that the shear flows are additive in panel 1. But according to conclusion 3, shear stress is additive in panel 3. Also, figure 15 shows that the strains are largest in panel 3. Which panel has the additive shear flows? If panel one does not have the additive shear flow, it may never reach large compressive strains, so how can the compressive strains be varied for this panel? Please explain.

Response: The shear flow is uniform in all the panels when only torsion is applied. The shear flow due to external shear loads is added/subtracted to the existing shear flow depending upon the direction of external shear load (as depicted in Fig. 4 of the draft). The authors agree with the reviewer that the panel no. 1 will never reach large compressive strain if it does not have additive shear flow. At the same time, it has to be noted that the section failure will be governed by the compressive strain in the panel 3 in which shear flow is additive. The analysis will stop as soon as

compressive strain reaches its failure limit in any one of the four panels. In the present discussion, it is panel-3, in which shear flows are additive.

15. Page 13, Line 304: no explanation is given for how the equivalent longitudinal and transverse reinforcement in each panel was determined.

Response: The following information has been added to the revised draft, in the section “Idealization of Cross-section”:

“The longitudinal and transverse reinforcement in the section also has to be distributed among the shear panels. **If the sections are symmetrical regarding reinforcement**, then longitudinal steel and transverse steel is distributed equally among all the shear panels. The transverse reinforcement is distributed equally among all the shear panels as it is symmetric for all the specimens adopted in the current study. The longitudinal steel area is assigned to that shear panel in which the longitudinal bar is located. In the cases of overlap of steel area between two shear panels, it is distributed as a function of the width of the shear panels that are overlapping. A detailed account of the distribution of longitudinal reinforcement can be in the work of Greene and Belarbi (2009).”

16. Page 13, Line 313 to 321: This list only shows the Missouri 2 specimen as having axial force. In Table 2, Rahal- Collins 1 and Rahal- Collins 2 also have an axial force given. Which one is correct?

Response: The list of lines 336-339 has been corrected to avoid the mismatch of information.

17. Page 13, Line 313 to 321: If axial force is included for columns, does the model account for spalling of the cover?

Response: No. Spalling of concrete cover is not considered in the present work. In the present model, the cover concrete area has also been included in all the calculations of torsion, shear and also axial loads. The authors agree that the spalling phenomenon occurs when axial loads are

present. The interaction of torsional, shear and axial loading on the spalling of concrete cover is not in the gambit of the present work. It is the scope of future work.

18. Page 13, Line 326: 1) the grammar in this sentence is confusing. 2) assuming a comparison is being made between two models: the comparison is purely qualitative. Just looking at the figures 14 a through e, the CASTM is much closer to experimental data than the proposed CASMM. So the validity of your statement is questionable. Instead, the comparison should be quantified or deleted.

Response: The comparisons are quantified in Tables 3 and 4. There are instances in which the predictions of CASMM are better than CASTM and vice versa. The ambiguous nature of the sentence is addressed by rephrasing the sentence in the revised draft as given below:

“The peak torque and the corresponding twist are captured reasonably well by the CA-SMM. The proposed model predicted the peak torque and twist more accurately for the specimen of Missouri, Rahal and Collins while the results of CA-STM are close to experimental peak values of Greene’s and Klus specimen. However, it can be observed from the Table 3 that the predictions in the peak torque and peak twist predictions of CASTM and CASMM are similar.”

19. Page 14, Line 331: Comparison of models based on peak values is also qualitative. Looking at the figures 14 this statement is questionable. The comparison should be quantitative or deleted.

Response: The comparisons are quantified in Tables 3 and 4. There are instances in which the predictions of CASMM are better than CASTM and even vice versa. The ambiguous nature of the sentence is addressed by rephrasing the sentence in the revised draft as given below:

“The peak torque and the corresponding twist are captured reasonably well by the CA-SMM. The proposed model predicted the peak torque and twist more accurately for the specimen of Missouri, Rahal and Collins while the results of CA-STM are close to experimental peak values of Greene’s and Klus specimen. However, it can be observed from the table 3 that the predictions in the peak torque and peak twist predictions of CASTM and CASMM are very close.”

20. Page 14, Line 338: Reference is made to figures 14 and 15. It is unclear whether the values shown in the figures are experimental or model predictions. It is unclear how it is useful to show only the

experimental or model predictions of strain. Both need to be shown together to evaluate the adequacy of the proposed model.

Response: The figures depict the predictions of the model. The experimental data of strains is not available in the literature. The authors presented the predicted strains to depict that the improved model is capable of capturing the behavior at the local level as well. Due to unavailability of experimental data, the predictions are not sufficed with experimental validation. The same information and the limitation are explained elaborately in the revised draft.

21. *Page 14, Line 352: Statement is made, “the model is capable of capturing the trend of strain variations in the section accurately.” The figures 14 and 15 that are the basis for this statement do not show a comparison of experimental and prediction strain. It is unclear what the trend of strain variation is. How can you claim the model accurately predicts something without showing a comparison?*

Response: The experimental results pertaining to the longitudinal and transverse strains are not available in the literature, due to which the comparison could not be presented. The authors want to present the strain distribution in the longitudinal and transverse steel to depict that the model is capable of calculating strains at the local level also. Depending upon the loading to which the panel is subjected to (Pure torsion/ torsion + shear/ torsion – shear), there are four different strains on four different panels, as depicted in fig. 15. Transverse steel reinforcement primarily resists loads of torsion and shear. Therefore, it is expected that the strains will increase smoothly until peak load and decreases after that. As the experimental data is not available, the authors want to depict from the graphs that the model is predicting the strains by the expected trend. The corresponding section “distribution of strains in reinforcement” has been elaborated to include the above details. The authors hope that the discussion is valid and adds value to the manuscript.

22. *Page 15, Line 373: Figure 16 does not show a variation in compressive strength or longitudinal reinforcement as stated in the text*

Response: The phrase is edited as given below. Fig. 16 depicts the parametric study of variation of concrete compressive strength, transverse and longitudinal reinforcements ratios. The authors

want to depict the same that the model can be adopted for parametric study also and the same results are presented in fig. 16.

“The parametric study of varying concrete compressive strength and longitudinal reinforcement ratio for predicting the torsion shear interaction is also presented in Fig. 16.”

23. *Page 16, Line 389: Conclusion number 3 was not directly discussed in the body of the paper. Not sure that the figures in this analytical study really demonstrated this conclusion as currently written.*

Response: Conclusion 3 is drawn from the analysis of strains presented in Fig. 16. The transverse strains are more in the panels in which shear stresses due to shear and torsion are additive. Therefore, the conclusion is made that the transverse reinforcement plays a key role in improving the torque-twist behaviour for members under combined loading of torsion and shear. The conclusion could be strongly established if the results are **sufficed** with the experimental validation.

24. *Page 25, Fig 6: this image was taken from another source and should be referenced*

Response: The figure is modified for a rectangular cross-section to suit the type of section investigated in this work. Relevant references to highlight the behavior are included in the text.

25. *Page 25, Fig 7: this image was taken from another source and should be referenced.*

Response: Fig. 7 has been adapted by the authors based on the previous work of Jeng 2009 and Ganganagoudar et al. 2016. References are included in the revised manuscript.

26. *Page 31, Fig 16: Rahal Collins series 2 was a single specimen in table 2, 3, and 4. In figure 16, one specimen is shown as an interaction curve of four points. Not sure how this is possible.*

Response: The specimen is same as in table 2,3 and 4. The interaction points are calculated for different T/V ratios. For Rahal Collins specimen, the results are compared with Experimental data available for T/V ratio of 1500mm.

27. Page 31, Fig 16: Klus specimen was shown as two specimens in table 2, three specimens in table 3, and excluded from table 4. These two or three specimens became 8 points on an interaction curve in figure 16. Not sure how this is possible.

Response: In total, Klus has conducted tests on eight specimens, which fall under different T/V ratios. Only a few of them were validated by the authors, and the validated ones were included in the Tables 2 & 3. Only three specimens are used in both the tables 2 and 3 (one under pure torsion and two other specimens of 2 different T/V ratios). In Table 4, the test data related to post-peak failure is not available for the Klus specimen and therefore it is omitted. However, all the experimental data of Klus's specimen (eight of them) for different T/V ratios are used in the validation of T-V interaction diagram (Figure 16). A note has been added to the Table 2 and 3 to convey the same information.

The manuscript has been resubmitted to your journal. We look forward to your positive response.

Sincerely,

Dr. S. Suriya Prakash.